CONFIGURATION ADJUSTMENT POTENTIAL OF THE VERY HIGH TEMPERATURE REACTOR PRISMATIC CORES WITH ADVANCED ACTINIDE FUELS

A Thesis

by

DAVID E. AMES II

Submitted to the Office of Graduate Studies of
Texas A&M University
in partial fulfillment of the requirements for the degree of

MASTER OF SCIENCE

August 2006

Major Subject: Nuclear Engineering

CONFIGURATION ADJUSTMENT POTENTIAL OF THE VERY HIGH TEMPERATURE REACTOR PRISMATIC CORES WITH ADVANCED ACTINIDE FUELS

A Thesis

by

DAVID E. AMES II

Submitted to the Office of Graduate Studies of
Texas A&M University
in partial fulfillment of the requirements for the degree of

MASTER OF SCIENCE

Approved by:

Chair of Committee,	Pavel V. Tsvetkov
Committee Members,	Kenneth L. Peddicord
	Donald G. Allen
Head of Department,	William E. Burchill

August 2006

Major Subject: Nuclear Engineering

ABSTRACT

Configuration Adjustment Potential of the Very High Temperature Reactor Prismatic Cores with Advanced Actinide Fuels. (August 2006)

David E. Ames II, B.S., University of Utah

Chair of Advisory Committee: Dr. Pavel Tsvetkov

Minor actinides represent the long-term radiotoxicity of nuclear wastes. As one of their potential incineration options, partitioning and transmutation in fission reactors are seriously considered worldwide. If implemented, these technologies could also be a source of nuclear fuel materials required for sustainability of nuclear energy.

The objective of this research was to evaluate performance characteristics of Very High Temperature Reactors (VHTRs) and their variations due to configuration adjustments targeting achievability of spectral variations. The development of realistic whole-core 3D VHTR models and their benchmarking against experimental data was an inherent part of the research effort. Although the performance analysis was primarily focused on prismatic core configurations, 3D pebble-bed core models were also created and analyzed.

The whole-core 3D models representing the prismatic block and pebble-bed cores were created for use with the SCALE 5.0 code system. Each of the models required the Dancoff correction factor to be externally calculated. The code system DANCOFF-MC was utilized to perform the Dancoff factor calculations.

The whole-core/system 3D models with multi-heterogeneity treatments were validated by the benchmark problems. Obtained results are in agreement with the available High Temperature Test Reactor data. Preliminary analyses of actinide-fueled VHTR configurations have indicated promising performance characteristics. Utilization of minor actinides as a fuel component would facilitate development of new fuel cycles and support sustainability of a fuel source for nuclear energy assuring future operation of Generation IV nuclear energy systems.

ACKNOWLEDGMENTS

I would like to offer my sincere thanks and gratitude to my adviser Dr. Pavel Tsvetkov, and committee members Dr. Kenneth Peddicord and Dr. Donald Allen, without whom this thesis would not have been possible. Especially Dr. Tsvetkov, who provided considerable guidance, help, and time; making himself available whenever needed throughout the duration of the project.

I would also like to acknowledge my family. Thank you for the continued support and all that you have done for me, and my friends from Salt Lake City, San Francisco, College Station, and everywhere in between.

This thesis is based upon work supported by the U.S. DOE under Award Number DE-FC07-05ID14655 (05-094).

TABLE OF CONTENTS

Page

CHAPTER Page

LIST OF FIGURES

FIGURE Page

LIST OF TABLES

TABLE Page

CHAPTER I

INTRODUCTION

I.A BACKGROUND

This chapter discusses current research and development efforts in the United States concerning the future of nuclear energy. The work described in this thesis was performed as part of the United States Department of Energy (DOE) Nuclear Energy Research Initiative (NERI) Project, "Utilization of Minor Actinides as a Fuel Component for Ultra-Long Life VHTR Configurations: Designs, Advantages, and Limitations". Objectives of the present research effort are stated in chapter I.B.

I.A.1 GENERATION-IV REACTOR SYSTEMS

Industrial nuclear power was introduced in the United States in the 1950s. Today it provides approximately 20 percent of the United States' electricity generation and about 17 percent of the world's electricity generation. Nuclear power has proven to be an environmentally safe, reliable, and economical to generate large supplies of electricity without releasing noxious gases into the atmosphere.

Even with the impressive track record of nuclear power to date, further advances in nuclear system energy design can broaden the opportunity for nuclear energy use in the future. This was the basis for the formation of the Generation-IV International Forum (GIF). Established in 2000, GIF investigates innovative nuclear energy system concepts

---

This thesis follows the style of *Nuclear Science and Engineering*.

for meeting future energy needs. It is an international assembly representing governments of countries where nuclear energy is viewed as a vital component of present and future energy needs. These countries are committed to joint development of the next generation of nuclear technology. Currently composed of 11 member countries (United States of America, Argentina, Brazil, Canada, France, Japan, South Korea, South Africa, Switzerland, United Kingdom, and the European Union) the forum serves to coordinate international research and development on promising new nuclear energy systems.

The GIF strives to develop Generation-IV nuclear energy systems that advance nuclear safety, address nuclear nonproliferation and physical protection issues, are competitively priced, minimize waste, and optimize natural resource utilization. Based on their potential to meet the above goals, six concepts have been selected by the GIF for further development [1].

The six Generation-IV systems selected are:

- Gas-Cooled Fast Reactor (GFR),
- Very High Temperature Reactor (VHTR),
- Supercritical Water Cooled Reactor (SCWR),
- Sodium Cooled Fast Reactor (SFR),
- Lead Cooled Fast Reactor (LFR), and
- Molten Salt Reactor (MSR).

I.A.2 THE VERY HIGH TEMPERATURE REACTOR (VHTR)

The United States Department of Energy has given priority to the VHTR concept making it the focus of intensive research programs. The VHTR is designed to be a high-efficiency system, which can supply electricity and process heat to a wide-range of high temperature and energy intensive applications. The VHTR is a passively safe design. The refractory core, low power density, and low excess reactivity enable this design feature.

The VHTR is a graphite moderated gas-cooled reactor that supplies heat with core outlet temperatures equal to or greater than 850 degree Celsius, which enables applications such as hydrogen production, process heat for the petrochemical industry, or sea water desalination. Its basic technology has been well established in former High Temperature Gas Reactors (HTGR), such as the German AVR and THTR prototypes, and the US Fort Saint Vrain and Peach Bottom prototypes. The VHTR extends the capabilities of HTGR's to achieve further improvements in thermal efficiency and open up additional high-temperature applications.

The reactor core can be a prismatic block core such as the High Temperature Test Reactor (HTTR) operating in Japan, or a pebble bed core such as the Chinese High Temperature Test Module (HTR-10). Both the prismatic and pebble bed cores have the same key design characteristics and use the same ceramic or TRISO (TRIstructual ISOtropic) coated fuel particles. The TRISO coating provides a miniature containment vessel for each fuel particle, allowing complete retention of fission fragments at high temperatures [2].

The prismatic block core is composed of fuel blocks, control rod guide blocks, and reflectors blocks. The fuel blocks consist of a hexagonal graphite block with borings in it for the placement of annular fuel compacts and helium coolant channels. The annular fuel compacts are composed of TRISO coated fuel particles embedded in a graphite matrix. The control rod guide blocks are hexagonal graphite blocks with borings for the control rods to pass through. The reflector blocks are simply solid graphite hexagonal blocks. These "fuel blocks, control rod guide blocks, and reflector blocks" are arranged side-to-side and stacked in columns to create the core.

The pebble bed core consists of TRISO coated fuel particles embedded into graphite billiard-ball size spheres, or fuel pebbles. These pebbles are loaded into the reactor core cavity formed by graphite reflector blocks. Gaseous coolant (helium) flows through the gaps of the pebble bed providing heat removal and transport to the heat exchanger or gas turbine. The pebble bed core provides the ability to perform continuous online refueling by circulating the pebbles through the core.

I.A.3 ADVANCED FUEL CYCLE INITIATIVE

To meet the projected goals of the GIF, continued research related to fuel cycles and the management of spent fuel is needed. This is a major reason why the United States Department of Energy (DOE) created the Advanced Fuel Cycle Initiative (AFCI). The AFCI will develop advanced fuel systems for Generation IV reactors and create fuel cycle technologies to considerably reduce the disposal of long-lived, highly radiotoxic transuranic isotopes while reclaiming spent fuel's valuable energy.

A key roadblock to expansion of nuclear power is the concern over management of the spent nuclear fuel. AFCI is developing the technology base for waste management

including partitioning and transmutation. AFCI's transmutation technology offers the potential to extract energy from spent nuclear fuel and to make it available to the national power grid [3].

I.A.4 U.S. DOE NERI PROJECT

The overall objective of the U.S. DOE Nuclear Energy Research Initiative (NERI) Project is to assess the possibility, advantages and limitations of achieving ultra-long life VHTRs with minor actinides as a fuel component. The analysis takes into consideration and compares capabilities of actinide-fueled VHTRs with pebble-bed and prismatic core designs to approach the reactor-lifetime long operation without intermediate refueling. The ultra-long life VHTR systems are developed and analyzed focusing on control, dynamics, safety, and proliferation-resistance during reactor lifetime long autonomous operation.

The project assesses the prospective relation and application for Generation IV VHTRs in the AFCI Program [2, 3]. Utilization of minor actinides, from light water reactor (LWR) fuel, as a fuel component, would facilitate development of new fuel cycles and support sustainability of a fuel source for nuclear energy assuring future operation of Generation IV nuclear energy systems. The ultra-long core life approach reduces the technical need for additional repositories. Furthermore, the developed VHTR configurations should improve marketability of the Generation IV VHTRs.

I.B RESEARCH OBJECTIVES

The work described in this thesis is within the scope of the NERI project, with focus placed on:

- Detailed 3D full-core model development,
- Validation and verification,
- Preliminary analysis of the VHTR cores, prismatic core designs, with advanced actinide fuels.

Prismatic core designs offer flexibility in component configuration, fuel utilization, and fuel management; making it possible to improve fissile properties of minor actinides by neutron spectrum shifting through configuration adjustments. As a result, under certain spectral conditions minor actinides would be able to contribute to the core neutron balance compensating for fuel depletion effects through their chain transformations. The resulting self-stabilization of advanced actinide fuels should allow prolonged operation on a single fuel loading up to ultra-long lifetimes.

The main anticipated advantages of the resulting VHTR prismatic core configurations are their inherent capabilities for utilization of minor actinides from spent LWR fuel, reduction of spent fuel flows, and handling per unit of produced energy. Consequently, if widely deployed, the developed designs would allow reducing the long-term radiotoxicity and heat load of high-level wastes sent to a geologic repository and enable recovery of the energy contained in spent fuel.

The objective of this thesis is to evaluate performance characteristics of VHTRs and their variations due to configuration adjustments targeting achievability of spectral variations. The development of realistic whole-core 3D VHTR models and their

benchmarking against experimental data is an inherent part of the research effort. Although the performance analysis is primarily focused on prismatic core configurations, 3D pebble-bed core models are also created and analyzed.

I.B.1 PROCEDURE

Most of the available well-established and validated computer code systems are oriented on LWRs. To apply them for VHTRs, a specialized approach of application is required. For instance, one of the most difficult phenomena related to analysis of VHTRs is the effects of the double heterogeneity on the resonance self-shielding of cross sections. The first level of heterogeneity (micro-level) is formed by coated fuel micro-particles that are randomly distributed in the fuel region of the graphite fuel pebble (pebble-bed core) or in the graphite compact (prismatic graphite block core). The second level of heterogeneity (macro-level) is formed by the randomly-packed bed of pebbles or by the prismatic blocks with compacts that compose the VHTR core. Consequently, the influence of the double heterogeneity involved in VHTRs has to be accounted for in the Dancoff factor calculation. Dancoff factors are used in resonance shielding calculations to adjust the first-flight escape probability of a fuel lump for the probability that a neutron that escapes will enter a neighboring fuel lump without interaction in between.

Previous work [4] has identified insufficiencies in the ability of code systems to accurately calculate a Dancoff correction factor for the VHTR fuel grains randomly distributed in fuel regions of fuel pebbles or compacts. To circumvent this limitation, the Dancoff factor for the fuel may be entered as an external parameter, in some cases, manually by the user. The Dancoff factor can be more accurately calculated by alternative means, which use, for example, the Monte Carlo method [5].

In the present study, state-of-the-art computer code systems will be utilized to create realistic modeling of the VHTR configurations. These include the SCALE (Standardized Computer Analysis for Licensing Evaluation) version 5 modular code system [6] and DANCOFF-MC: A Computer Program for Monte Carlo Calculation of Dancoff Factors in Irregular Geometries [7]. Two separate models will be created; one being the prismatic graphite block type core design and the other the pebble-bed type core design. The prismatic core model will be based on available information for Japan's operating High Temperature Test Reactor (HTTR). The pebble-bed core will be based on China's operating High Temperature Test Module (HTR-10) [8]. The existing HTTR and HTR-10 configurations will serve as the initial prototype designs and also as examples of small-scale VHTRs.

The developed computational models must adequately represent the actual reactor systems at the full core level with explicit geometry representation while at the same time provide a computational run time allowing completion of configuration variations within realistic time limits. This will include balancing the built-in model assumptions and sources of uncertainty to achieve reliable results. As a guideline, computational time for benchmark evaluations should be kept under 12 hours, in order to produce desired output results and remain within time limitations allowing parametric studies and multiple configuration variations.

Following the international benchmark practices and accepted accuracy standards, the models require validation by experiment-to-code and code-to-code benchmarking procedures, with the goal of 10 percent prediction accuracy or better in computational studies. If results demonstrate higher discrepancy, but the discrepancy can be adequately

explained by the model assumptions, then it will be concluded that the experimental benchmark testing is passed conditionally. In any case, the ability to explain differences between code and experiment results is expected. The benchmarking project will use actual test results from the HTTR and HTR-10 programs [8]. Continuation of the project and its success will be vitally dependent on the successful completion of the benchmark calculations.

Once benchmark calculations have been completed, further analysis will be conducted on the prismatic fuel block core VHTR model. The pebble-bed type VHTR model will be made available to fellow researchers involved with the encompassing U.S. DOE NERI Project of evaluating the advantages and limitations of VHTRs with minor actinides as a fuel component.

As mentioned previously, the Dancoff correction factor is an important parameter of VHTRs. To provide a clear understanding, sensitivity calculations with respect to Dancoff correction factors will be conducted. This entails performing multiple computational runs for a range of Dancoff factors followed by analysis of the results.

For the purposes of the project, energy-dependent fluxes in the fuel compacts will be computed and analyzed for various locations and for different core configurations. Based on the observed core features, preliminary conclusions will be made on achievability of different spectral conditions in the VHTR core. The core performance characteristics will be compared to demonstrate the potential for use of minor actinides as a fuel component.

CHAPTER II

APPLIED CODE SYSTEMS

A description of the utilized code systems and their limitations will be discussed in this chapter. The VHTR whole-core/system 3D computational models with explicit multi-heterogeneity treatments were developed using SCALE (Standardized Computer Analysis for Licensing Evaluation) version 5 [6] and DANCOFF-MC: A Computer Program for Monte Carlo Calculation of Dancoff Factors in Irregular Geometries [7]. Both code systems are part of the Radiation Safety Information Computational Center (RSICC), a Department of Energy Specialized Information Analysis Center (SIAC) authorized to collect, analyze, maintain, and distribute computer software and data sets in the areas of radiation transport and safety.

The 3D VHTR full-core models were created for the developed benchmark problems to compare with experimental data in order to validate the models before subsequently evaluating performance characteristics of VHTRs and their variations due to configuration adjustments targeting achievability of spectral variations. The experimental data were provided by IAEA-TECDOC-1382, “Evaluation of High Temperature Gas Cooled Reactor Performance: Benchmark Analysis Related to Initial Testing of the HTTR and HTR-10” [8]. Computational models of the existing HTTR and HTR-10 cores were created for the benchmarking process.

II.A SCALE 5

The 3D whole-core VHTR models were created using SCALE 5. The SCALE modular code system is developed and maintained by Oak Ridge National Laboratory (ORNL) and is widely accepted around the world for criticality safety analysis.

The developed model called upon the Criticality Safety Analysis Sequence No. 6 (CSAS6) control module [9]. CSAS6 was developed within the SCALE code system to provide automated, problem-dependent, cross-section processing followed by calculation of the neutron multiplication factor for the system being modeled using KENO-VI [10]. The code system includes several problem-independent multigroup cross-section libraries. The 238-Group ENDF/B-V neutron library [11] was used for all calculations.

The only sequence in CSAS6 is CSAS26. By default CSAS26 follows the execution path BONAMI, NITAWL-III, XSDRNPM, and KENO-VI [12-14]. BONAMI performs resonance self-shielding calculations for nuclides that have Bonderanko data associated with their cross-sections. As input, the program requires the presence of shielding factor data on the AMPX master library. As output, BOMAMI produces a problem-dependent master library and is always used in conjunction with NITAWL-III.

NITAWL-III applies the Nordheim Integral Technique to perform neutron cross-section processing in resonance energy range. This technique involves a fine energy group calculation of the slowing-down flux across each resonance with subsequent flux weighting of the resonance cross-sections. The major function of NITAWL is its conversion of cross-section libraries form a problem-independent to a problem-dependent form.

XSDRNPM uses one-dimensional discrete ordinates transport code to perform neutron calculations to create a homogenized cell-weighted mixture cross-section based on the specific unit cell. These cell-weighted cross-sections are used for subsequent system analysis by way of KENO-VI.

KENO-VI is a mutigroup Monte Carlo code applied to determine effective multiplication factors for three-dimensional systems. The geometry package in KENO-VI is capable of modeling any volume that can be constructed using quadratic equations.

A flow chart of the CSAS6 control module path used for the VHTR modeling is provided in Fig. 1.

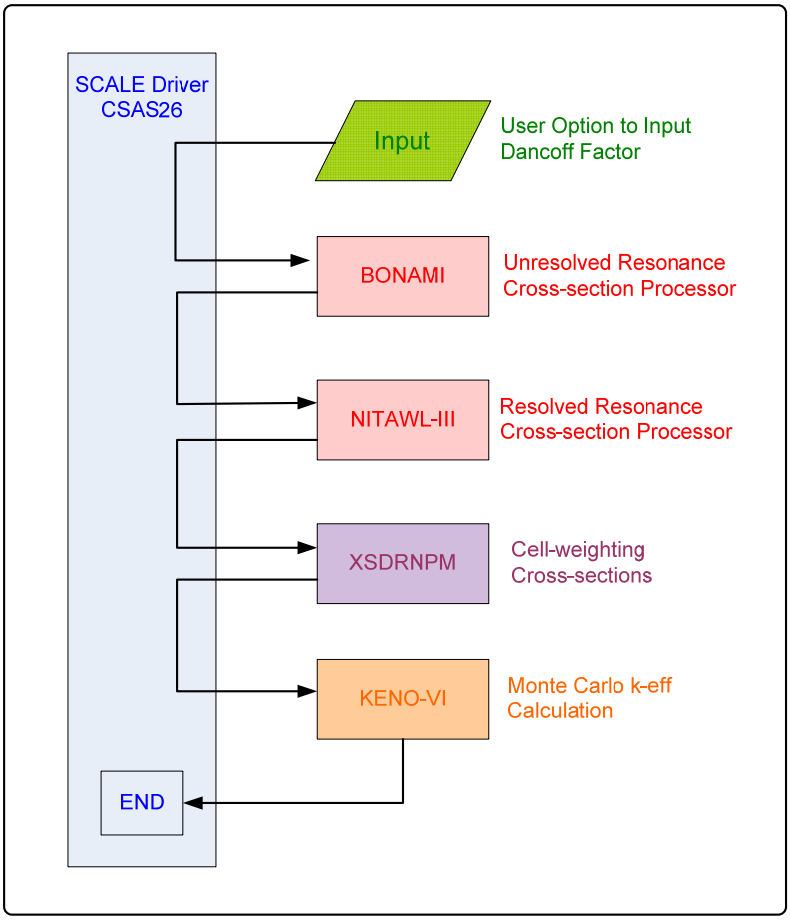

Fig. 1: Flow Chart of the CSAS6 Control Module

The inherent limitations in CSAS6 are as follows [9]:

1. Double heterogeneity such as HTGR or Pebble Bed fuel, where uranium encased in small graphite spheres are used to make larger spheres or rods which are then placed in a regular lattice.
2. Two-dimensional (2-D) effects such as fuel rods in assemblies where some positions are filled with control rod guide tubes, burnable poison rods and/or fuel rods of different enrichments. The cross sections are processed as if the rods are in an infinite lattice of rods.
3. The NITAWL-III Nordheim integral treatment assumes no resonance overlap from other resonances or other material regions.
4. The treatment of an external moderator assumes an asymptotic flux present at the absorber-moderator interface.
5. The treatment of spatial transport uses the first-flight escape probability for the absorber, the two-region reciprocity theorem, and Dancoff factors. For configurations with double and multi-heterogeneity features, proper Dancoff factors must be computed externally and provided as part of the input data.
6. The Nordheim integral treatment assumes no flux profile interference from resonance material in adjacent zones.

II.B DANCOFF-MC

The computer program code DANCOFF-MC was developed to calculate, by the Monte Carlo method, the Dancoff correction factor, which is used to determine the flux reduction in the resonance integral calculations [7].

There are two equivalent definitions for the Dancoff correction factor (or simply Dancoff factor). The original or 'historic' definition was developed by Dancoff and Ginsburg, who showed that in a closely packed lattice the in-current of resonance neutrons into the fuel is reduced, as compared to the in-current into a single fuel rod in an infinite moderator, because of the shadowing effect of adjacent rods. The relative reduction of the in-current is called the Dancoff correction [15]. The more commonly used definition today is related to the method of collision probabilities. This definition of the Dancoff factor is the probability that a neutron emitted isotropically from the surface of the fuel region of the fuel element under consideration will have its next collision in the fuel region of a surrounding fuel element [16]. By means of Monte Carlo-type simulation, DANCOFF-MC calculates the Dancoff factor base on the later definition.

The DANCOFF-MC program has been developed to obtain Dancoff factors in an arbitrary arrangement of cylindrical fuel pins or spherical fuel pellets, providing a high degree of generality: different fuel region diameters, clads and gaps with varying sizes, annular rods, arbitrary positions of rods or pellets, and different macroscopic cross-sections for each fuel element and its clad are all allowed.

The program calculates the Dancoff factor using the collision probability definition. Neutrons are started from the surface of the fuel lump and tracked until they intersect another fuel lump. Using the Monte Carlo method in DANCOFF-MC means to

select randomly the position where a neutron is emitted and the direction in which it travels. Analytical formulas are used to calculate both the lengths traveled in different material regions and the transport probabilities along any given path.

The DANCOFF-MC program is limited by the complexity of the problem. Restrictions include that the rods and pellets cannot be mixed in the same arrangement. The cylinders' axis must be parallelly positioned in rod arrangements. Calculation of ‘grey-effect’ for annular geometries is not available.

II.C COMBINED CODE SYSTEMS

Numerous papers presenting various techniques and algorithms for determining the Dancoff factor have been published and several methods are used for the calculation of Dancoff factors in different fuel lattices [17, 18]. However, these methods, developed for regular lattices of macroscopic fuel dimensions, are not directly applicable to VHTR fuel [5]. In addition, reactor physics code systems generally provide for the automatic calculation of the Dancoff factor, and the user is not always aware of the extent of approximation involved or the validity of the method in the actual application [19].

The SCALE code system provides the option for the Dancoff factor to be provided as an external input parameter. Therefore, DANCOFF-MC will be utilized to determine the Dancoff correction factor for the system. The factor will then be introduced into the VHTR model developed within the SCALE code system as illustrated in Fig. 1. By using this technique, the accuracy of the models is expected to be improved.

CHAPTER III

VHTR MODEL

III.A VHTR PRISMATIC CORE

The following sections detail the developed 3D full-core models of the VHTR prismatic configurations. The model description as well as validation and verification efforts are based on Japan's operating High Temperature Test Reactor (HTTR). The first section (III.A.1) provides general information related to the HTTR program and why it was selected. The next section (III.A.2) describes in detail the VHTR computational model and explains how it functions.

III.A.1 HTTR

The HTTR of the Japan Atomic Energy Research Institute (JAERI) is a graphite-moderated and helium gas-cooled reactor with 30 MW in thermal output and outlet coolant temperature of 850°C for rated operation and 950°C for high temperature test operation [8].

The major objectives of the HTTR are to establish and upgrade the technological basis for advanced high temperature gas-cooled reactors and to conduct various irradiation tests for innovative high temperature basic research. The major specifications for the HTTR are given in Table I.

Table I. Design Specifications for the HTTR

Thermal Power	30 MW
Outlet coolant temperature	950 C
Inlet coolant temperature	395 C
Primary coolant pressure	4 MPa
Core structure	Graphite
Equivalent core diameter	230 cm
Effective core height	290 cm
Average power density	2.5 W/cc
Fuel	UO_2
Uranium enrichment	3 to 10 wt.%
Type of fuel	Pin-in-block
Burn-up period	660 days
Coolant material	Helium gas
Flow direction in core	Downward
Reflector thickness	
Top	116 cm
Side	99 cm
Bottom	116 cm
Number of fuel assemblies	150
Number of fuel columns	30
Number of pairs of control rods	16
In core	7
In reflector	9

The HTTR was selected because of the reference material available. The reference material provided: general design features, reactor layout, core configuration, material properties, and other relevant information to develop the computational model. Also supplied were actual experimental test results to be utilized for experiment-to-code benchmarks and several analytical code results for code-to-code benchmark tests [8]. Taking advantage of the performed benchmark studies, the HTTR configurations are also used as initial prototype designs representing small-scale VHTR concepts.

III.A.2 VHTR PRISMATIC CORE MODEL

The VHTR model is a nearly explicit representation of the existing HTTR core configuration. The model was created in the SCALE code system utilizing the CSAS6/KENO-VI module, which allows flexible geometry representations. The geometry package in KENO-VI is capable of modeling any volume that can be constructed by quadratic equations (second order surfaces).

The general procedure for creating the model was to build the four types of prismatic hexagonal blocks that compose the HTTR, then to arrange these blocks in an array of rows and columns to construct the core. The four prismatic blocks are: fuel assembly blocks, replaceable reflector blocks, control rod guide blocks, and irradiation blocks.

III.A.2.1 THE FUEL ASSEMBLY BLOCK

The fuel assembly block consists of 4 main components: a hexagonal graphite block, fuel rods, burnable poison rods, and helium coolant channels. The core contains 150 fuel assembly blocks, which construct 30 columns (5 fuel blocks stacked vertically) within the core. Although these fuel blocks share the same general characteristics, there are subtle differences between them. For instance, individual fuel blocks can have different fuel enrichments (12 enrichments: 3.3% – 9.8%), one of two types of burnable poison rods, and either 31 or 33 annular fuel rods. This translates to 48 different types of fuel assembly blocks in the core, which can be identified by fuel enrichment and type of burnable poison rod.

The general parameters shared by the fuel blocks are as follows. A fuel assembly consists of fuel rods, coolant channels, and two burnable poison rods, which are

assembled in a hexagonal graphite block to create a pin-in-block type assembly. The fuel graphite block is 36 cm in width across the flats and 58 cm in height. The block has either 31 or 33 vertical borings (depending on number of fuel rods) with a diameter of 4.1 cm for placement of the annular fuel rods. In addition, each fuel graphite block has three burnable poison insertion holes measuring 50 cm in height and 1.5 cm in diameter. Two are loaded with burnable poison rods, while the third is left empty. In the center of each block is a fuel handling hole. Fig. 2 shows the arrangement and dimensions of the fuel graphite block. The measurements and material properties of the block are given in Table II.

The annular fuel rod consists of a fuel compact with an outer graphite sleeve. The graphite sleeve has an inner diameter of 2.6 cm, outer diameter of 3.4 cm, and height of 58 cm. The compact has an inner diameter of 1.0 cm, outer diameter of 2.6 cm, height of 54.6 cm, and is composed of fuel particles imbedded in a graphite matrix. Details on the treatment of the fuel compacts (homogenized fuel region) are presented in chapter III.A.2.6. The rods are inserted into the vertical holes of the graphite fuel block. Helium gas coolant flows through the gaps that are created between the holes and the rods.

The burnable poison rod is 1.4 cm in diameter and 50 cm in height. It is made up of two neutron absorber sections (20 cm in height) separated by a graphite section (10 cm in height). Fig. 3 was generated by KENO 3D, which is part of the SCALE code system. It illustrates an example of the fuel assembly block that was used in the computational model. Tables III and IV list the properties of the fuel rod and burnable poison rods.

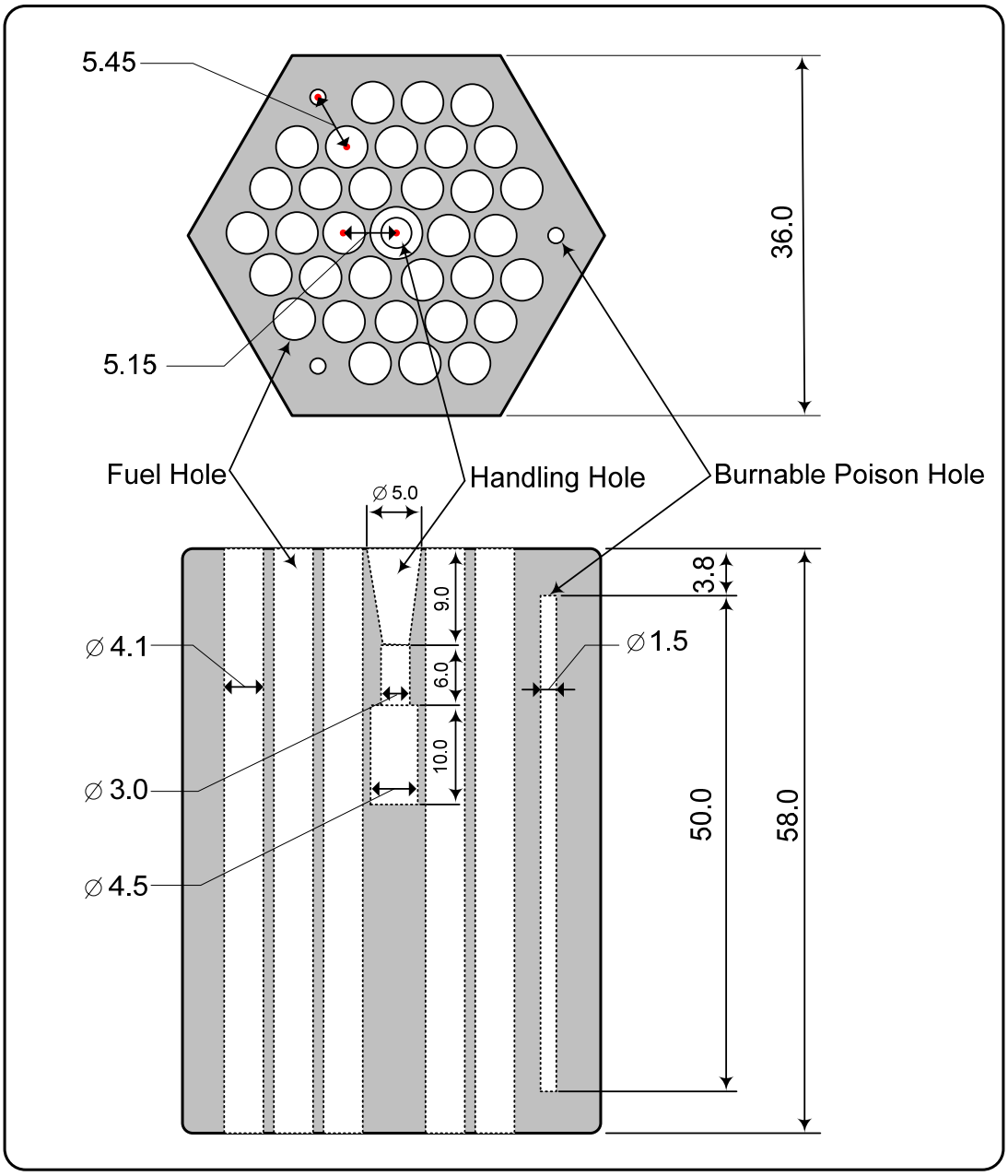

Fig.2. Fuel Graphite Block (measurements in cm)

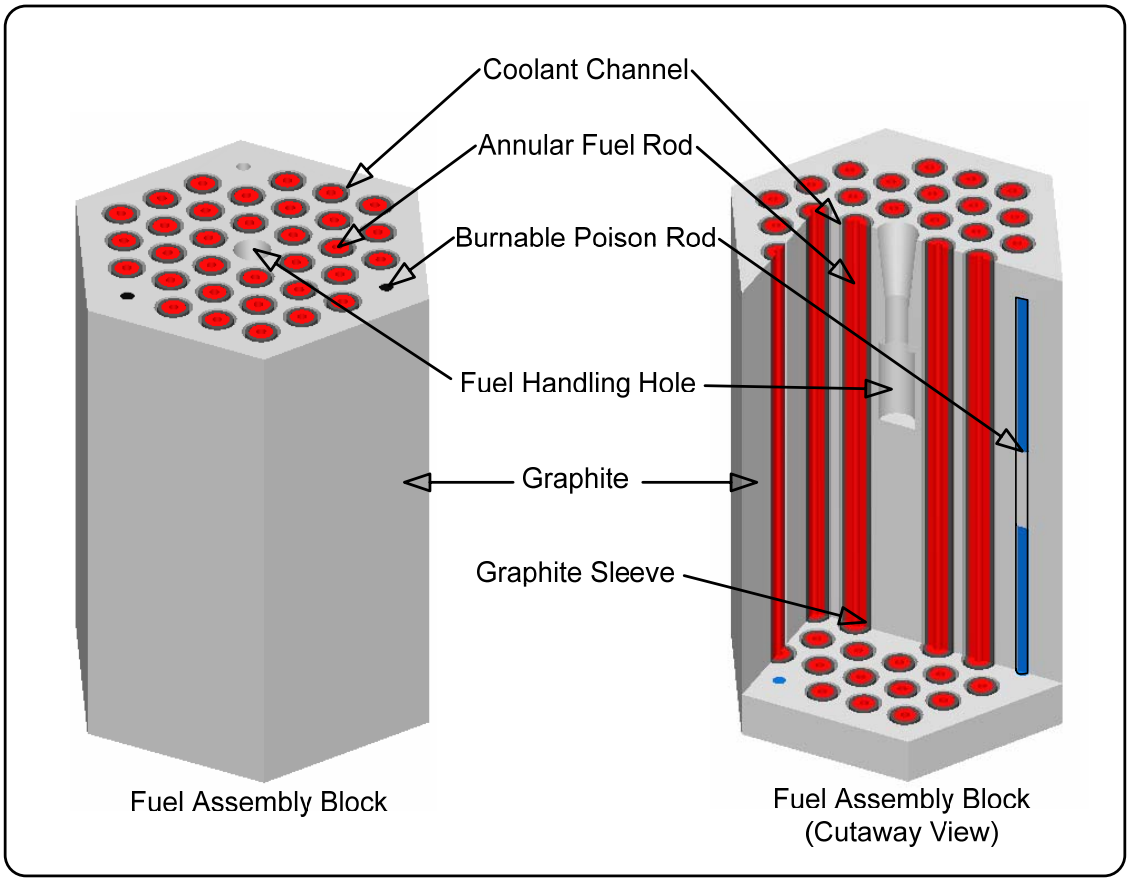

Fig.3. HTTR Fuel Block Assembly (KENO 3D)

Table II. Fuel Graphite Block Properties

Type	Pin-in-block
Configuration	Hexagonal
Material	IG-110 Graphite
Density	1.770 g/cc
Impurity	0.40 ppm B_{nat}
Height	58.0 cm
Width across the flats	36.0 cm
Number of fuel holes in block	33 or 31
Fuel hole diameter	4.1 cm
Fuel hole height	58.0 cm
Number of burnable poison holes	3
Burnable poison hole diameter	1.5 cm
Burnable poison hole height	50.0 cm

Table III. Fuel Rod Properties

Fuel Compact	
Number of fuel particles	182,200
Graphite matrix density	1.690 g/cc
Graphite matrix Impurity	0.82 ppm B_{nat}
Diameter-inner	1.0 cm
Diameter-outer	2.6 cm
Effective height of fuel rod	54.6 cm

Graphite Sleeve	
Material	Graphite
Density	1.770 g/cc
Impurity	0.37 ppm B_{nat}
Diameter-inner	2.6 cm
Diameter-outer	3.4 cm
Height	57.7 cm

Table IV. Burnable Poison Rod Properties

Type	**H-I**	**H-II**
Absorber section material	B_4C-C	B_4C-C
Density	1.79 g/cc	1.82 g/cc
Natural boron concentration	2.22 wt.%	2.74 wt.%
Diameter	1.39 cm	1.39 cm
Height	2.0 cm	2.5 cm
B-10 abundance ratio	18.7 wt.%	18.7 wt.%
Graphite section density	1.77 g/cc	1.77 g/cc
Diameter	1.40 cm	1.40 cm
Height	10 cm	10 cm

III.A.2.2 REPLACEABLE REFLECTOR BLOCK

The replaceable reflector block has the same external form as the fuel assembly block, 36 cm in width across the flats and 58 cm in height with a handling hole in the center of the block. There are two types of reflector blocks; one being a solid graphite block, and the other having helium coolant channels in it.

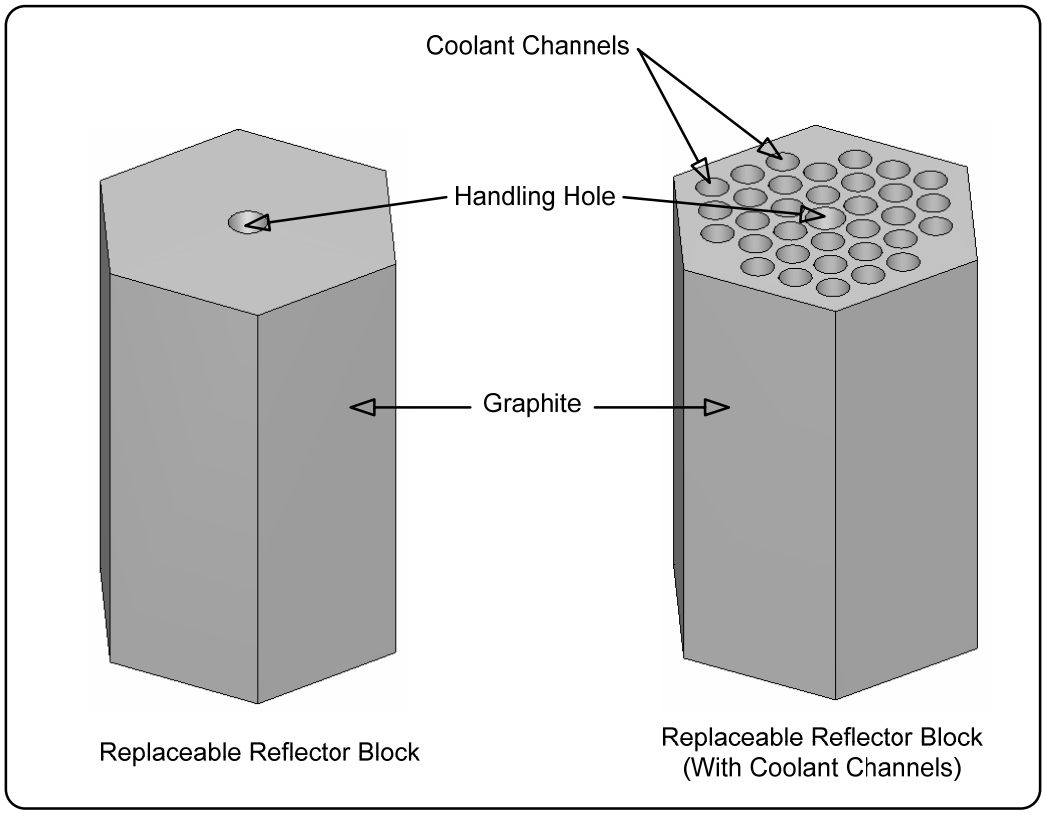

Fig.4. Replaceable Reflector Blocks (KENO 3D)

The reflector blocks with the coolant channels are stacked directly above and below the fuel assembly blocks. This creates a fuel column, being composed of 2 replaceable reflector blocks on top, 5 fuel assembly blocks in the middle, and 2 replaceable reflector blocks on the bottom (total of 9 blocks). The blocks have the same

dimensions as the fuel graphite block within the same column, with the exception of not having the three burnable poison insertion holes. This allows the helium gas to flow into the core, through the fuel assemble blocks, and then exit the core. Examples of the replaceable reflector blocks are provided in Fig. 4, with the properties listed in Table V.

Table V. Replaceable Reflector Block Properties

Configuration	Hexagonal
Material	IG-110 Graphite
Density	1.760 g/cc
Impurity	0.37 ppm B_{nat}
Height	58.0 cm
Width across the flats	36.0 cm
Number of coolant holes if applicable	33/31
Coolant hole diameter	4.1 cm
Coolant hole height	58.0 cm

III.A.2.3 CONTROL ROD GUIDE BLOCK

There are 144 control rod guide blocks in the core. They form 16 control rod guide columns in the core (9 blocks stacked vertically). The block consists of a hexagonal graphite block with three large vertical borings. Just as the fuel block, it is 58 cm in height and 36 cm in width across the flats.

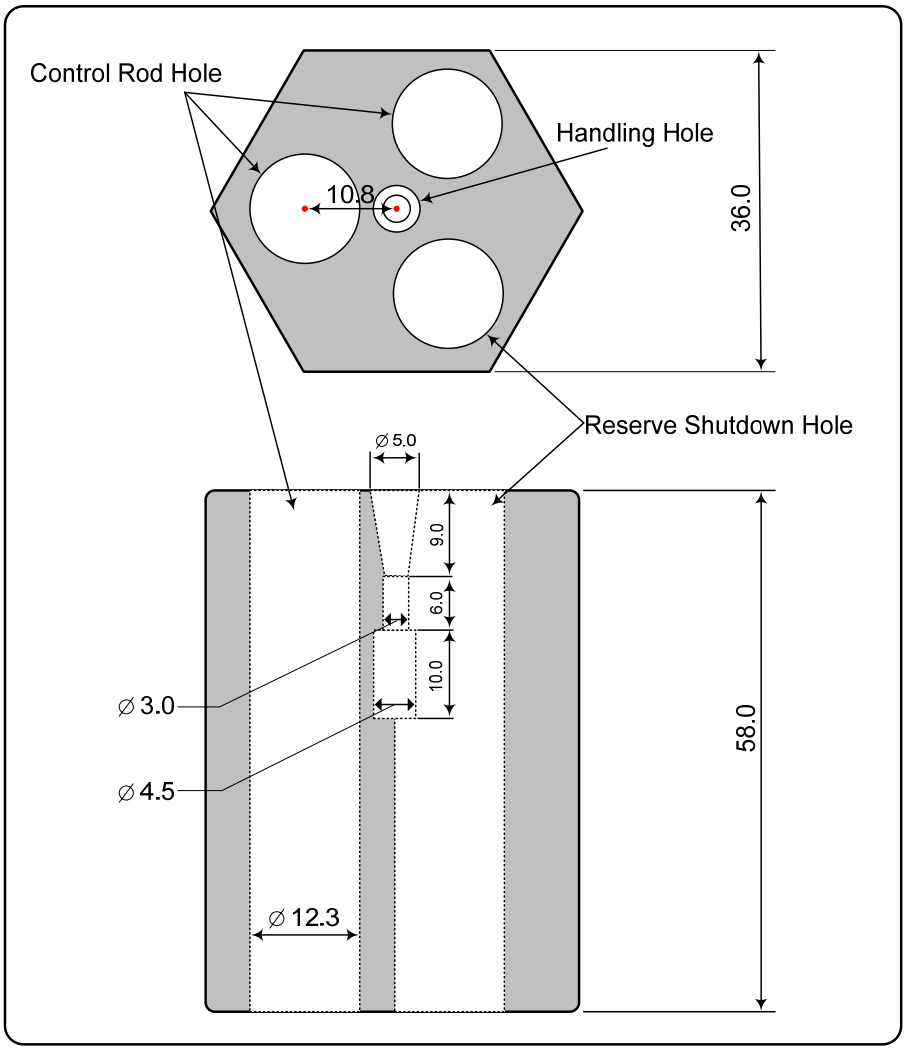

Fig. 5. Control Rod Guide Block (measurements in cm) [2]

The holes created by the borings have a 12.3 cm diameter and extend through the entire length of the block. Two of the holes are used for the control rods to pass through, while the third is left empty to serve as the reserve shutdown system. In the center of each block is a fuel handling hole. Fig. 5 shows the arrangement and dimensions of the fuel graphite block and Table VI lists the properties of the block.

Table VI. Control Rod Guide Block Properties

Material	IG-110 Graphite
Density	1.770 g/cc
Impurity	0.40 ppm B_{nat}
Height	58.0 cm
Width across the flats	36.0 cm
Number of control rod holes in block	2
Control rod hole diameter	12.3 cm
Control rod hole height	58.0 cm
Number of reserve shutdown holes in block	1
Reserve shutdown hole diameter	12.3 cm
Reserve shutdown hole height	58.0 cm

There are 16 pairs of control rods, 7 in the active core and 9 in the replaceable reflector region. A pair of control rods is inserted into the holes of a control rod guide column. Each control rod consists of 10 annular neutron absorber section (B_4C/C) having an inner diameter of 6.5 cm, outer diameter of 10.5 cm, and height of 29 cm. Each section is separated by 2.2 cm, which translates to an overall rod height of 310 cm.

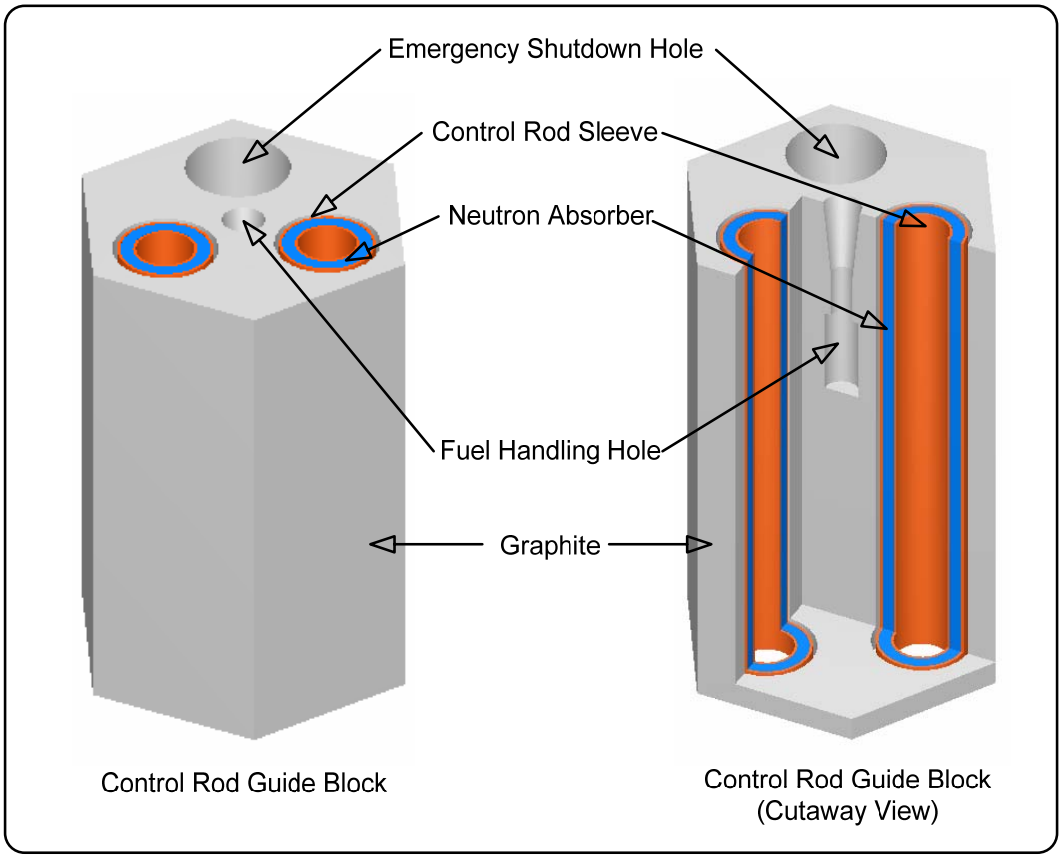

Fig 6. Control Rod Guide Block with Control Rods (KENO 3D)

The annular absorber sections are incased by a sleeve constructed of Alloy 800 H with a thickness of 0.35 cm. Fig. 6 illustrates an example of the control rod guide block with control rods inserted. The figures come directly from the computational model. The properties of the control rod are provided in Table VII.

Table VII. Control Rod Properties

Neutron Absorber Sections (annular)	
Number of neutron absorber sections in each control rod	10
Material	B_4C and C
Density	1.9 g/cc
Diameter-inner	7.5 cm
Diameter-outer	10.5 cm
Height	29.0 cm
Effective height	290 cm (10 neutron absorber sections)
Spacing between neutron absorber sections	2.2 cm
Control Rod Sleeve	
Material	Alloy 800H
Thickness	0.35 cm
Control Rod	
Number of control rods	32 (16 pairs)
Number of control rods in active core	14 (7 pairs)
Number of control rods in replaceable reflector region	18 (9 pairs)
Diameter-inner	6.5 cm
Diameter-outer	11.3 cm
Height	310 cm

III.A.2.4 IRRADIATION BLOCK

The irradiation block is identical to the control rod guide block, but the holes in the irradiation block are only used for nuclear instrumentation. There are 27 irradiation blocks that makeup three irradiation columns (9 blocks vertically stacked per column). In the case of the model, the holes in the blocks were left empty.

III.A.2.5 BUILDING THE MODEL

The four types of prismatic hexagonal blocks just described are stacked vertically to make a column. The columns are classified by the type of block, making four types of columns: 1) fuel assembly block column, 2) control rod block column, 3) replaceable reflector block column, and 4) irradiation block column.

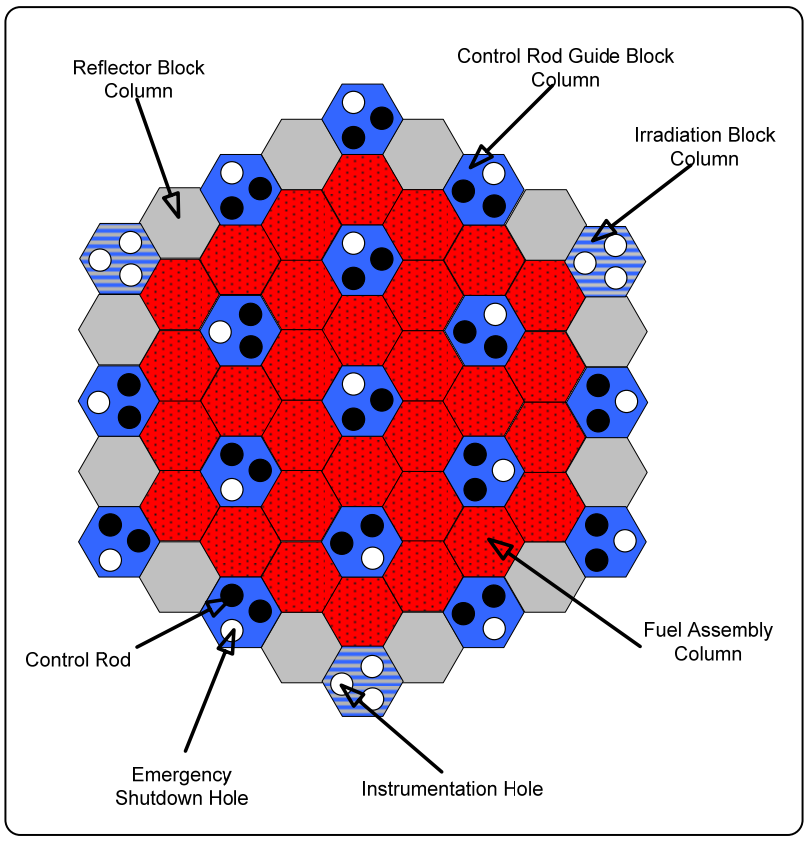

Fig. 7. Hexagonal Array of Prismatic Columns

Each column consists of nine blocks, resulting in a height of 522 cm. The columns are then arranged side-to-side in a hexagonal array to construct the model. A horizontal cross-section of the model showing the arrangement of the columns is provided in Fig. 7.

The core components (array of prismatic hexagonal columns) are horizontally surrounded by a permanent reflector having a diameter of 430 cm. The structures outside of the permanent reflector region were neglected in the calculation models. KENO 3D was used to provide an actual cross-sectional view of the model, as shown in Fig. 8.

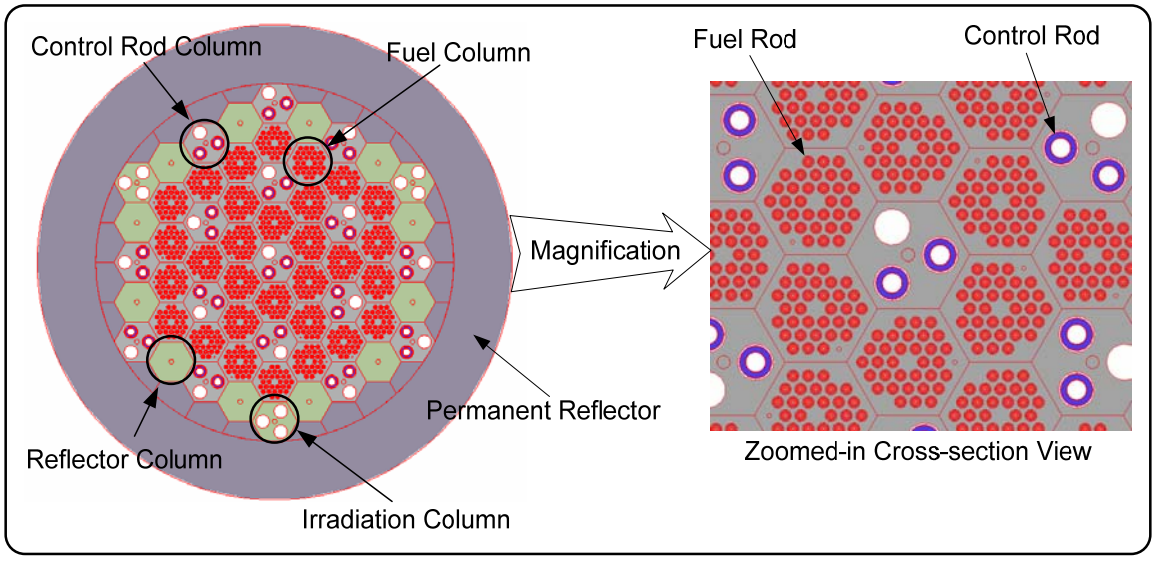

Fig. 8. Horizontal Cross-Section of VHTR Model (KENO 3D)

The complete VHTR model has an overall height of 522 cm and a diameter of 430 cm. The fueled region or active core is 290 cm in height and 230 cm in effective

diameter. Fig. 9 is a 3D cutaway view of the VHTR model, which shows the active core. In this particular figure the control rods are fully inserted in the core.

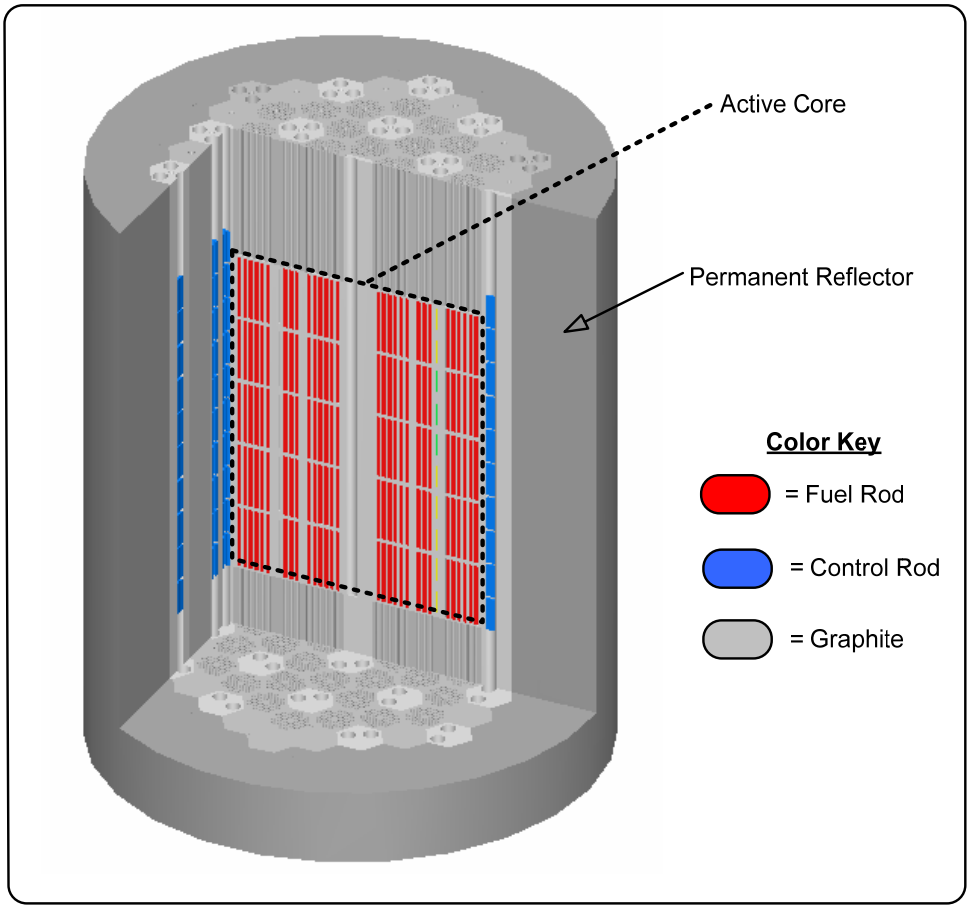

Fig.9. Three-Dimensional Cutaway View of VHTR Model (KENO 3D)

III.A.2.6 HOMOGENIZED FUEL REGION

The computational model is a very detailed model of the HTTR in which practically all components are modeled explicitly, with the exception of the fuel compacts. The fuel compact consists of TRISO coated fuel particles imbedded within a graphite matrix in the form of an annular rod (fuel compact properties listed in Table III). Each compact contains about 182,000 coated fuel particles, which consist of a spherical fuel kernel of low enriched UO_2 with TRISO coating. The coating is made up of a low-density, porous pyrolytic carbon (PyC) buffer layer adjacent to the fuel kernel, followed by high density isotropic PyC layer, a silicon carbide barrier layer and a final outer PyC layer. Table VIII lists the properties of the TRISO fuel particles.

Table VIII. TRISO Fuel Particle Properties

	material	density (g/cc)	radius (cm)
Fuel kernel	UO_2	10.41	0.0300
1st coating	PyC	1.14	0.0359
2nd coating	PyC	1.89	0.0390
3rd coating	SiC	3.20	0.0419
4th coating	PyC	1.87	0.0465

The particles have 12 different uranium enrichments, ranging from 3.3 weight percent to 9.8 weight percent, provided in Table IX.

Table IX. Uranium Enrichments

number	1	2	3	4	5	6	7	8	9	10	11	12
wt. %	3.301	3.864	4.290	4.794	5.162	5.914	6.254	6.681	7.189	7.820	9.358	9.810

In the computational model the TRISO fuel particles are homogenized with the graphite matrix of the fuel compacts. An illustration showing an example of the TRISO fuel particle, the fuel compact (with section removed to show imbedded fuel particles), and the homogenized fuel compact is provided in Fig. 10.

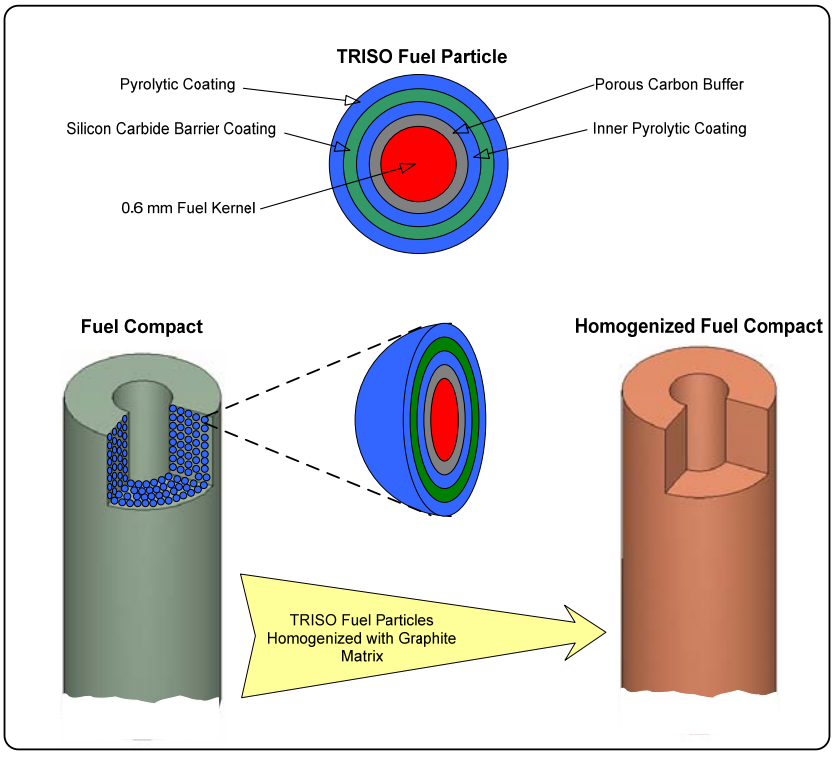

Fig. 10. TRISO Fuel Particle and Homogenized Fuel Compact

The homogenization of the fuel compact was accomplished by creating an array of spheres assembled in a triangular-pitch (dodecahedral) lattice. The SCALE module CSAS6 allows for this arrangement, which closely represents the actual TRISO fuel particles inside a fuel compact. The unit cell of the triangular-pitch lattice contains three regions: 1) UO_2 fuel kernel, 2) homogenized mixture of the coating layers, and 3)

graphite matrix of the fuel compact. A cross-section view through a cell is represented by Fig. 11.

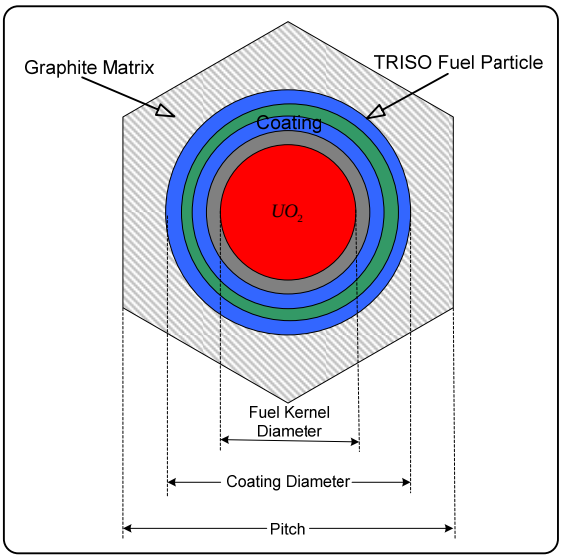

Fig. 11. Arrangement of Materials in Triangular Pitch Unit Cell

Given the number of fuel particles per fuel compact and the geometric makeup of each, the unit cell measurements were determined and are listed in Table X.

Table X. Unit Cell Measurements

Fuel Kernel Diameter	Coating Diameter	Pitch
0.05967 cm	0.0929 cm	0.1162

As part of the unit cell specifications in the computational model, CSAS6 allows the Dancoff correction factor to be manually entered by the user. As stated previously (chapter II.C), the accuracy of the model can be improved by determining the Dancoff factor using the code system DANCOFF-MC. The input values needed to accomplish

this are: lattice type, radius of the environment (number of pitches equal to the radius of the fuel compact), outer fuel radius, outer coating radius, pitch, total macroscopic cross-section of the coating, and total macroscopic cross-section of the graphite matrix. Just as with the unit cell lattice used in homogenizing the fuel region, an array of spheres assembled in a triangular-pitch (dodecahedral) lattice was utilized. The macroscopic cross-sections were determined for the materials at 0.0253 eV or 2200 m/sec. The input values are listed in Table XI.

Table XI. DANCOFF-MC Input Values

Environment	$\Sigma_{coating}$	$\Sigma_{moderator}$	**Fuel Radius**	**Coating Radius**	**Pitch**
10.345	0.37	0.402	0.029 cm	0.46cm	0.116 cm

DANCOFF-MC does not allow for the exact modeling of the annular fuel compact so an equivalent cylinder shaped fuel compact was used instead. Fig. 12 shows the fuel compact used for the Dancoff factor calculation.

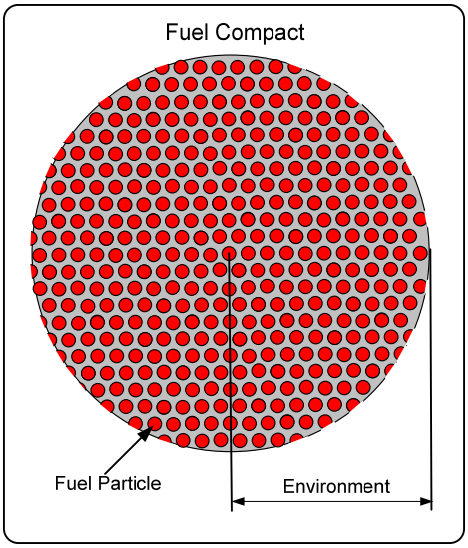

Fig. 12. Fuel Compact Arrangement in DANCOFF-MC

The results produced by running DANCOFF-MC are listed in Table XII.

Table XII. DANCOFF-MC Results

Number of fuel lumps taken into account	Dancoff factor	Standard deviation	Number of cycles executed
5705	0.8493	0.00009	5000000

III.A.2.7 MAP OF VHTR MODEL CORE

Being that the fuel assembly blocks can have a number of different arrangements: 31 or 33 fuel rods, 12 different uranium fuel enrichments (Table IX), and two types of burnable poison rods; a system to identify their position in the core was developed. It separates the fuel columns into four fuel zones and assigns a number to the rows that construct the columns.

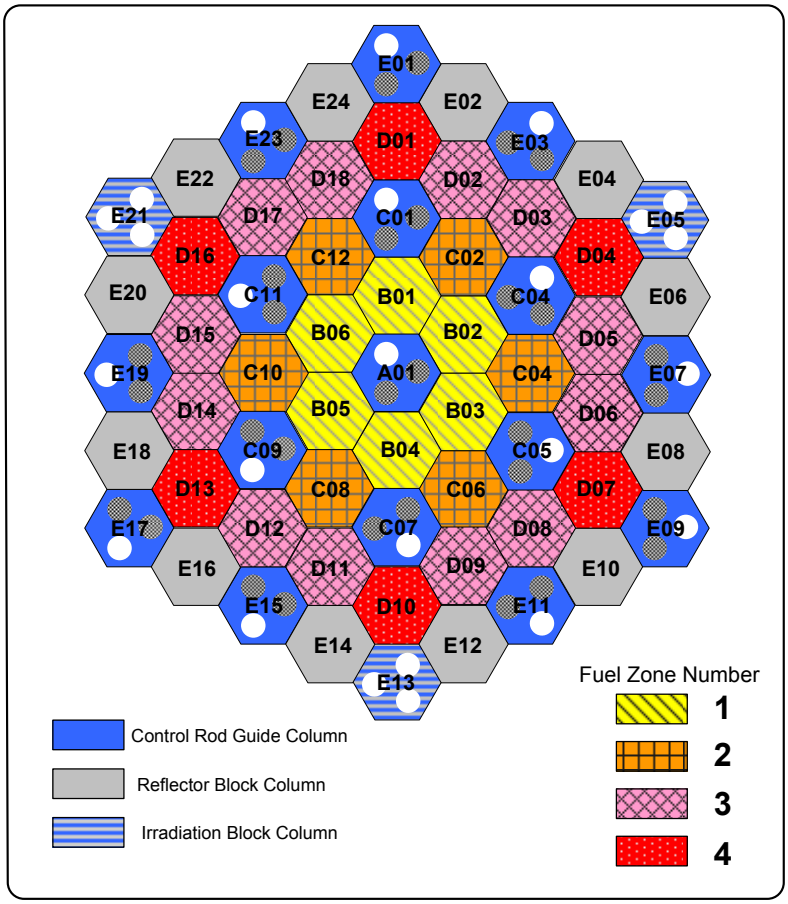

Fig. 13. Map of Core and Fuel Zones

There are five rows (representing the five fuel assembly blocks in the fuel column), the first being the top row and the fifth being the bottom row. In addition, it is

important to know the radial positions in the core. This is accomplished by naming each hexagonal block. A map of the core is provided in Fig. 13 and Table XIII identifies were the fuel assembly blocks are placed.

Table XIII. Core Arrangement

Layer number from top fuel block	Items	Fuel zone number			
		1	2	3	4
1	Uranium enrichment (wt. %) Number of fuel rods in graphite block Type of burnable poisons	6.681 33 H-I	7.820 33 H-I	9.358 31 H-I	9.810 31 H-I
2	Uranium enrichment (wt. %) Number of fuel rods in graphite block Type of burnable poisons	5.162 33 H-II	6.254 33 H-II	7.189 31 H-II	7.820 31 H-II
3	Uranium enrichment (wt. %) Number of fuel rods in graphite block Type of burnable poisons	4.290 33 H-II	5.162 33 H-II	5.914 31 H-II	6.254 31 H-II
4	Uranium enrichment (wt. %) Number of fuel rods in graphite block Type of burnable poisons	3.301 33 H-I	3.864 33 H-I	4.290 31 H-I	4.794 31 H-I
5	Uranium enrichment (wt. %) Number of fuel rods in graphite block Type of burnable poisons	3.301 33 H-I	3.864 33 H-I	4.290 31 H-I	4.794 31 H-I

III.A.2.8 VHTR MODEL SPECIFICATIONS

The completed computational model has over 8,500 lines of code in the form of a text input file. There are 7,290 geometry regions in the model and its large size and complexity makes computational time a concern. The files were run on a 2005 Dell Precision 670 Elite Workstation with 4GB of RAM and 3.80GHz processor speed. To produce a runtime of 12 hours, a total sample size of 200,000 was used. The total sample size is the product of the number of histories per generation (1,000) and the total number of generations run (200).

III.B VHTR PEBBLE BED CORE

The following sections detail the VHTR pebble bed core 3D computational model. For verification and validation purposes, the model is implemented from China's operating 10MW High Temperature Gas cooled reactor test Module (HTR-10). The first section (III.B.1) provides general information related to the HTR-10. The next section (III.B.2) describes in detail the pebble-bed reactor computational model and explains how it functions.

III.B.1 HTR-10

The HTR-10 is a graphite moderated helium gas cooled pebble bed reactor. The design represents the features of the modular HTGR. The objective of the HTR-10 program is to verify and demonstrate the technical and safety features of the modular HTGR and to establish an experimental base for developing nuclear process heat applications [8]. Table XIV presents the main design parameters of the HTR-10.

Table XIV. HTR-10 Design Parameters

Reactor thermal power	10 MW
Primary helium pressure	3.0 MPa
Active core volume	5 m^3
Reactor core diameter	180 cm
Average core height	197 cm
Average helium temperature at reactor outlet	700 °C
Average helium temperature at reactor inlet	250 °C
Helium mass flow rate at full power	4.3 kg/s
Main steam pressure at steam generator outlet	4.0 MPa
Main steam temperature at steam generator	440 °C
Feed water temperature	104 °C
Fuel-to-graphite ball ratio	0.57/0.43
Number of control rods in side reflector	10
Number of absorber ball units in side reflector	7
Nuclear fuel	UO_2
Heavy metal loading per fuel element	5 g
Enrichment of fresh fuel element	17%
Number of fuel elements in equilibrium core	27,000
Fuel loading mode	multi-pass

The HTR-10 was selected because of the reference material available. The reference material provided: general design features, reactor layout, core configuration, material properties, and other relevant information to develop the computational model. Also supplied were actual experimental test results to be utilized for experiment-to-code benchmarks and several analytical code results for code-to-code benchmark tests [8].

III.B.2 VHTR PEBBLE BED CORE MODEL

The pebble bed core consists of a fuel region (active core) that has a diameter of 180 cm and a height of 197 cm. The fuel region is surrounded by graphite reflectors, which consist of top, bottom, and side reflectors. A vertical cross-sectional view of the modeled structure is shown in Fig. 14.

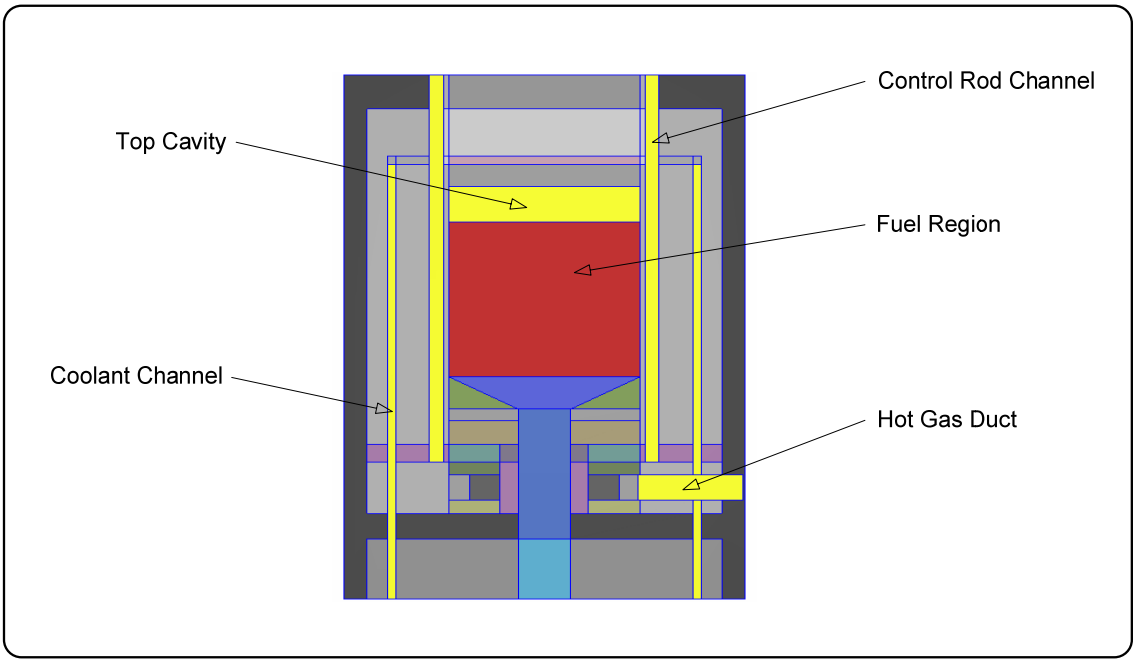

Fig. 14. Vertical Cross-Sectional View of the VHTR Model (KENO 3D)

The side reflector contains an inner and outer ring of borings. The inner ring consists of twenty borings of which thirteen have a diameter of 13cm (ten control rod channels and three irradiation channels). The remaining seven are absorber ball channels, which have a rectangular cross section in the middle (10cm by 6cm) and semicircles at the ends (diameter of 6cm). The outer ring consists of twenty borings for the helium inlet flow channels (boring diameter of 8cm). These channels are shown in the horizontal cross-sectional view of the model in Fig. 15.

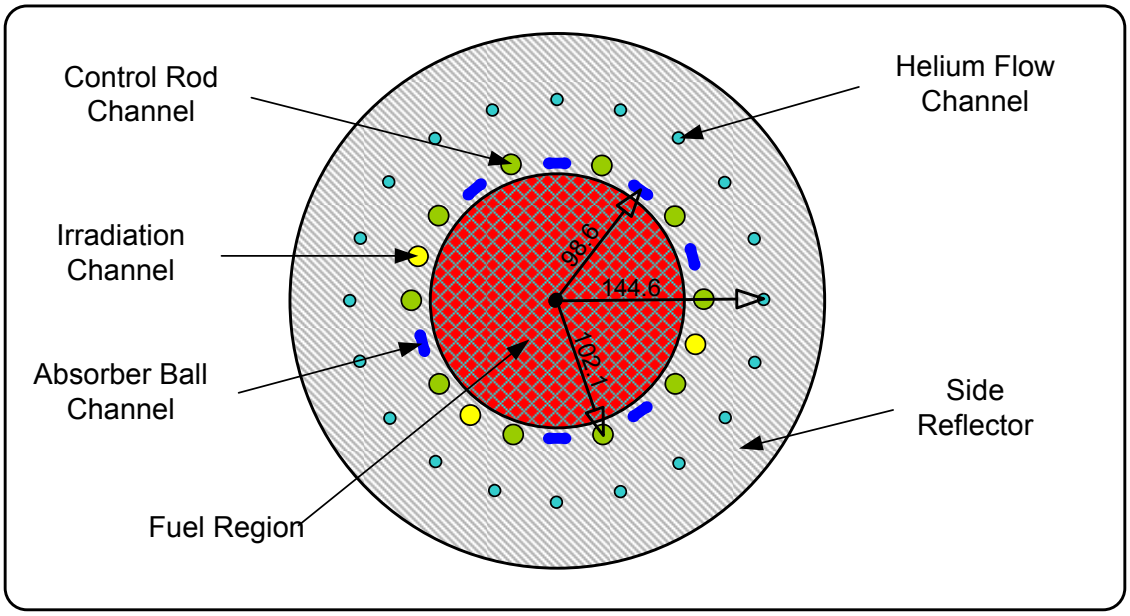

Fig. 15. Horizontal Cross-Section (KENO 3D)

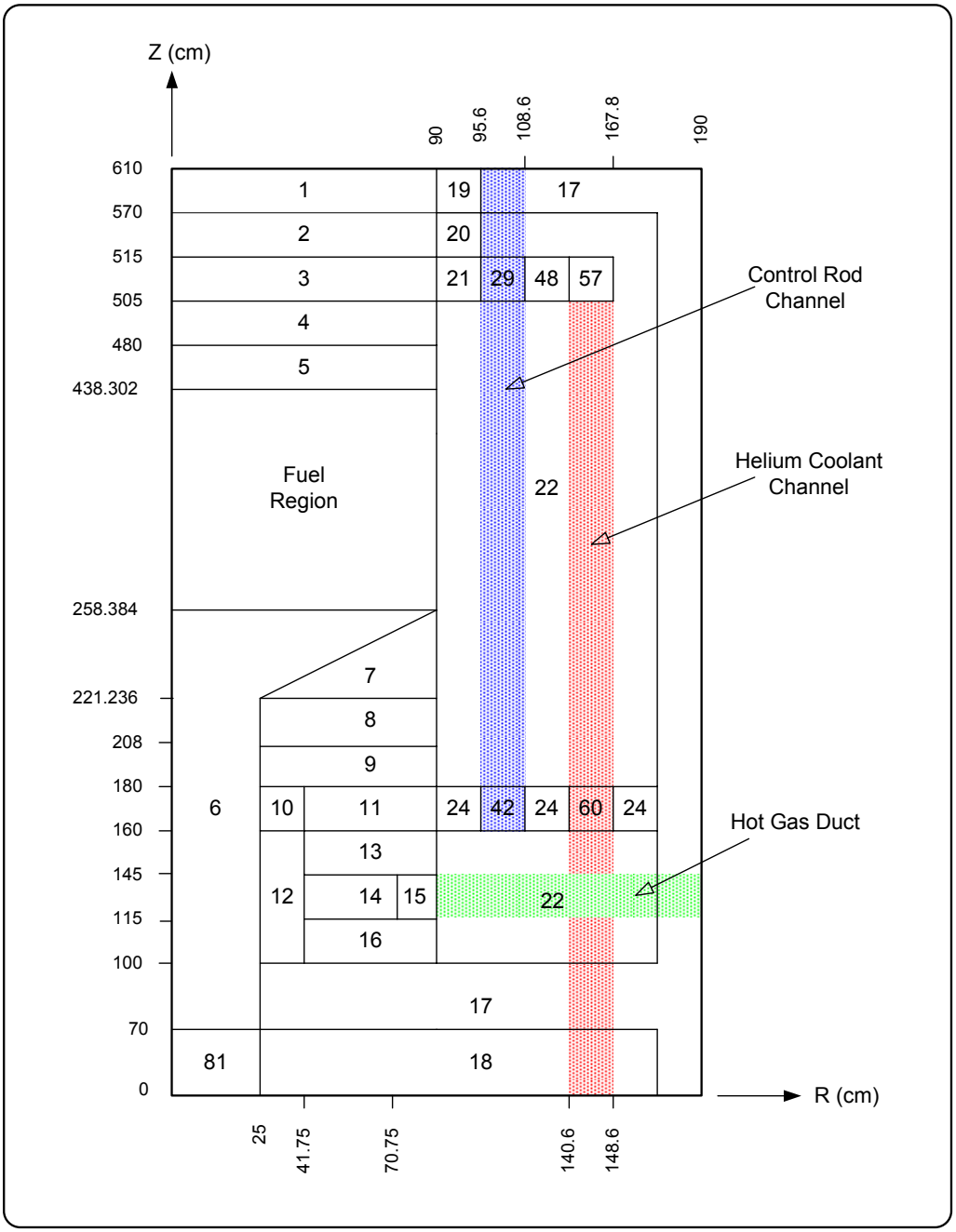

Fig. 16. Vertical Cross-Section with Zone Identification Numbers

The model is divided into zones according to material properties. Figure 16 provides the two-dimensional vertical cross-section of the model with zone identification numbers, while Table XV gives the material description and atom densities of these specific zones.

Table XV. Homogenized Atom Density of Nuclide in Reflector Zones ($1/cm \cdot barn$)

Zone number	Carbon	Natural boron	Remarks
1	7.29410E-02	3.29811E-03	Boronated carbon bricks
2	8.51462E-02	4.57148E-07	Top graphite reflector
3	1.45350E-02	7.80384E-08	Cold helium chamber
4	8.02916E-02	4.31084E-07	Top reflector
5			Top core cavity
6	5.38275E-02	2.88999E-07	Dummy balls, simplified as graphite of lower density
7	8.51047E-02	4.56926E-07	Bottom reflector with hot helium borings
8	7.81408E-02	4.19537E-07	Bottom reflector structures
9	8.23751E-02	4.42271E-07	Bottom reflector structures
10	8.43647E-02	2.98504E-04	Bottom reflector structures
11	8.17101E-02	1.56416E-04	Bottom reflector structures
12	8.50790E-02	2.09092E-04	Bottom reflector structures
13	8.19167E-02	3.58529E-05	Bottom reflector structures
14	5.41118E-02	5.77456E-05	Bottom reflector structures
15	3.32110E-02	1.78309E-07	Bottom reflector structures
16	8.81811E-02	3.58866E-05	Bottom reflector structures
17	7.65984E-02	3.46349E-03	Boronated carbon bricks
18	7.97184E-02	0.00000E+00	Carbon bricks
19	7.61157E-02	3.44166E-01	Boronated carbon bricks
20	8.78374E-02	4.71597E-07	Graphite reflector structure
21	5.79696E-02	3.11238E-07	Graphite reflector structure
22	8.82418E-02	4.73769E-07	Graphite reflector structure
24	8.79541E-02	1.68369E-04	Graphite reflector structure
29	5.24843E-02	1.81969E-07	Graphite reflector structure
42	8.79637E-02	1.62903E-04	Graphite reflector structure
48	5.82699E-02	3.12850E-07	Graphite reflector structure
57	7.28262E-02	3.91003E-07	Graphite reflector structure
60	8.79538E-02	1.68369E-04	Graphite reflector, cold helium flow region
81	7.97184E-02	0.00000E+00	Dummy balls, but artificially taken as carbon bricks

III.B.3 FUEL REGION

The fuel region or active core contains about 27,000 spherical fuel elements, which form a pebble bed that is 180cm in diameter, 197cm in average height, and has volume of about 5m³. A spherical fuel element has a diameter of 6cm and consists of TRISO coated fuel particles embedded in graphite matrix. The coated fuel particle consists of a UO_2 kernel with diameter of 0.5mm, which is coated with a buffer layer of low density pyrolytical carbon (PyC), an inner layer of high density PyC, a layer of silicon carbide (SiC), and outer high density PyC layer. Each fuel element has about 8,300 coated fuel particles and contains 5g uranium with ^{235}U enrichment of 17%. Table XVI and Figure 17 show the characteristics and schematic of the fuel element.

Table XVI. Fuel Element Characteristics

Diameter of ball	6.0 cm
Diameter of fuel zone	5.0 cm
Density of graphite in matrix and outer shell	1.73 g/cm³
Heavy metal (uranium) loading (weight) per ball	5.0 g
Enrichment of U-235 (weight)	17%
Equivalent natural boron content of impurities in uranium	4 ppm
Equivalent natural boron content of impurities in graphite	1.3 ppm
Volumetric filling fraction of balls in the core	0.61
Fuel kernel	
Radius of the kernel	0.025 cm
UO_2 density	10.4 g/cm³
Coatings	
Coating layer materials (starting from kernel)	PyC / PyC / SiC / PyC
Coating layer thickness (mm)	0.09 / 0.04 / 0.035 / 0.04
Coating layer density (g/cm³)	1.1 / 1.9 / 3.18 / 1.9
Dummy (no fuel) elements	
Diameter of ball	6.0 cm
Density of graphite	1.73 g/cm³
Equivalent natural boron content of impurities in graphite	1.3 ppm

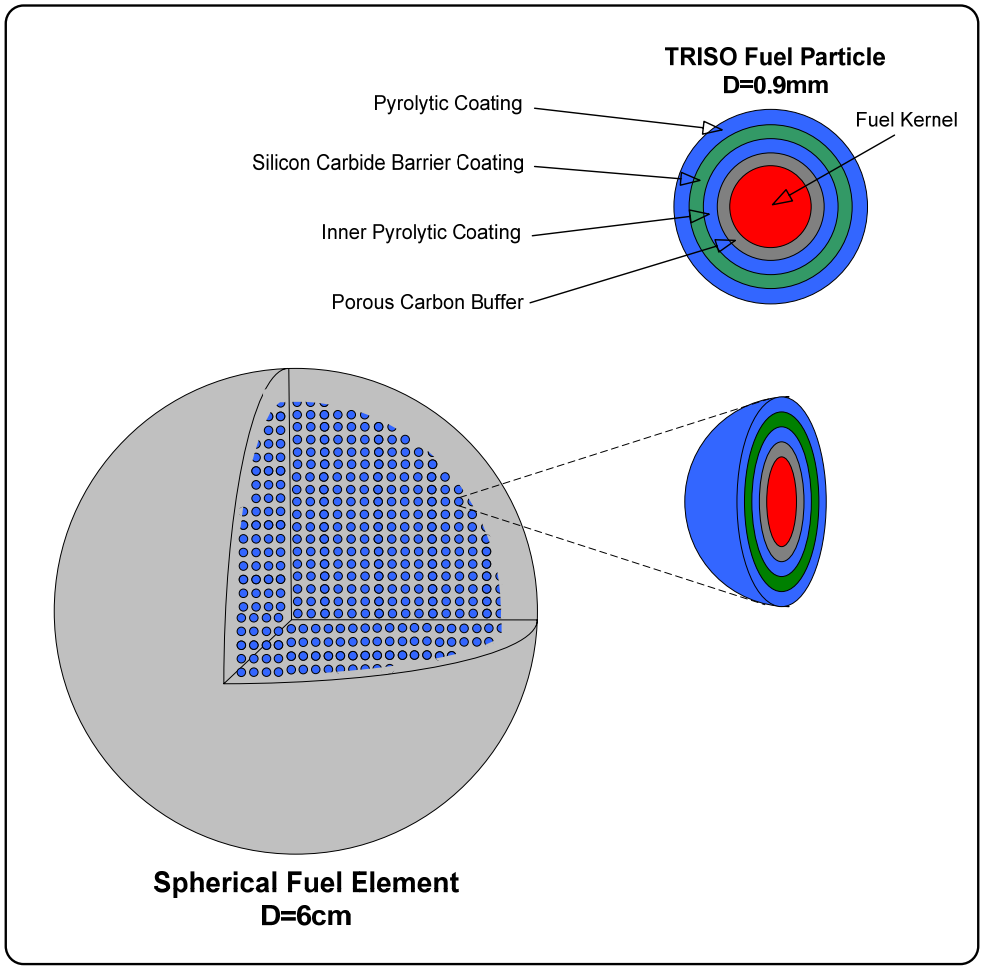

Fig. 17. Fuel Element Schematic

The fuel region of the model was regarded in two different ways. One was to homogenize the entire fuel region and the other was to homogenize only the fuel pebbles. This approach resulted in two models that will be identified as: the homogenized model and the homogenized fuel pebble model. Other than the fuel region, the models are exactly the same.

III.B.3.1 HOMOGENIZED MODEL

The homogenized model simplifies the fuel region by smearing the fuel pebbles with the graphite matrix, moderator pebbles, and void space; creating one homogeneous region. To accomplish this, the SCALE module CSAS6 was utilized to create a triangular-pitch (dodecahedral) lattice. The unit cell of the triangular-pitch lattice contains three regions: 1) UO_2 fuel kernel, 2) homogenized mixture of the coating layers, and 3) mixture consisting of the graphite matrix of the fuel pebble, moderator pebbles, and void space created between fuel and moderator pebbles. A cross-section view through a cell is represented in Fig. 18.

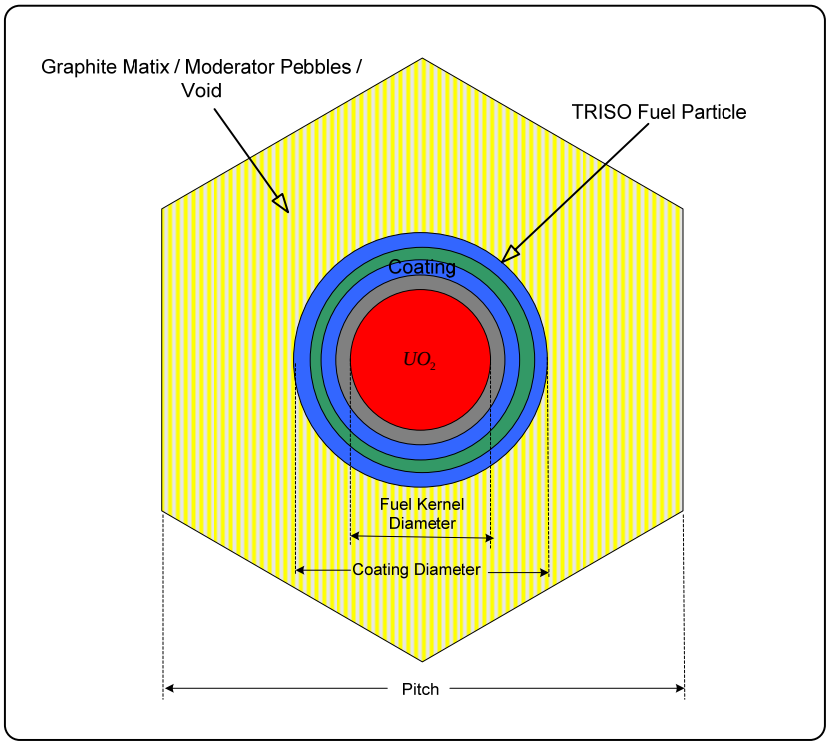

Fig. 18. Triangular-Pitch Unit Cell (homogenized model)

Given the number of fuel elements and particles per fuel element, the number of dummy balls, and the geometric makeup of the fuel region, the unit cell measurements were determined and are listed in Table XVII.

Table XVII. Unit Cell Measurements (homogenized model)

Fuel Kernel Diameter	Fuel Coating Diameter	Pitch
0.050 cm	0.091 cm	0.3562 cm

III.B.3.1.a HOMOGENIZED MODEL SPECIFICATIONS

The completed computational model has over 290 lines of code. There are 113 geometry regions in the model. The files were run on a 2005 Dell Precision 670 Elite Workstation with 4GB of RAM and 3.80GHz processor speed. A total sample size of 200,000 was used, which resulted in a runtime of about 4 hours. The total sample size is the product of the number of histories per generation (1,000) and the total number of generations run (200).

III.B.3.2 HOMOGENIZED FUEL PEBBLE MODEL

The homogenized fuel pebble model is a more accurate and detailed representation of the pebble-bed core. Instead of homogenizing the entire fuel region, only the TRISO fuel particles are homogenized with the graphite matrix of the fuel pebbles. An illustration showing an example of the TRISO fuel particle, the fuel pebble (with section removed to show imbedded fuel particles), and the homogenized fuel pebble is provided in Fig. 19.

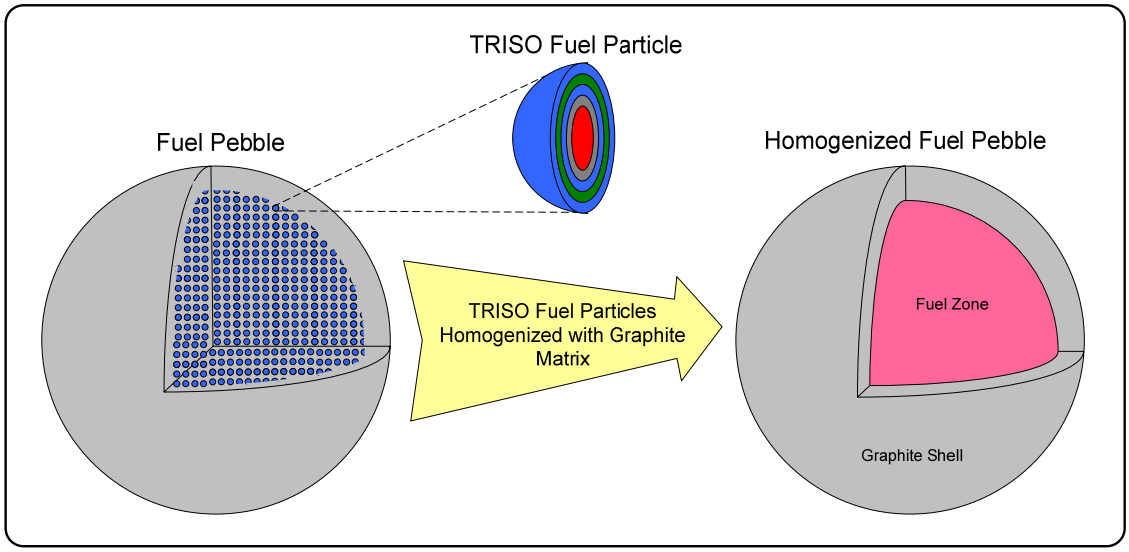

Fig. 19. TRISO Fuel Particle and Homogenized Fuel Pebble

The homogenization of the fuel pebble was accomplished by creating an array of spheres assembled in a triangular-pitch (dodecahedral) lattice. The SCALE module CSAS6 allows for this arrangement, which closely represents the actual TRISO fuel particles inside a fuel pebble. The unit cell of the triangular-pitch lattice contains three regions: 1) UO_2 fuel kernel, 2) homogenized mixture of the coating layers, and 3) graphite matrix of the fuel pebble. A cross-section view through a cell is represented by Fig. 20.

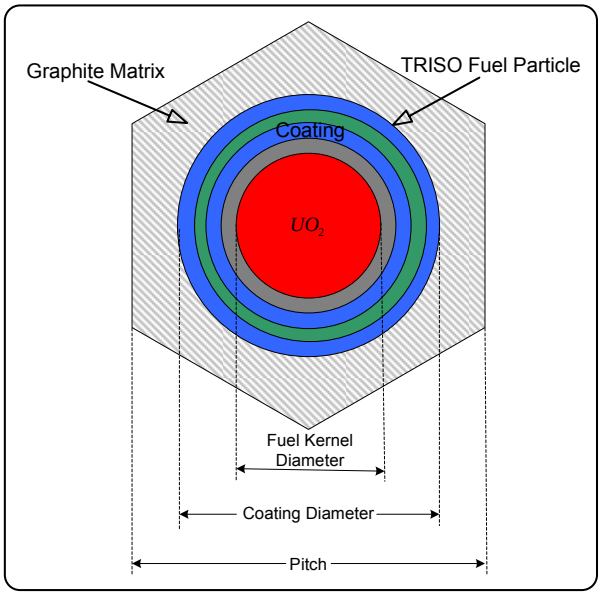

Fig. 20. Triangular Pitch Unit Cell (homogenized fuel pebble model)

The measured values for the unit cell are listed in Table XVIII.

Table XVIII. Unit Cell Measurements (homogenized fuel pebble model)

Fuel Kernel Diameter	Fuel Coating Diameter	Pitch
0.050 cm	0.091 cm	0.2085 cm

A random packing of pebbles cannot be modeled by SCALE, therefore the fuel region was approximated using a body-centered cubic (BCC) lattice. The BCC unit cell contains a center fuel pebble and sectioned moderator pebble in the corners. The diameter of the moderator pebble can be reduced or increased to produce the desired fuel-to-moderator pebble ratio. The BCC lattice was chosen because the two pebble content of the unit cell minimizes the size adjustment for the moderator pebble. The size of the unit cell is determined by the volumetric packing fraction (specified as 0.61). Table XIX summarizes the geometry specifications on the pebble-bed core model, and Fig. 21 shows the BCC unit cell and lattice. To fully load the fuel region of the pebble-bed core the BCC unit cell was extended to a 27 by 27 by 21 lattice.

Table XIX. Pebble-Bed Geometry Specifications

Parameter	Value
Fuel-to-moderator pebble ratio	57:30
Fuel pebble radius	3.0 cm
Fueled region radius	2.5 cm
Packing fraction	0.61
Moderator Pebble Radius	2.731 cm
BCC unit cell size	6.8873 cm

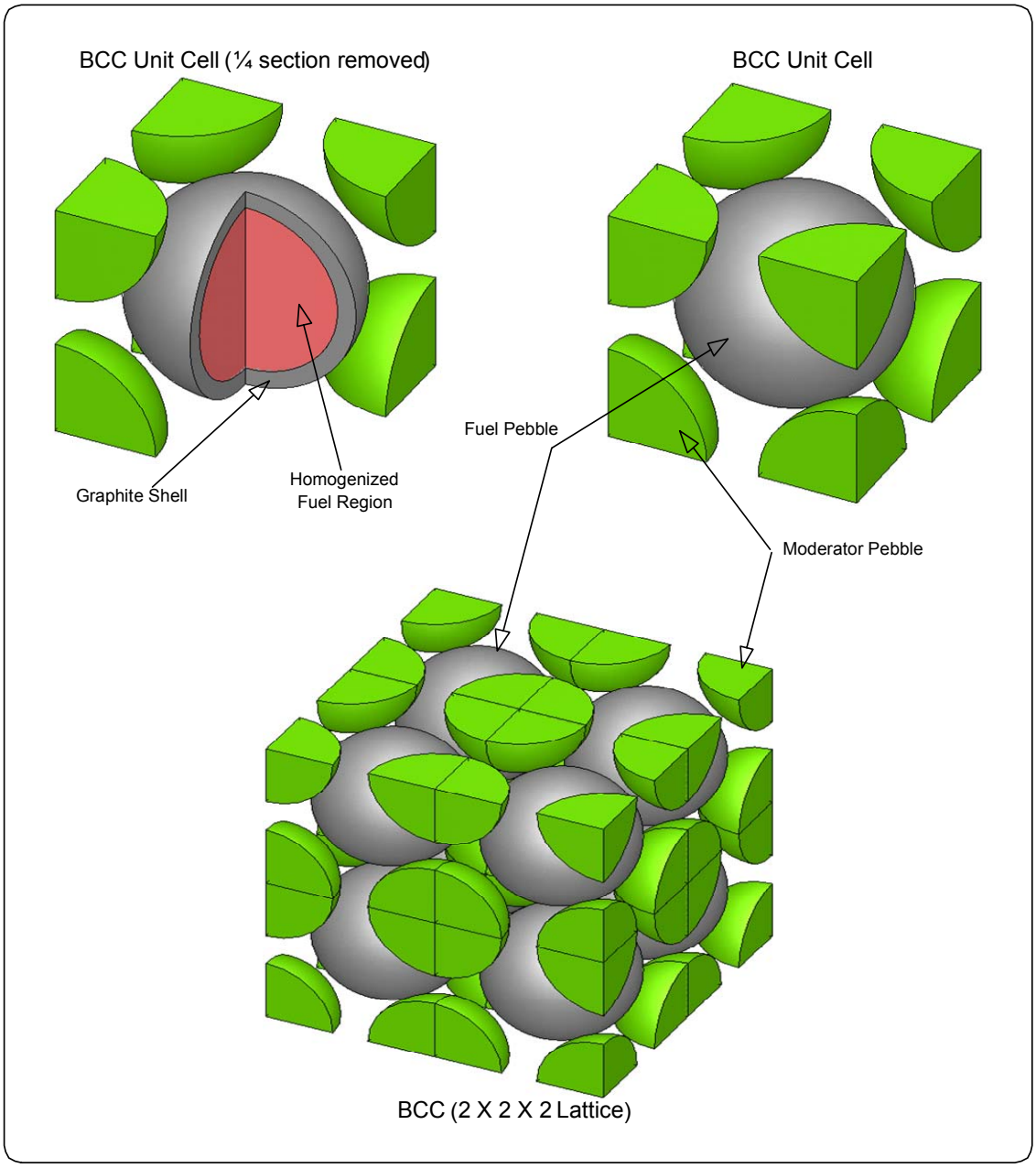

Fig. 21. BCC Unit Cell Schematic (KENO 3D)

III.B.3.2.a HOMOGENIZED FUEL PEBBLE MODEL SPECIFICATIONS

The completed computational model has over 340 lines of code in the form of a text input file. There are 124 geometry regions in the model. The files were run on a 2005 Dell Precision 670 Elite Workstation with 4GB of RAM and 3.80GHz processor speed. A total sample size of 200,000 was used, which resulted in a runtime of about 4 hours. The total sample size is the product of the number of histories per generation (1,000) and the total number of generations run (200).

CHAPTER IV

VALIDATION OF THE VHTR PRISMATIC CORE MODEL (MODEL-TO-EXPERIMENT BENCHMARK ANALYSIS)

The benchmark problems are related to start-up core physics tests and include the analysis of the effective multiplication factor of fully loaded core with control rods fully withdrawn and fully inserted, control rod position at criticality, and isothermal temperature coefficient of reactivity.

All calculations were performed for a core temperature of 300K unless otherwise specified. A Dancoff correction factor of 0.8493, as calculated by DANCOFF-MC, was used for all benchmark tests. A total sample size of 200,000 was used in all cases. The total sample size is the product of the number of histories per generation (1,000) and the total number of generations run (200). General descriptions of the benchmark tests are provided below.

IV.A SUITE OF BENCHMARK PROBLEMS

The effective multiplication factor $\left(k_{eff}\right)$ was evaluated with the control rods fully withdrawn and inserted. When the control rods are fully withdrawn, their upper limit is the upper face of the top reflector block of the core (116 cm above the active core) with the exception of the six pair of control rods located on the perimeter of the core. The control rods of these six columns have an upper limit of 72.5 cm, which translates to 43.5 cm above the active core. When the control rods are fully inserted, the lower ends of all the control rods are on the same plane with the bottom face of the active core.

The control rod insertion depths were evaluated at the critical condition for the fully loaded core. All control rod insertion levels are adjusted on the same level except three pairs of control rods that are located at columns E03, E09, and E17 of the most outer region in the side reflectors, as shown in Fig. 13 of Chapter III.A.2.7. These three pairs of control rods are fully withdrawn for the calculation. When fully withdrawn, the upper limit is the upper face of the first replaceable reflector block (116 cm above the active core). The control rod critical positions are measured from the bottom of the active core. Control rod insertion depths were calculated for core temperatures of 300K, 418K and 480K.

Isothermal temperature coefficients for the fully-loaded core were evaluated using the effective multiplication factors according to the following relationship:

$$\rho_n = \frac{k_{n+1} - k_n}{k_{n+1} \cdot k_n} \cdot \frac{1}{T_{n+1} - T_n}, \qquad (1)$$

where:

ρ_n: Temperature coefficient between T_n and T_{n+1} $\left(\Delta k/k/K\right)$

T_n: Core temperature at n^{th} measurement $\left(K\right)$

T_{n+1}: Core temperature at $n+1^{th}$ measurement $\left(K\right)$

k_n: Effective multiplication factor at T_n

k_{n+1}: Effective multiplication factor at T_{n+1}.

The critical control rod positions are changed with temperature elevation in the real reactor operation. However, the control rod position is not changed in the calculation to obtain the reactivity difference.

IV.B SUMMARY OF BENCHMARK RESULTS

Following the established international benchmark program practices, in the present analysis 10% discrepancy between computed values and the available experimental values was considered as the model acceptability threshold. In addition to experiment-to-code benchmark studies, code-to-code benchmark analysis was also performed to provide further understanding of the modeled system performance. The results of the analysis showing comparison to experimental data are summarized in Table XX. Experimental data for prismatic core configurations are available from the HTTR program [8].

Table XX. Experiment-to-Code Benchmark Analysis

Benchmark		VHTR model (calculated)	HTTR (experimental)	Error (%)
Control Rods Fully Withdrawn	k_{eff}	1.1255 ± 0.0018	1.1363 ± 0.041	-0.95
Control Rods Fully Inserted	k_{eff}	0.7254 ± 0.0018	0.685 ± 0.010	+5.90
Critical Insertion Depth of Control Rods (core temperature 300K)	cm	181.6	177.5 ± 0.5	+2.31
Critical Insertion Depth of Control Rods (core temperature 418K)	cm	195.7	190.3 ± 0.5	+2.84
Temperature Coefficient α_T	Δ k/k/K	(-1.61 ± 0.25) E-4	-1.42E-4	+13.38

The experiment-to-code benchmark analysis resulted in successful validation of the VHTR prismatic core model. Obtained computational results are in agreement with the available experimental data.

The case for control rods fully withdrawn resulted in a discrepancy of about 1%. The observed larger deviation of computational results from experimental values occurred when the control rods were fully inserted, resulting in a 6% discrepancy. This is

due to ambiguity of available information regarding the control rods and core configuration. The benchmark case for the critical insertion depth of control rods, which translated to the control rods being inserted roughly halfway into the core, predictably reduced the discrepancy by about half.

The computed value of the isothermal temperature coefficient (α_T) deviates by 13% from the corresponding experimental value. However, the experimental value is within the standard deviation limits of the computational result. It is expected that increasing the sample size of the model would result in reducing the discrepancy to within the 10% range. However, for the benchmark calculations a computational run time of 12 hours or less was targeted and higher accuracy results were not obtained in the present analysis.

IV.C PROTOTYPE VHTR CONFIGURATION

The HTTR configuration with fully withdrawn control rods was chosen as a prototype VHTR configuration. The best agreement with experimental data was observed for that case. Table XXI summarizes basic reactor physics characteristics obtained for the prototype VHTR configuration.

Table XXI. Basic Reactor Physics of the HTTR with Fully Withdrawn Control Rods

k_{eff}	Fission-Inducing Energy (eV)	System Mean Free Path (cm)	Fission Neutron Yield
1.1255 ± 0.0018	0.0846757 ± 0.0002343	2.72263 ± 0.00084	2.43846 ± 0.00001

It is proposed that through configuration adjustments, spectrum shifting can be achieved, with the end result of improving fissile properties of minor actinides. With that

concept in mind, an analysis of the energy-dependent neutron flux in the core was performed for the prototype VHTR configuration.

The average energy dependent neutron flux obtained for the fuel compacts located in the central region of the core is provided in Figure 22. The flux profile matched expectations for the VHTR system with exception of the high energy range of the profile. At energies of about 1.0E+6 eV a peak was expected, but instead there was a noticeable dip followed by a lower peak.

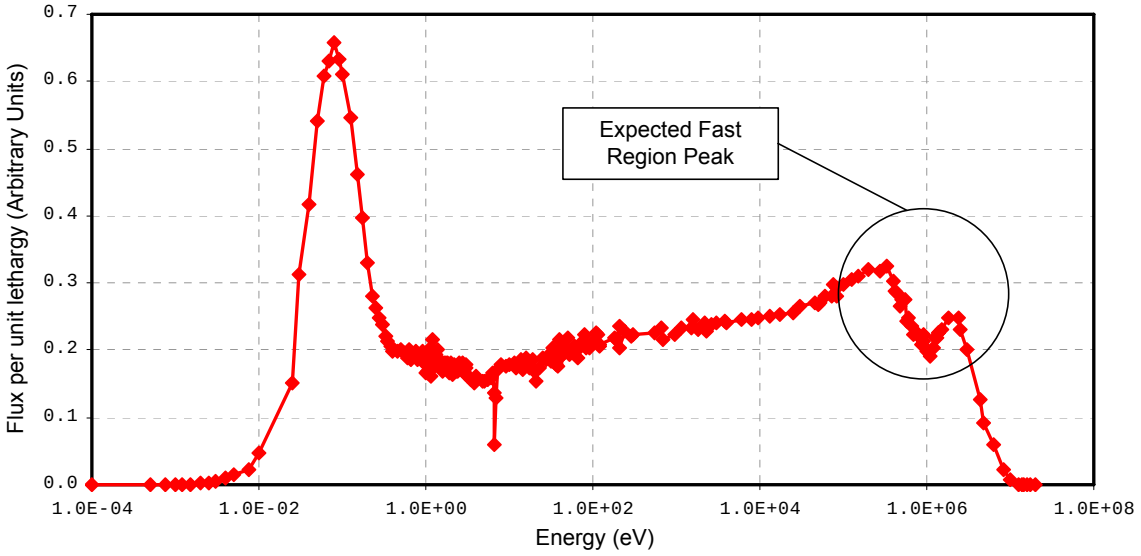

Fig. 22. Energy-Dependent Neutron Flux in the Central Fuel Compacts

This phenomenon can be explained by the streaming of fast neutrons through the void spaces in the core. To illustrate this, the computational model was modified and the void spaces (coolant channels and prismatic block handling holes), which under normal conditions are filled with helium, were replaced by reactor grade graphite. Fig. 23 shows the observed effects. Comparison of the modified configuration to the case with

explicitly-modeled void spaces gives an illustration of fast neutron streaming through the VHTR core.

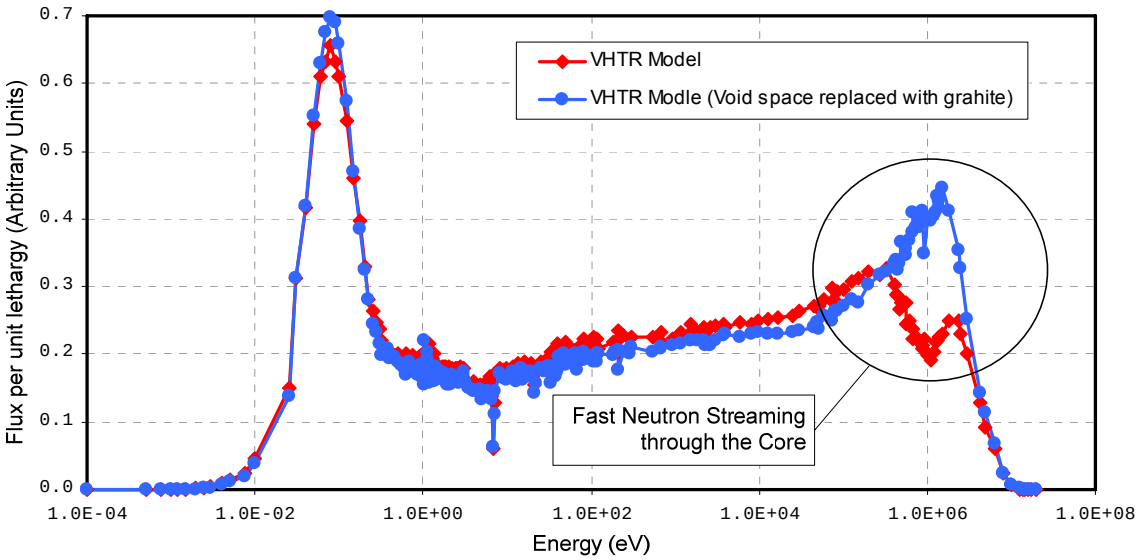

Fig. 23. Energy-Dependent Neutron Flux in the Fuel Compacts: Neutron Streaming Effects

The VHTR model contains 12 fuel enrichments in the core. Differences in the neutron fluxes are expected in each case. An example is given in Fig. 24, where the averaged neutron fluxes obtained for the fuel compacts containing the lower (3.3%) and higher (9.8%) enrichments are given. Also noted is the placement of the compacts in the core. The 3.3% enrichment is located in the central-lower region of the core, and the 9.8% enrichment being in the upper-outer region of the core. For exact location refer to Table XIII and Fig. 13 of Chapter III.

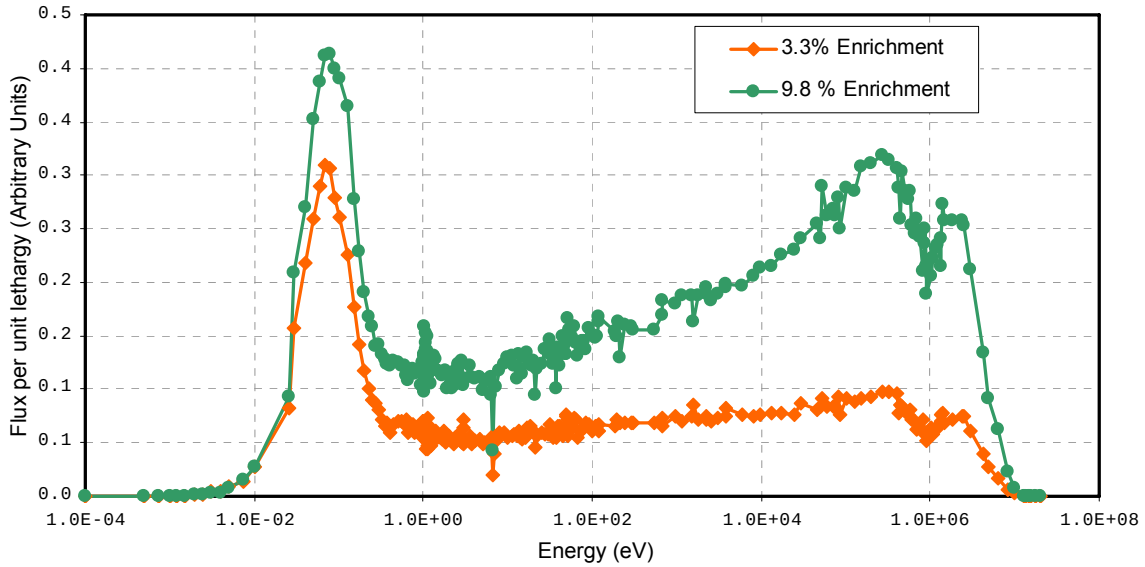

Fig. 24. Energy-Dependent Neutron Flux in the Fuel Compacts: Different Fuel Enrichments

CHAPTER V

SENSITIVITY OF THE VHTR CORE PERFORMANCE TO THE NEUTRON-KERNEL INTERACTIONS

As defined above, the Dancoff correction factor is an important parameter that characterizes a probability for neutrons to interact with fuel kernels. To provide an understanding of how this parameter affects the core performance, a sensitivity analysis with respect to the Dancoff correction factor was conducted. This entails performing multiple criticality calculations for a range of Dancoff factors.

The sensitivity analysis was performed for the critical HTTR core, which was experimentally determined to have control rod insertion depths of 177.5 cm. The computational model was altered to match this case. A total of nine Dancoff factors ranging from 0.20 (typical pebble-bed core range) to 0.95 (upper range for prismatic cores) were evaluated at two temperatures, 300K and 700K. The results are summarized in Table XXII. The Dancoff factor for the HTTR is expected to be in the 0.7 to 0.9 range. Detailed comparisons for the HTR-10 pebble-bed core and other VHTRs can be performed in a similar manner.

Table XXII. Dancoff Factor and Corresponding k_{eff} Values

Temp=300K	
Dancoff factor	k_{eff}
0.2	0.9507
0.3	0.9559
0.4	0.9656
0.5	0.971
0.6	0.9731
0.7	0.9811
0.8	0.9951
0.9	1.0103
0.95	1.022

Temp=700K	
Dancoff factor	k_{eff}
0.2	0.8858
0.3	0.8885
0.4	0.896
0.5	0.8971
0.6	0.9096
0.7	0.912
0.8	0.9295
0.9	0.9437
0.95	0.9506

The results are shown in Figs. 25 & 26. As illustrated in Fig. 25 the Dancoff factor, at which the HTTR would be critical, is 0.8536, considering that the model is 100% accurate. It is also easy to observe that the Dancoff factor has a significant effect on the system and must be considered carefully when evaluating core performance. As example, when the Dancoff factor changes from 0.70 to 0.95 it results in a Δk_{eff} of 0.041 and the system jumps from sub-critical to super-critical.

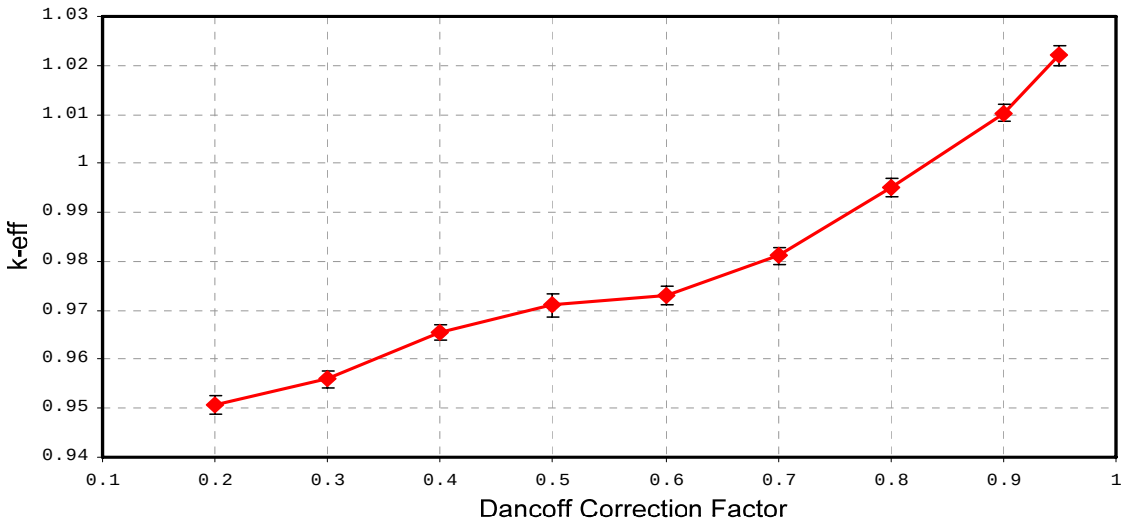

Fig. 25. Sensitivity of k-eff to the Dancoff Correction Factor for 300 K

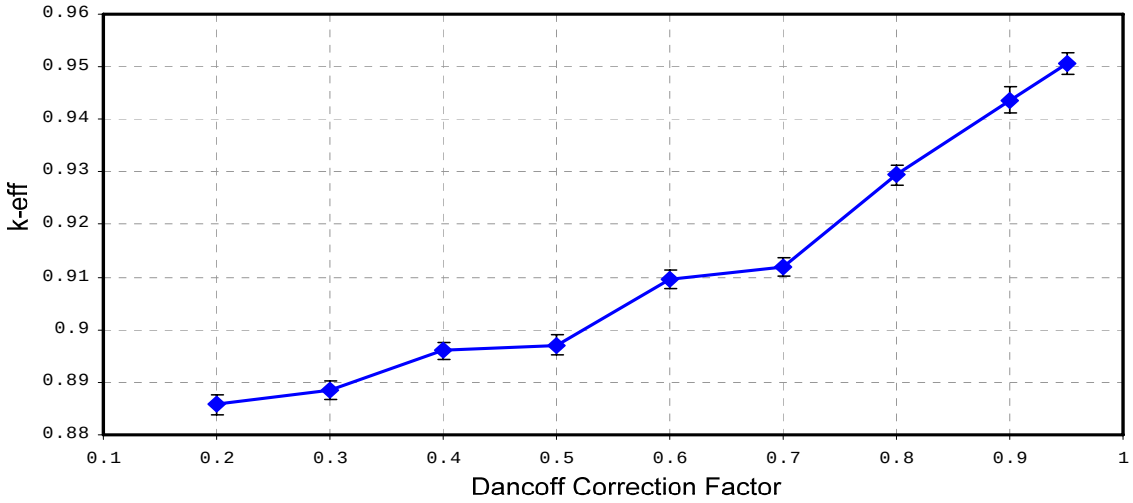

Fig. 26. Sensitivity of k-eff to the Dancoff Correction Factor for 700 K

CHAPTER VI

CONFIGURATION ADJUSTMENT IN SMALL-SCALE VHTRS

The work presented in this chapter is part of the preliminary analysis of configuration adjustments in small-scale VHTR prismatic cores, including annular and cylindrical core designs, and advanced actinide fuel loadings.

The HTTR is currently the only operating VHTR prismatic core design, making it a focal point of VHTR related research. The HTTR was designed according to established objectives, which categorize it as a small-scale VHTR. The core size of the HTTR corresponds to about half of that of the future VHTRs [20]. These future reactors will most likely consist of annular core designs, whereas the HTTR is a cylindrical core design.

An annular core is one of the promising core types for the future VHTRs because of its high inherent safety characteristics following a loss of coolant accident. The decay heat removal is enhanced by introduction of the annular core because the heat transfer path will be shortened due to the relatively thin active core region. As a result, the fuel temperature in a loss of coolant accident can be maintained at less than the fuel temperature limit of 1600 °C [21].

The prismatic whole-core 3D model was adjusted from the original cylindrical core of the HTTR to that of an annular core. The process included changing the fuel in the core from a mixture of uranium enrichments (12 types) to just one enrichment throughout the entire core (8 wt%). To create the annular core the model was

reconfigured by replacing the fuel assembly block columns located in the inner region of the core with the replaceable reflector block columns in the outer region, and vice versa. An exact representation of the configuration adjustment is provided in Fig. 27.

The original cylindrical core was modified by changing the uranium enrichment to 8 wt% in order to analyze and compare data from both core arrangements.

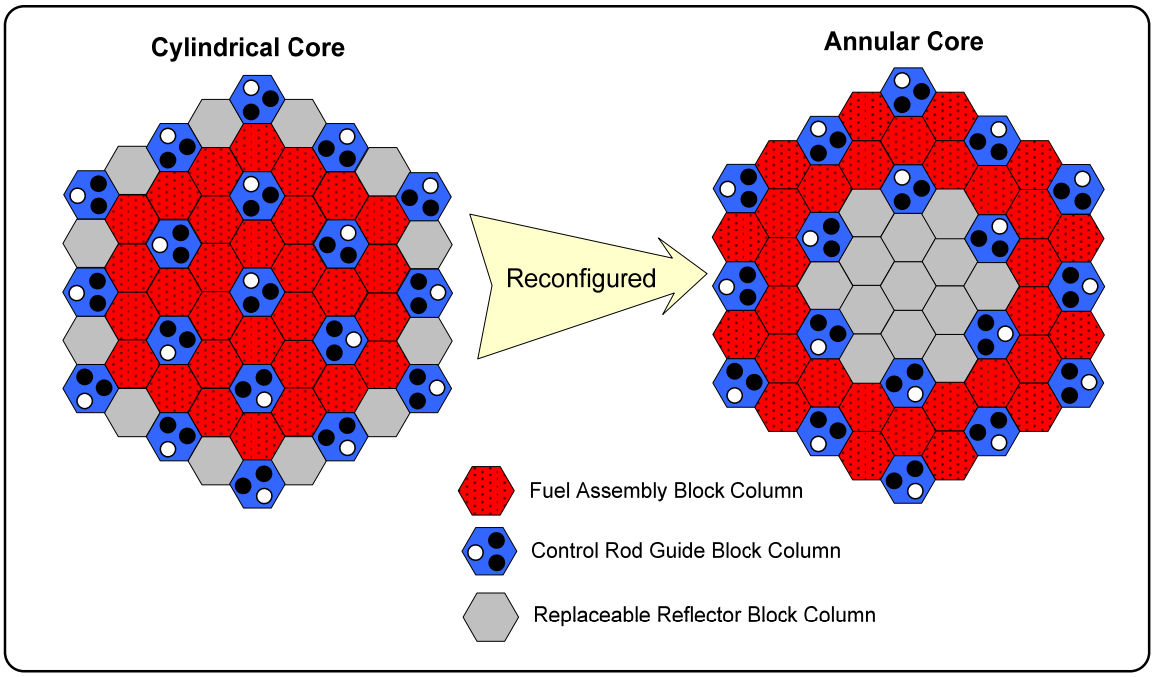

Fig. 27. Cylindrical and Annular Core Configurations

The cylindrical and annular cores were modeled so that energy distributions could be obtained for different regions of interest in the cores. Three horizontal planes within the cores were created. The top plane consists on the hexagonal blocks that are located in the upper most row of the active core. Likewise, the middle and bottom planes consist of the hexagonal blocks that make up the center and lower most rows of the active core. Fig. 28 shows the horizontal planes in a 3D view of the cylindrical core model (same

placement for the annular core). In addition, the annular core model also has the option to obtain energy distributions for the ring of inner and outer fuel assembly columns that compose the annular fuel region.

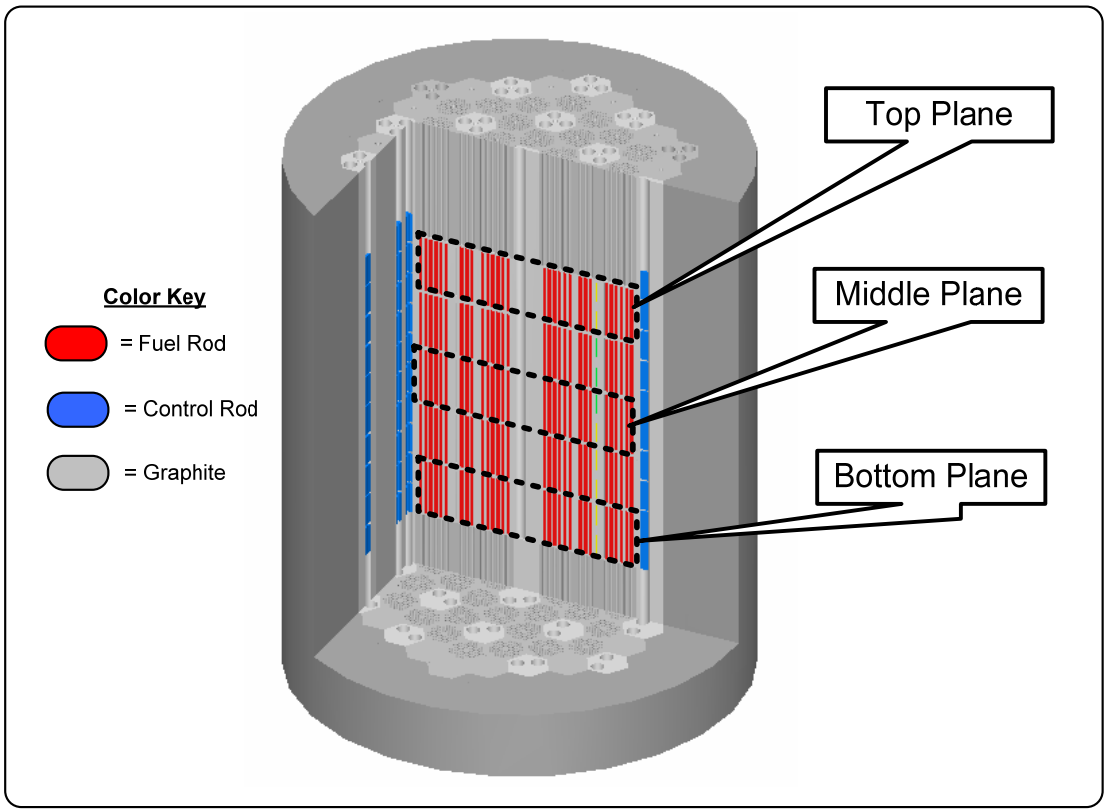

Fig. 28. Horizontal Planes of VHTR Models

The core temperature for the models representing the cylindrical and annular cores was increased to 950°C to better represent the operating environment for VHTRs. The number of histories per generation was increased to 2,000 and the total number of generations run was 210, giving a total sample size 420,000. Using the same Dell Workstation as for the benchmark calculations, the computational runtime for the reconfigured models is about 24 hours each.

VI.A MULTIPLICATION CHARACTERISTICS AND ENERGY DISTRIBUTIONS

The effective multiplication factor for the cylindrical and annular core configurations were calculated and are listed in Table XXIII. Both core configurations resulted in very similar supercritical systems. The fuel placement in the annular configuration is on the periphery of the core, while the fuel in the cylindrical core is distributed in a more compact arrangement. The result is that the effective multiplication factor for the annular core is less than the cylindrical core.

Table XXIII. Effective Multiplication Factor for Cylindrical and Annular Core Configurations

Core Configuration	k_{eff}
Cylindrical	1.0992 ± 0.0012
Annular	1.0775 ± 0.0012

The middle horizontal plane was selected to evaluate and make comparisons between both core configurations. The average energy-dependent neutron flux obtained for the fuel compacts located in the middle horizontal plane of the cylindrical and annular core configurations is provided in Fig. 29. As expected, the profile for each is nearly identical; however, the cylindrical core produces a slightly greater flux.

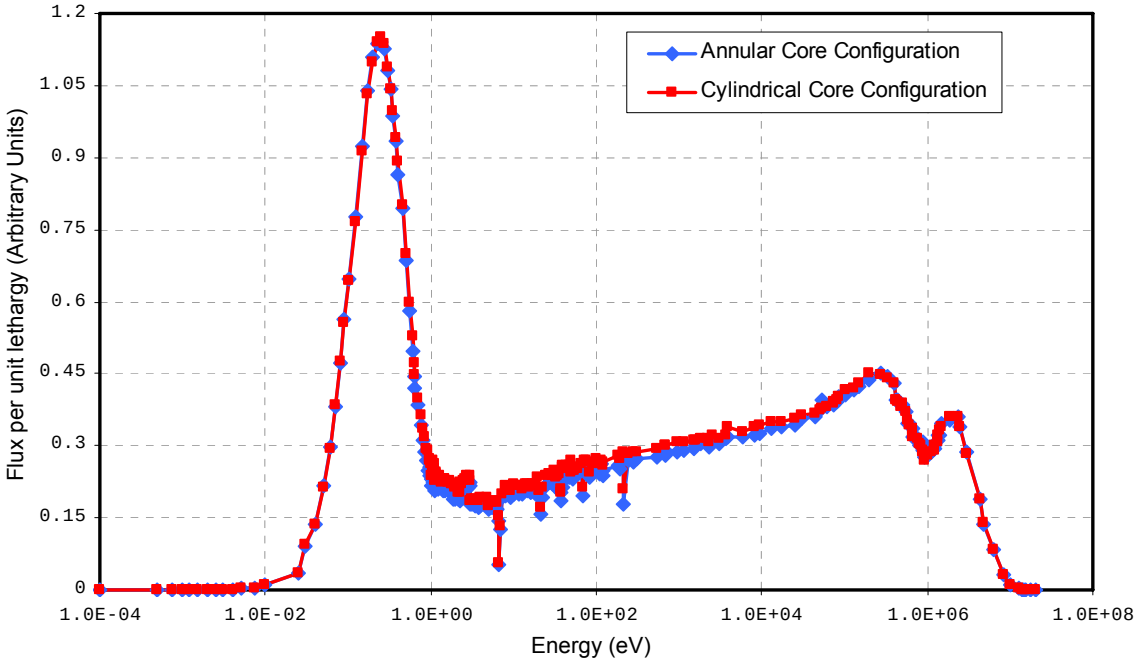

Fig. 29. Energy-Dependent Neutron Flux in the Fuel Compacts for the Middle Horizontal Plane

An evaluation of the neutron flux for all available positions in the annular core was performed. The average energy-dependent neutron flux obtained for the fuel compacts located in the top, middle, and bottom horizontal planes of the annular core configuration are provided in Fig. 30. Likewise, the fluxes for the inner and outer ring of fuel assembly columns are shown in Fig. 31. As indicated by the flux profiles, the highest flux is experienced in the middle horizontal plane of the outer fuel assembly columns.

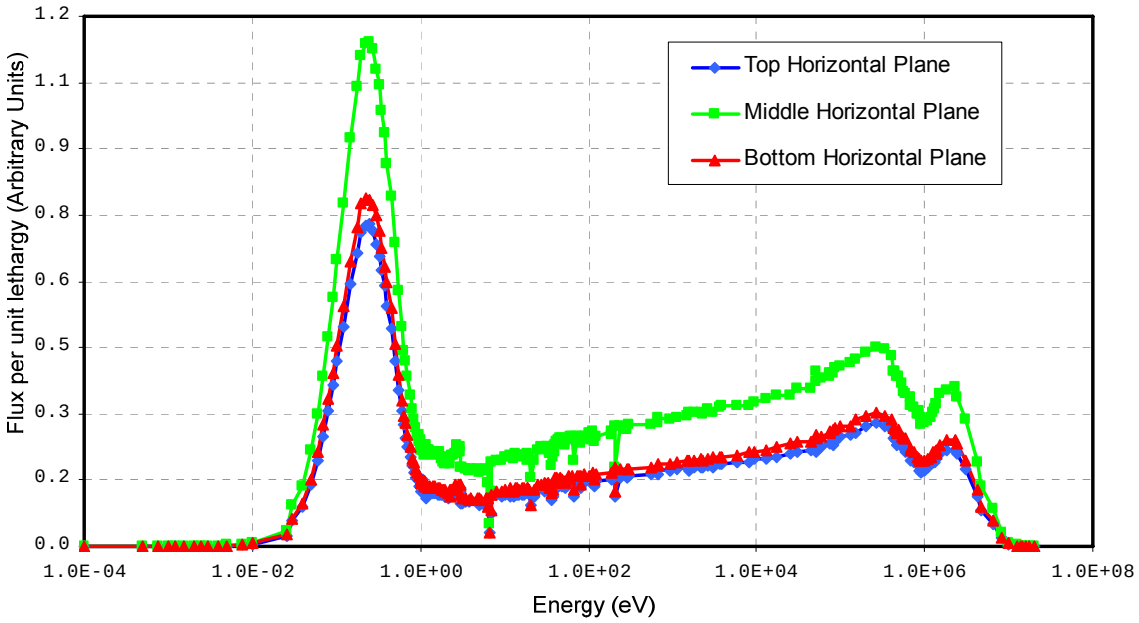

Fig. 30. Energy-Dependent Neutron Flux in the Fuel Compacts Located in the Specified Horizontal Planes for the Annular Core Configuration

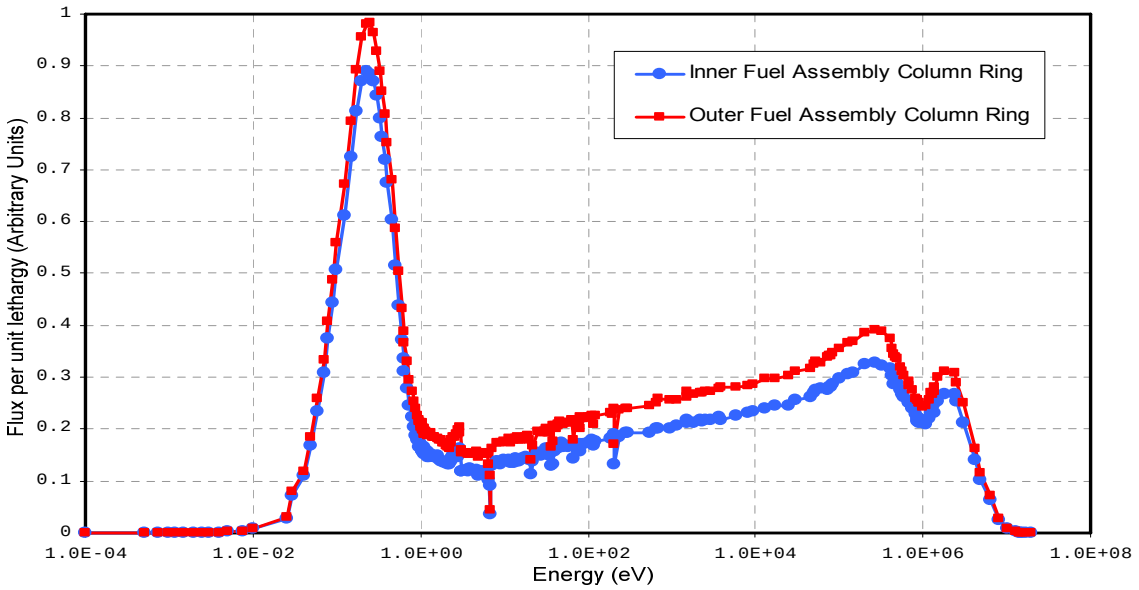

Fig. 31. Energy-Dependent Neutron Flux in the Fuel Compacts Located in the Inner and Outer Fuel Assembly for the Annular Core Configuration

VI.B SAFETY ANALYSIS

The VHTR systems achieve their safety through their design approach, the materials used, and the fuel form. The key safety features of VHTRs, in addition to the radionuclide retention capability of the TRISO fuel particle, is a small operational excess reactivity, a large negative temperature coefficient, and a passive heat removal capability of the reactor design. The combination of the small excess reactivity and large negative temperature coefficient stops the nuclear fission process with only a moderate temperature rise in the core even if the control and shutdown systems fail. In addition, the introduction of an annular core allows fuel decay heat to be conducted through the reactor structures to the vessel cavity and then to the atmosphere without outside intervention. This provides the reactor with a high degree of inherent safety, in turn, making the temperature coefficient a major component for safety analysis within VHTRs.

The benchmark project included calculating the isothermal temperature coefficient for the fully-loaded HTTR core; the procedure is described in Chapter IV.A. The calculations were extended to the cylindrical and annular configured cores. The change in temperature (ΔT) for the analysis was 100°C and the effective multiplication factor was determined at 950°C and 1050°C. Table XXIV. shows the calculated values obtained for the isothermal temperature coefficients.

Table XXIV. Isothermal Temperature Coefficients

Core Configuration	Isothermal Temperature Coefficient $(\Delta k/k/°C)$
HTTR	(-9.626 ± 2.409) $\times 10^{-5}$
Cylindrical	(-6.670 ± 1.415) $\times 10^{-5}$
Annular	(-7.817 ± 1.474) $\times 10^{-5}$

As indicated in Table XXIV, the isothermal temperature coefficients for each core configuration is within the standard deviation limits of one another. For preliminary safety analysis it is sufficient to note that the isothermal temperature coefficients for each case have negative values.

VI.C FUEL LOADINGS CONTAINING ADVANCED ACTINIDES

The fuel compacts within the cylindrical and annular core configurations were loaded with the following fuels in order to perform an introductory analysis of the resulting system's behavior:

- Uranium Dioxide (UO_2)
- Uranium Carbide (UC)
- Transuranics (TRU)
- Minor Actinides (MA)
- Reactor Grade Plutonium (RGPu)

The average energy-dependent flux in the fuel compacts (for each loading: UO_2, UC, TRU, MA, and RGPu) located in the middle horizontal plane of the cylindrical and annular core configurations are shown in Figs. 32 & 33. The two core configurations produce almost identical flux profiles for the specified fuel loadings.

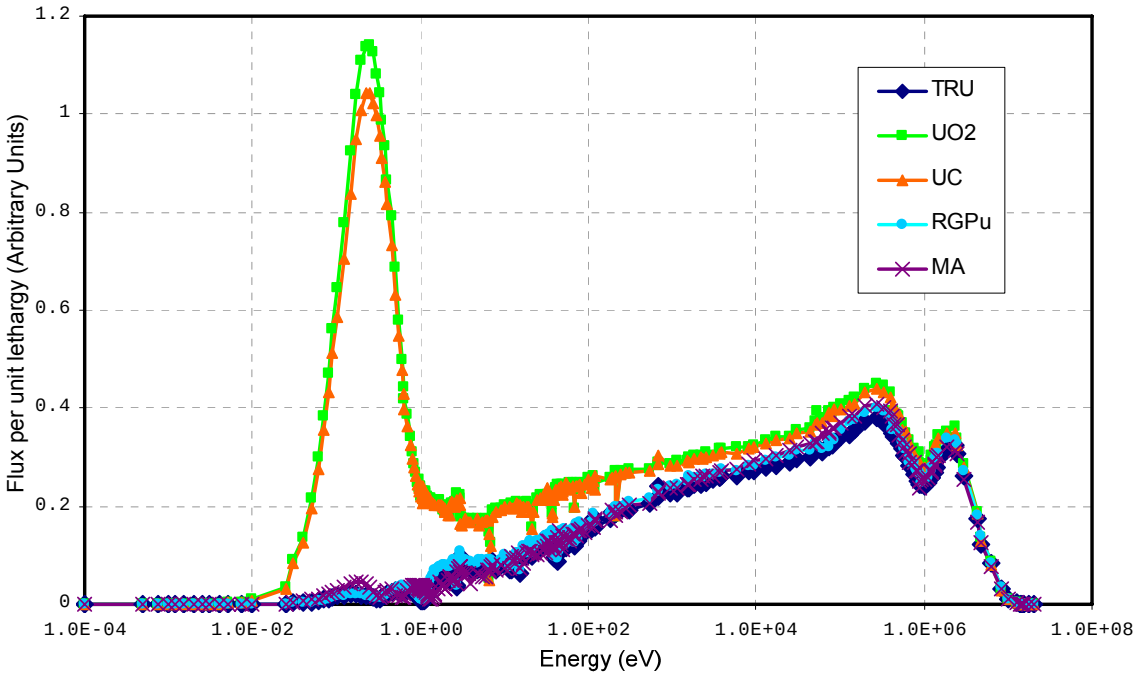

Fig. 32. Energy-Dependent Neutron Flux in the Fuel Compacts for the Annular Core Configuration (advanced actinides)

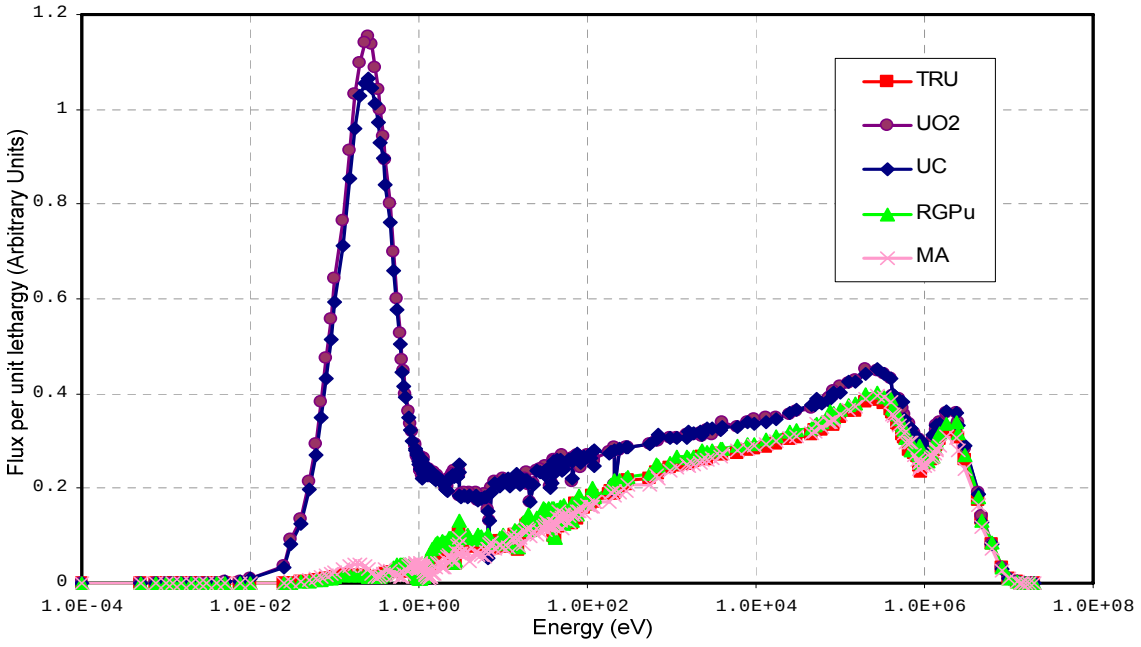

Fig. 33. Energy-Dependent Neutron Flux in the Fuel Compacts for the Cylindrical Core Configuration (advanced actinides)

Although Figs. 32 & 33 do not show much contrast between the two core configurations, the plots provide a good comparison between the individual fuel loadings in each. The uranium based fuels display the same general profile, marked by the large peak in the thermal region. The UO_2 has a larger thermal peak, but is approximately the same as the UC flux profile at other energies. This affect can be attributed to a higher absorption rate of carbide in UC at thermal energies as compared to UO_2's dioxide.

The TRU, RGPu, and MA fuels produce a similar flux profile, marked by a peak in the fast region and by the absence of a thermal peak. To gain better insight, the average energy-dependent neutron flux for these fuel loadings is provided in Fig. 34. As shown, a definite fast spectrum is evident. The MA loading has the highest peak followed by the RGPu and TRU loadings.

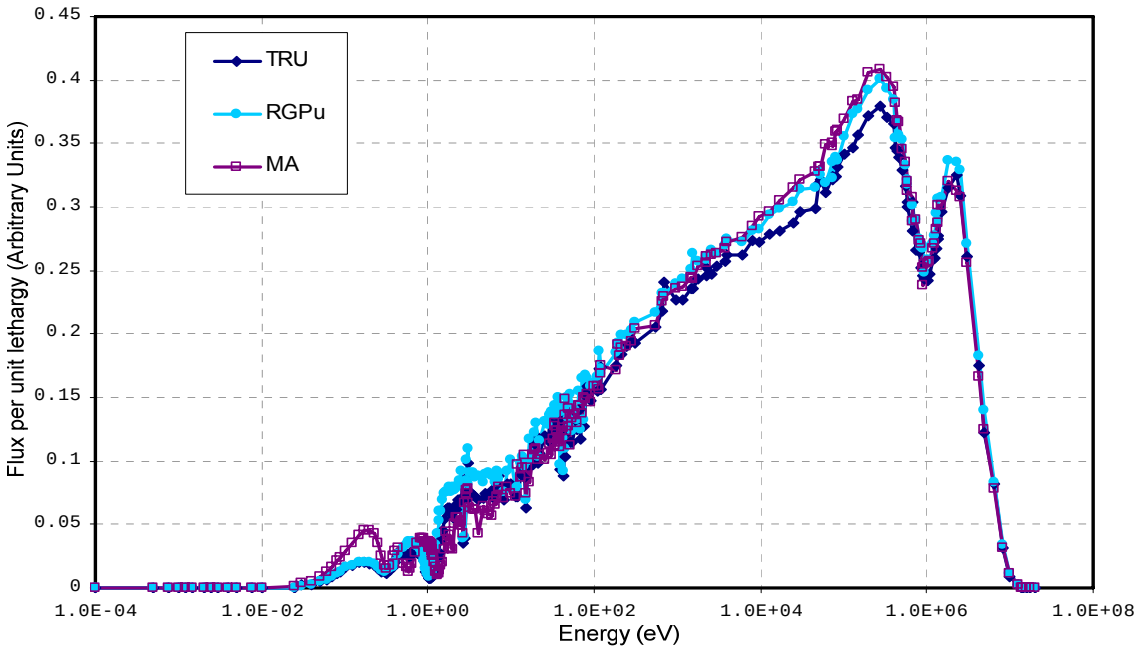

Fig. 34. Energy-Dependent Neutron Flux in the Fuel Compacts for the Annular Core Configuration with TRU, RGPu and MA fuel loadings

Table XXV summarizes basic reactor physics characteristics obtained for the fuel loadings in the (a) cylindrical core configuration and the (b) annular core configuration. Only the MA fuel loading does not produce a critical system.

Table XXV. Basic Reactor Physics of the Cylindrical and Annular Core Configurations

(a) Cylindrical Core Configuration

Fuel	k-eff	Fission-Inducing Energy (eV)	System Mean Free Path (cm)	Fission Neutron Yield
UO2, mixed LEU	1.0191 ± 0.0017	0.22505 ± 0.00047	2.68572 ± 0.00081	2.43867 ± 0.00001
UO2, 8% LEU	1.0992 ± 0.0012	0.25040 ± 0.00038	2.68974 ± 0.00059	2.43859 ± 0.00001
UC, 8% LEU	1.1097 ± 0.0014	0.26387 ± 0.00043	2.69138 ± 0.00061	2.43871 ± 0.00001
TRU	1.01365 ± 0.00091	9.43126 ± 0.04593	2.72176 ± 0.00074	2.90387 ± 0.00004
MA	0.07737 ± 0.00013	1851.18 ± 24.2224	2.71479 ± 0.00086	3.28834 ± 0.00004
RGPu	1.2052 ± 0.0010	9.31957 ± 0.04185	2.72503 ± 0.00083	2.90006 ± 0.00004

(b) Annular Core Configuration

Fuel	k-eff	Fission-Inducing Energy (eV)	System Mean Free Path (cm)	Fission Neutron Yield
UO2, 8% LEU	1.0775 ± 0.0012	0.24094 ± 0.00039	2.64085 ± 0.00043	2.43861 ± 0.00001
UC, 8% LEU	1.0897 ± 0.0015	0.25301 ± 0.00042	2.64241 ± 0.00045	2.43870 ± 0.00001
TRU	1.01485 ± 0.00089	7.28925 ± 0.03847	2.66688 ± 0.00064	2.90356 ± 0.00004
MA	0.07777 ± 0.00013	1427.12 ± 18.1571	2.66471 ± 0.00066	3.28914 ± 0.00004
RGPu	1.19567 ± 0.00096	7.32365 ± 0.03207	2.66678 ± 0.00065	2.89993 ± 0.00004

Evidence is provided to support the proposition that the MAs could be blended with the uranium based fuels to create a fuel loading that would produce a critical system. The UO_2 portion of the fuel would provide the thermal energy peak needed for criticality. Fig. 35 shows the UO_2 and MA fuel loading energy-dependent neutron fluxes.

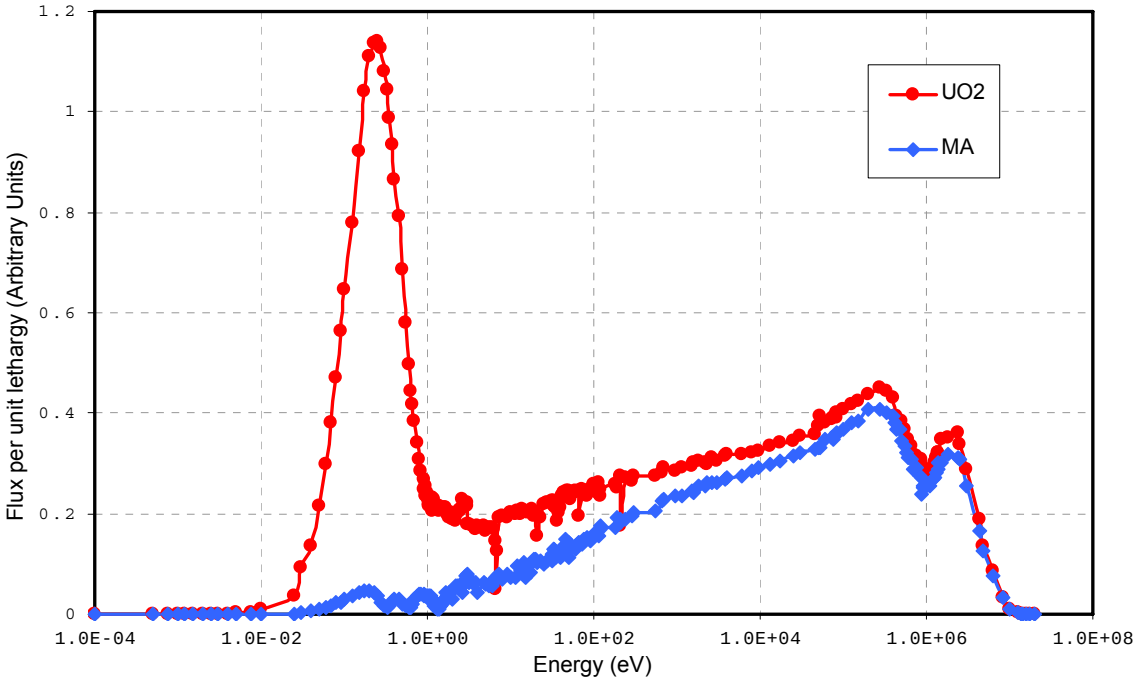

Fig. 35. Energy-Dependent Neutron Flux in the Fuel Compacts for the Annular Core Configuration with UO2 and MA fuel loadings

As a preliminary safety analysis, the isothermal temperature coefficients for each fuel loading case was evaluated. The temperature range (ΔT) was 100°C and the effective multiplication factor was determined at 950°C and 1050°C. Table XXVI. shows the calculated values obtained for the isothermal temperature coefficients for specified fuel loadings and core configuration. As noted, the coefficients in all cases are negative values.

Table XXVI. Isothermal Temperature Coefficients for Specified Fuel Loadings

a) Cylindrical Core Configuration

Fuel	Isothermal Temperature Coefficient $(\Delta k/k/°C)$
UO2, mixed LEU	(-9.6259 ± 2.4089) $\times 10^{-5}$
UO2, 8% LEU	(-6.6697 ± 1.4149) $\times 10^{-5}$
UC, 8% LEU	(-7.6986 ± 1.5083) $\times 10^{-5}$
TRU	(-7.0970 ± 1.1481) $\times 10^{-5}$
MA	(-1.5725 ± 0.2989) $\times 10^{-3}$
RGPu	(-3.5261 ± 0.9778) $\times 10^{-5}$

b) Annular Core Configuration

Fuel	Isothermal Temperature Coefficient $(\Delta k/k/°C)$
UO2, 8% LEU	(-7.8172 ± 1.4741) $\times 10^{-5}$
UC, 8% LEU	(-6.4452 ± 1.6266) $\times 10^{-5}$
TRU	(-5.0847 ± 1.2284) $\times 10^{-5}$
MA	(-1.6410 ± 0.3079) $\times 10^{-3}$
RGPu	(-3.2794 ± 1.0801) $\times 10^{-5}$

CHAPTER VII

CONCLUSIONS

Detailed 3D full-core VHTR models were developed. The preliminary analysis of configuration adjustments in VHTR prismatic cores was performed including fuel loadings with advanced actinide fuels. As an inherent part of the process, the models were validated and verified by performing experiment-to-code benchmarking procedures, which provided substantiation for obtained data and results. Although the performance analysis was primarily focused on prismatic core configurations, 3D pebble-bed core models were also created and analyzed.

Configuration adjustments were performed on the VHTR cylindrical core benchmark model to create an annular core design. The annular core is a more relevant core layout; to be used in future VHTR systems because it provides superior safety features. Preliminary analysis of the annular core model show promising performance characteristics.

Fuel loadings consisting of advanced actinide fuels were evaluated in the models. Initial studies indicate strong potential for the use of minor actinides as a fuel component in VHTRs. The preliminary analysis of the fuel loadings concluded the research work of this thesis, but continued research will be performed as a PhD. Project.

The success of the performed research has provided a seamless transition to future research plans. The final objective of future research is to assess the possibility,

advantages and limitations of achieving ultra-long life VHTRs with minor actinides as a fuel component.

A number of challenges lie ahead for the successful completion of future research. These challenges include but are not limited to:

- Large power configurations (power reactor),
- Configuration adjustments and heterogeneity treatments,
- Uncertainty effects of nuclear data and design parameters,
- Depletion and error propagation,
- Loadings containing minor actinides (ultra-long life VHTR configurations)

The completion of this thesis has provided the ground work for additional research which aims to aid in the energy crisis that faces future generations. The main advantages of the resulting ultra-long life VHTR configurations are their inherent capabilities for utilization of minor actinides from spent LWR fuel, reduction of spent fuel flows and handling per unit of produced energy, and their potential for autonomous operation with minimized maintenance. Consequently, if widely deployed, the developed designs would allow reducing the long-term radiotoxicity and heat load of high-level waste sent to a geologic repository and enable recovery of the energy contained in spent fuel.

This research effort enhances capabilities of the Generation IV VHTR and transforms it to a technology that can deliver electricity, hydrogen, and assist in spent fuel treatment while being inherently safe, environmentally friendly, and proliferation resistant. The technology is also going to be cost-effective because of actinide recycling,

high burn-up, and reactor lifetime long autonomous operation expanding deployment to developing countries and remote areas.

REFERENCES

1. "The US Generation IV Implementation Strategy", 03-GA50439-06, September, 2003, Office of Nuclear Energy, Science, and Technology, USDOE (2003).
2. "Generation IV Nuclear Energy Systems Ten Year Program Plan Volume I", March 27, 2005, Office of Nuclear Energy, Science, and Technology, USDOE (2005).
3. "Report to Congress on Advanced Fuel Cycle Initiative: The Future Path for Advanced Spent Fuel Treatment and Transmutation Research", 03-GA50439-06, January, 2003, Office of Nuclear Energy, Science, and Technology, USDOE (2003).
4. E. E. BENDE, A. H. HOGENBIRK, J. L. KLOOSTERMAN and H. VAN DAM, "Analytical Calculation of the Average Dancoff Factor for a Fuel Kernel in a Pebble-Bed High-Temperature Reactor," *Nuc. Sci. Eng*. **133**, 147-162 (1999).
5. J. VALKO, P. V. TSVETKOV, J. E. HOOGENBOOM, "Calculation of the Dancoff Factor for Pebble-Bed Reactors", *Nucl. Sci. Eng.*, **135**, 304 (2000).
6. SCALE: A Modular Code System for Performing Standardized Computer Analysis for Licensing Evaluation, NUREG/CR-0200, Rev. 7 (ORNL/NUREG/CR/CSD-2R7), 3 vols., April 2004. Available from the Radiation Safety Information Computational Center at Oak Ridge National Laboratory as CCC-545.

7. S. FEHER and P.F.A. DE LEEGE, "DANCOFF-MC: A Computer Program for Monte Carlo Calculation of Dancoff Factors in Irregular Geometries," IRI-131-95-003 (June 1997).

8. "Evaluation of High Temperature Gas-cooled Reactor Performance: Benchmark Analysis Related to Initial Testing of the HTTR and HTR-10", IAEA-TECDOC-1382, International Atomic Energy Agency, Vienna, Austria (2003).

9. D. F. HOLLENBACH and L. M. PETRIE, "CSAS6: Control Module for Enhanced Criticality Safety Analysis with KENO-VI," Vol. I, Sect. C6 of *SCALE: A Modular Code System for Performing Standardized Computer Analysis for Licensing Evaluation*, NUREG/CR-0200, Rev. 7 (ORNL/NUREG/CR/CSD-2R7), 3 vols., April 2004. Available from the Radiation Safety Information Computational Center at Oak Ridge National Laboratory as CCC-545.

10. D. F. HOLLENBACH, L. M. PETRIE, and N. F. LANDERS, "KENO-VI: A General Quadratic Version of the KENO Program," Vol. II, Sect. F17 of *SCALE*: *A Modular Code System for Performing Standardized Computer Analysis for Licensing Evaluation*, NUREG/CR-0200, Rev. 7 (ORNL/NUREG/CR/CSD-2R7), 3 vols., April 2004. Available from the Radiation Safety Information Computational Center at Oak Ridge National Laboratory as CCC-545.

11. W. C. JORDAN and S. M. BOWMAN, "SCALE Cross-Section Libraries," Vol. III, Sect. M4 of SCALE: A Modular Code System for Performing Standardized Computer Analysis for Licensing Evaluation, NUREG/CR-0200, Rev. 7 (ORNL/NUREG/CR/CSD-2R7), 3 vols., April 2004. Available from the

Radiation Safety Information Computational Center at Oak Ridge National Laboratory as CCC-545.

12. N. M. GREENE, "BONAMI: Resonance Self-Shielding by the Bondarenko Method," Vol. II, Sect. F1 of *SCALE: A Modular Code System for Performing Standardized Computer Analysis for Licensing Evaluation*, NUREG/CR-0200, Rev. 7 (ORNL/NUREG/CR/CSD-2R7), 3 vols., April 2004. Available from the Radiation Safety Information Computational Center at Oak Ridge National Laboratory as CCC-545.

13. N. M. GREENE, L. M. PETRIE, and R. M. WESTFALL, "NITAWL-III: SCALE System Module for Performing Resonance Shielding and Working Library Production," Vol. II, Sect. F2 of *SCALE: A Modular Code System for Performing Standardized Computer Analysis for Licensing Evaluation*, NUREG/CR-0200, Rev. 7 (ORNL/NUREG/CR/CSD-2R7), 3 vols., April 2004. Available from the Radiation Safety Information Computational Center at Oak Ridge National Laboratory as CCC-545.

14. N. M. GREENE and L. M. PETRIE, "XSDRNPM: A One-Dimensional Discrete-Ordinates Code for Transport Analysis," Vol. II, Sect. F3 of *SCALE: A Modular Code System for Performing Standardized Computer Analysis for Licensing Evaluation*, NUREG/CR-0200, Rev. 7 (ORNL/NUREG/CR/CSD-2R7), 3 vols., April 2004. Available from the Radiation Safety Information Computational Center at Oak Ridge National Laboratory as CCC-545.

15. S.M. DANCOFF and M. GINSBURG: "Surface Resonance Absorption if a Closed-Packed Lattice", CP-2157 (October 1944).

16. G.I. BELL and S. GLASSTONE: *Nuclear Reactor Theory*, Chap. II.5, Van Nostrand Reinhold Company, New York (1970).

17. A. SAUER, "How to Use the Code DANCOFF-III: A Computer Code for the IBM 7040," Allgemeine Elektrizitats Gesellschaft (1966).

18. J. R. KNIGHT, "SUPERDAN: Computer Programs for Calculating the Dancoff factor of Spheres, Cylinders, and Slabs," ORNL/NUREGCSD/TM-2, RSIC/PSR-282, Oak Ridge National Laboratory (1978).

19. S. FEHÉR, J.E. HOOGENBOOM, P.F.A. DE LEEGE and J. VALKÓ: "Monte Carlo Calculation of Dancoff Factors in Irregular Geometries", *Nucl. Sci. Eng.*, **117**, 227 (1994).

20. KUNITOMI, K., "Development of New Type of HTGR", (Proc. 73rd JSME Fall Annual Meeting), JSME, Japan, 1995.

21. T. A. TAIWO, T. K. KIM, W. S. YANG, and H. S. KHALIL, "Evaluation of High Temperature Gas-Cooled Reactor Physics Experiments as VHTR Benchmark Problems", ANL-GenIV-059, Argonne National Laboratory, September 2005.

APPENDIX A

EXAMPLE SCALE 5 INPUT FILE

```
SCALE 5 Input File (Benchmark Case with Control Rods Fully Withdrawn)
'Input generated by GeeWiz 5.0 Compiled on 04-30-2004
=csas26
httr(CRs removed):UO2=10.41,2E5hist,keff=1.1363,nsk=10
238groupndf5
read comp
'Fuel kernel, 12 different enrichments:
 uo2         21 den=10.41 1 300 92234 0.005407837 92235 3.301 92238
               96.69359 end
 uo2         22 den=10.41 1 300 92234 0.005407837 92235 3.864 92238
               96.13059 end
 uo2         23 den=10.41 1 300 92234 0.005407837 92235 4.29 92238
               95.70459 end
 uo2         24 den=10.41 1 300 92234 0.005407837 92235 4.794 92238
               95.20059 end
 uo2         25 den=10.41 1 300 92234 0.005407837 92235 5.162 92238
               94.83259 end
 uo2         26 den=10.41 1 300 92234 0.005407837 92235 5.914 92238
               94.08059 end
 uo2         27 den=10.41 1 300 92234 0.005407837 92235 6.254 92238
               93.74059 end
 uo2         28 den=10.41 1 300 92234 0.005407837 92235 6.681 92238
               93.31359 end
 uo2         29 den=10.41 1 300 92234 0.005407837 92235 7.189 92238
               92.80559 end
 uo2         30 den=10.41 1 300 92234 0.005407837 92235 7.82 92238
               92.17459 end
 uo2         31 den=10.41 1 300 92234 0.005407837 92235 9.358 92238
               90.63659 end
 uo2         32 den=10.41 1 300 92234 0.005407837 92235 9.81 92238
               90.18459 end
'Control Rod Sleeve:
 wtptsleeve      7  8.08  11 13000 0.4 6000 0.08 24000 21 29000 0.3
                 26000 44.44 25000 1 28000 32 15031 0.02 16000 0.01
                 14000 0.35 22000 0.4 1 300 end
'Graphite fuel and Control rod block:
 c-graphite  1 den=1.77 0.9999996 300 end
 b           1 den=1.77 4.0e-07 300 end
'Boron Burnable Poison Rod (H-I):
 b4c         2 den=1.79 1 300 5010 18.7 5011 81.3 end
'Boron Burnable Poison Rod (H-II):
 b4c         3 den=1.82 1 300 5010 18.7 5011 81.3 end
'Boron Control Rod:
 b4c         8 den=1.9 1 300 end
'Graphite Replaceable and Side Blocks:
 c-graphite  9 den=1.76 0.9999996 300 end
 b           9 den=1.76 3.7e-07 300 end
'Graphite Permanent Reflector Block:
 c-graphite  10 den=1.732 0.999998 300 end
 b           10 den=1.732 1.91e-06 300 end
'Graphite Sleeve (Fuel rod):
 c-graphite  14 den=1.77 0.9999996 300 end
 b           14 den=1.77 3.7e-07 300 end
'Helium:
 he          5 1 300 end
```

```
'Fuel Coating:
 b-10        11 0 7.221155e-09 300 end
 b-11        11 0 2.924932e-08 300 end
 c-graphite  11 0 0.07291468 300 end
 si          11 0 0.01017942 300 end
'Graphite Matrix (Fuel Compact):
 b           12 den=1.69 8.2e-07 300 end
 c-graphite  12 den=1.69 0.99999918 300 end
'Fuel Coating:
 b-10        40 0 7.221155e-09 300 end
 b-11        40 0 2.924932e-08 300 end
 c-graphite  40 0 0.07291468 300 end
 si          40 0 0.01017942 300 end
'Graphite Matrix (Fuel Compact):
 b           41 den=1.69 8.2e-07 300 end
 c-graphite  41 den=1.69 0.99999918 300 end
'Fuel Coating:
 b-10        42 0 7.221155e-09 300 end
 b-11        42 0 2.924932e-08 300 end
 c-graphite  42 0 0.07291468 300 end
 si          42 0 0.01017942 300 end
'Graphite Matrix (Fuel Compact):
 b           43 den=1.69 8.2e-07 300 end
 c-graphite  43 den=1.69 0.99999918 300 end
'Fuel Coating:
 b-10        44 0 7.221155e-09 300 end
 b-11        44 0 2.924932e-08 300 end
 c-graphite  44 0 0.07291468 300 end
 si          44 0 0.01017942 300 end
'Graphite Matrix (Fuel Compact):
 b           45 den=1.69 8.2e-07 300 end
 c-graphite  45 den=1.69 0.99999918 300 end
'Fuel Coating:
 b-10        46 0 7.221155e-09 300 end
 b-11        46 0 2.924932e-08 300 end
 c-graphite  46 0 0.07291468 300 end
 si          46 0 0.01017942 300 end
'Graphite Matrix (Fuel Compact):
 b           47 den=1.69 8.2e-07 300 end
 c-graphite  47 den=1.69 0.99999918 300 end
'Fuel Coating:
 b-10        48 0 7.221155e-09 300 end
 b-11        48 0 2.924932e-08 300 end
 c-graphite  48 0 0.07291468 300 end
 si          48 0 0.01017942 300 end
'Graphite Matrix (Fuel Compact):
 b           49 den=1.69 8.2e-07 300 end
 c-graphite  49 den=1.69 0.99999918 300 end
'Fuel Coating:
 b-10        50 0 7.221155e-09 300 end
 b-11        50 0 2.924932e-08 300 end
 c-graphite  50 0 0.07291468 300 end
 si          50 0 0.01017942 300 end
'Graphite Matrix (Fuel Compact):
 b           51 den=1.69 8.2e-07 300 end
 c-graphite  51 den=1.69 0.99999918 300 end
'Fuel Coating:
```

```
 b-10        52 0 7.221155e-09 300 end
 b-11        52 0 2.924932e-08 300 end
 c-graphite  52 0 0.07291468 300 end
 si          52 0 0.01017942 300 end
'Graphite Matrix (Fuel Compact):
 b           53 den=1.69 8.2e-07 300 end
 c-graphite  53 den=1.69 0.99999918 300 end
'Fuel Coating:
 b-10        54 0 7.221155e-09 300 end
 b-11        54 0 2.924932e-08 300 end
 c-graphite  54 0 0.07291468 300 end
 si          54 0 0.01017942 300 end
'Graphite Matrix (Fuel Compact):
 b           55 den=1.69 8.2e-07 300 end
 c-graphite  55 den=1.69 0.99999918 300 end
'Fuel Coating:
 b-10        56 0 7.221155e-09 300 end
 b-11        56 0 2.924932e-08 300 end
 c-graphite  56 0 0.07291468 300 end
 si          56 0 0.01017942 300 end
'Graphite Matrix (Fuel Compact):
 b           57 den=1.69 8.2e-07 300 end
 c-graphite  57 den=1.69 0.99999918 300 end
'Fuel Coating:
 b-10        58 0 7.221155e-09 300 end
 b-11        58 0 2.924932e-08 300 end
 c-graphite  58 0 0.07291468 300 end
 si          58 0 0.01017942 300 end
'Graphite Matrix (Fuel Compact):
 b           59 den=1.69 8.2e-07 300 end
 c-graphite  59 den=1.69 0.99999918 300 end
'Fuel Coating:
 b-10        60 0 7.221155e-09 300 end
 b-11        60 0 2.924932e-08 300 end
 c-graphite  60 0 0.07291468 300 end
 si          60 0 0.01017942 300 end
'Graphite Matrix (Fuel Compact):
 b           61 den=1.69 8.2e-07 300 end
 c-graphite  61 den=1.69 0.99999918 300 end
end comp
read celldata
'Unit Cell Specifications, cell-weighted cross sections (cellmix=m) to
be used in KENOVI:
  latticecell sphtriangp fuelr=0.02985 21 cladr=0.04645 11
  hpitch=0.058077 12 cellmix=121 end
           more data
           IIM=50
           ICM=100
           COF=3
           EPS=0.0001
           PTC=0.000001
           DAN(21)=0.8493
           end more
  latticecell sphtriangp fuelr=0.02985 22 cladr=0.04645 40
  hpitch=0.058077 41 cellmix=122 end
           more data
           IIM=50
```

```
         ICM=100
         COF=3
         EPS=0.0001
         PTC=0.000001
         DAN(22)=0.8493
         end more
latticecell sphtriangp fuelr=0.02985 23 cladr=0.04645 42
hpitch=0.058077 43 cellmix=123 end
         more data
         IIM=50
         ICM=100
         COF=3
         EPS=0.0001
         PTC=0.000001
         DAN(23)=0.8493
         end more
latticecell sphtriangp fuelr=0.02985 24 cladr=0.04645 44
hpitch=0.058077 45 cellmix=124 end
         more data
         IIM=50
         ICM=100
         COF=3
         EPS=0.0001
         PTC=0.000001
         DAN(24)=0.8493
         end more
latticecell sphtriangp fuelr=0.02985 25 cladr=0.04645 46
hpitch=0.058077 47 cellmix=125 end
         more data
         IIM=50
         ICM=100
         COF=3
         EPS=0.0001
         PTC=0.000001
         DAN(25)=0.8493
         end more
latticecell sphtriangp fuelr=0.02985 26 cladr=0.04645 48
hpitch=0.058077 49 cellmix=126 end
         more data
         IIM=50
         ICM=100
         COF=3
         EPS=0.0001
         PTC=0.000001
         DAN(26)=0.8493
         end more
latticecell sphtriangp fuelr=0.02985 27 cladr=0.04645 50
hpitch=0.058077 51 cellmix=127 end
         more data
         IIM=50
         ICM=100
         COF=3
         EPS=0.0001
         PTC=0.000001
         DAN(27)=0.8493
         end more
latticecell sphtriangp fuelr=0.02985 28 cladr=0.04645 52
```

```
  hpitch=0.058077 53 cellmix=128 end
           more data
           IIM=50
           ICM=100
           COF=3
           EPS=0.0001
           PTC=0.000001
           DAN(28)=0.8493
           end more
  latticecell sphtriangp fuelr=0.02985 29 cladr=0.04645 54
  hpitch=0.058077 55 cellmix=129 end
           more data
           IIM=50
           ICM=100
           COF=3
           EPS=0.0001
           PTC=0.000001
           DAN(29)=0.8493
           end more
  latticecell sphtriangp fuelr=0.02985 30 cladr=0.04645 56
  hpitch=0.058077 57 cellmix=130 end
           more data
           IIM=50
           ICM=100
           COF=3
           EPS=0.0001
           PTC=0.000001
           DAN(30)=0.8493
           end more
  latticecell sphtriangp fuelr=0.02985 31 cladr=0.04645 58
  hpitch=0.058077 59 cellmix=131 end
           more data
           IIM=50
           ICM=100
           COF=3
           EPS=0.0001
           PTC=0.000001
           DAN(31)=0.8493
           end more
  latticecell sphtriangp fuelr=0.02985 32 cladr=0.04645 60
  hpitch=0.058077 61 cellmix=132 end
           more data
           IIM=50
           ICM=100
           COF=3
           EPS=0.0001
           PTC=0.000001
           DAN(32)=0.8493
           end more
end celldata
read param
           gen=200
           npg=1000
           nsk=10
           FLX=yes
           FDN=yes
           PKI=yes
```

```
            FAR=yes
            GAS=yes
            MKP=yes
            FMP=yes
            MKU=yes
            FMU=yes
            SMU=yes
            NUB=yes
            CFX=yes
end param
read geometry
unit 121
com='fuel hole (center gap, fuel, graphite sleeve, coolant)'
 cylinder 2  2.05  54.6  0
 cylinder 3  0.5  54.6  0
 cylinder 4  1.3  54.6  0
 cylinder 5  1.7  54.6  0
 media 5 1 3
 media 121 1 4 -3
 media 14 1 5 -4 -3
 media 5 1 2 -3 -4 -5
 boundary 2
unit 122
com='fuel hole (center gap, fuel, graphite sleeve, coolant)'
 cylinder 2  2.05  54.6  0
 cylinder 3  0.5  54.6  0
 cylinder 4  1.3  54.6  0
 cylinder 5  1.7  54.6  0
 media 5 1 3
 media 122 1 4 -3
 media 14 1 5 -4 -3
 media 5 1 2 -3 -4 -5
 boundary 2
unit 123
com='fuel hole (center gap, fuel, graphite sleeve, coolant)'
 cylinder 2  2.05  54.6  0
 cylinder 3  0.5  54.6  0
 cylinder 4  1.3  54.6  0
 cylinder 5  1.7  54.6  0
 media 5 1 3
 media 123 1 4 -3
 media 14 1 5 -4 -3
 media 5 1 2 -3 -4 -5
 boundary 2
unit 124
com='fuel hole (center gap, fuel, graphite sleeve, coolant)'
 cylinder 2  2.05  54.6  0
 cylinder 3  0.5  54.6  0
 cylinder 4  1.3  54.6  0
 cylinder 5  1.7  54.6  0
 media 5 1 3
 media 124 1 4 -3
 media 14 1 5 -4 -3
 media 5 1 2 -3 -4 -5
 boundary 2
unit 125
com='fuel hole (center gap, fuel, graphite sleeve, coolant)'
```

```
 cylinder 2  2.05  54.6  0
 cylinder 3  0.5  54.6  0
 cylinder 4  1.3  54.6  0
 cylinder 5  1.7  54.6  0
 media 5 1 3
 media 125 1 4 -3
 media 14 1 5 -4 -3
 media 5 1 2 -3 -4 -5
 boundary 2
unit 126
com='fuel hole (center gap, fuel, graphite sleeve, coolant)'
 cylinder 2  2.05  54.6  0
 cylinder 3  0.5  54.6  0
 cylinder 4  1.3  54.6  0
 cylinder 5  1.7  54.6  0
 media 5 1 3
 media 126 1 4 -3
 media 14 1 5 -4 -3
 media 5 1 2 -3 -4 -5
 boundary 2
unit 127
com='fuel hole (center gap, fuel, graphite sleeve, coolant)'
 cylinder 2  2.05  54.6  0
 cylinder 3  0.5  54.6  0
 cylinder 4  1.3  54.6  0
 cylinder 5  1.7  54.6  0
 media 5 1 3
 media 127 1 4 -3
 media 14 1 5 -4 -3
 media 5 1 2 -3 -4 -5
 boundary 2
unit 128
com='fuel hole (center gap, fuel, graphite sleeve, coolant)'
 cylinder 2  2.05  54.6  0
 cylinder 3  0.5  54.6  0
 cylinder 4  1.3  54.6  0
 cylinder 5  1.7  54.6  0
 media 5 1 3
 media 128 1 4 -3
 media 14 1 5 -4 -3
 media 5 1 2 -3 -4 -5
 boundary 2
unit 129
com='fuel hole ((center gap, fuel, graphite sleeve, coolant)'
 cylinder 2  2.05  54.6  0
 cylinder 3  0.5  54.6  0
 cylinder 4  1.3  54.6  0
 cylinder 5  1.7  54.6  0
 media 5 1 3
 media 129 1 4 -3
 media 14 1 5 -4 -3
 media 5 1 2 -3 -4 -5
 boundary 2
unit 130
com='fuel hole (center gap, fuel, graphite sleeve, coolant)'
 cylinder 2  2.05  54.6  0
 cylinder 3  0.5  54.6  0
```

```
 cylinder 4  1.3  54.6  0
 cylinder 5  1.7  54.6  0
 media 5 1 3
 media 130 1 4 -3
 media 14 1 5 -4 -3
 media 5 1 2 -3 -4 -5
 boundary 2
unit 131
com='fuel hole ((center gap, fuel, graphite sleeve, coolant)'
 cylinder 2  2.05  54.6  0
 cylinder 3  0.5  54.6  0
 cylinder 4  1.3  54.6  0
 cylinder 5  1.7  54.6  0
 media 5 1 3
 media 131 1 4 -3
 media 14 1 5 -4 -3
 media 5 1 2 -3 -4 -5
 boundary 2
unit 132
com='fuel hole ((center gap, fuel, graphite sleeve, coolant)'
 cylinder 2  2.05  54.6  0
 cylinder 3  0.5  54.6  0
 cylinder 4  1.3  54.6  0
 cylinder 5  1.7  54.6  0
 media 5 1 3
 media 132 1 4 -3
 media 14 1 5 -4 -3
 media 5 1 2 -3 -4 -5
 boundary 2
unit 3
com='burnable poison, h-i (boron section)'
 cylinder 3  0.70  20  0
 media 2 1 3
 boundary 3
unit 39
com='burnable poison, h-ii (boron section)'
 cylinder 3  0.70  20  0
 media 3 1 3
 boundary 3
unit 12
com='burnable poison (empty space)'
 cylinder 1  0.75  50  0
 media 5 1 1
 boundary 1
unit 4
com='fuel handling hole (upper)'
 cone 4  2.5  58  1.5  49
 media 5 1 4
 boundary 4
unit 5
com='fuel handling hole (middle)'
 cylinder 5  1.5  49  43
 media 5 1 5
 boundary 5
unit 6
com='fuel handling hole (lower)'
 cylinder 6  2.25  43  33
```

```
 media 5 1 6
 boundary 6
unit 36
com='top replaceable reflector block coolant hole (31/33 holes)'
 cylinder 1  2.05  116  0
 media 5 1 1
 boundary 1
unit 35
com='bottom replaceable reflector block coolant hole (31/33 holes)'
 cylinder 1  2.05  58  0
 media 5 1 1
 boundary 1
unit 37
com='very bottom replaceable reflector block coolant hole (6 holes)'
 cylinder 1  4.6  58  0
 media 5 1 1
 boundary 1
unit 14
com='fuel column (33-pin) zone-1 #1: empty bp hole at 120 degree'
 rhexprism 1  18  406  -116
 rhexprism 10  18  0  -116
 rhexprism 20  18  406  290
 rhexprism 30  18  290  0
 hole 37   origin  x=5.15 y=8.92 z=-116
 hole 37   origin  x=5.15 y=-8.92 z=-116
 hole 37   origin  x=-5.15 y=8.92 z=-116
 hole 37   origin  x=-5.15 y=-8.92 z=-116
 hole 37   origin  x=10.3 y=0 z=-116
 hole 37   origin  x=-10.3 y=0 z=-116
 hole 35   origin  x=0 y=8.92 z=-58
 hole 35   origin  x=0 y=-8.92 z=-58
 hole 35   origin  x=2.575 y=4.46 z=-58
 hole 35   origin  x=2.575 y=-4.46 z=-58
 hole 35   origin  x=2.575 y=13.38 z=-58
 hole 35   origin  x=2.575 y=-13.38 z=-58
 hole 35   origin  x=-2.575 y=4.46 z=-58
 hole 35   origin  x=-2.575 y=-4.46 z=-58
 hole 35   origin  x=-2.575 y=13.38 z=-58
 hole 35   origin  x=-2.575 y=-13.38 z=-58
 hole 35   origin  x=5.15 y=0 z=-58
 hole 35   origin  x=5.15 y=8.92 z=-58
 hole 35   origin  x=5.15 y=-8.92 z=-58
 hole 35   origin  x=-5.15 y=0 z=-58
 hole 35   origin  x=-5.15 y=8.92 z=-58
 hole 35   origin  x=-5.15 y=-8.92 z=-58
 hole 35   origin  x=7.725 y=4.46 z=-58
 hole 35   origin  x=7.725 y=-4.46 z=-58
 hole 35   origin  x=7.725 y=13.38 z=-58
 hole 35   origin  x=7.725 y=-13.38 z=-58
 hole 35   origin  x=-7.725 y=4.46 z=-58
 hole 35   origin  x=-7.725 y=-4.46 z=-58
 hole 35   origin  x=10.3 y=0 z=-58
 hole 35   origin  x=10.3 y=8.92 z=-58
 hole 35   origin  x=10.3 y=-8.92 z=-58
 hole 35   origin  x=-10.3 y=0 z=-58
 hole 35   origin  x=-10.3 y=8.92 z=-58
 hole 35   origin  x=-10.3 y=-8.92 z=-58
```

```
hole 35   origin  x=12.875 y=4.46 z=-58
hole 35   origin  x=12.875 y=-4.46 z=-58
hole 35   origin  x=-12.875 y=4.46 z=-58
hole 35   origin  x=-12.875 y=-4.46 z=-58
hole 35   origin  x=-15.45 y=0 z=-58
hole 121   origin  x=0 y=8.92 z=1.7
hole 121   origin  x=0 y=-8.92 z=1.7
hole 121   origin  x=2.575 y=4.46 z=1.7
hole 121   origin  x=2.575 y=-4.46 z=1.7
hole 121   origin  x=2.575 y=13.38 z=1.7
hole 121   origin  x=2.575 y=-13.38 z=1.7
hole 121   origin  x=-2.575 y=4.46 z=1.7
hole 121   origin  x=-2.575 y=-4.46 z=1.7
hole 121   origin  x=-2.575 y=13.38 z=1.7
hole 121   origin  x=-2.575 y=-13.38 z=1.7
hole 121   origin  x=5.15 y=0 z=1.7
hole 121   origin  x=5.15 y=8.92 z=1.7
hole 121   origin  x=5.15 y=-8.92 z=1.7
hole 121   origin  x=-5.15 y=0 z=1.7
hole 121   origin  x=-5.15 y=8.92 z=1.7
hole 121   origin  x=-5.15 y=-8.92 z=1.7
hole 121   origin  x=7.725 y=4.46 z=1.7
hole 121   origin  x=7.725 y=-4.46 z=1.7
hole 121   origin  x=7.725 y=13.38 z=1.7
hole 121   origin  x=7.725 y=-13.38 z=1.7
hole 121   origin  x=-7.725 y=4.46 z=1.7
hole 121   origin  x=-7.725 y=-4.46 z=1.7
hole 121   origin  x=10.3 y=0 z=1.7
hole 121   origin  x=10.3 y=8.92 z=1.7
hole 121   origin  x=10.3 y=-8.92 z=1.7
hole 121   origin  x=-10.3 y=0 z=1.7
hole 121   origin  x=-10.3 y=8.92 z=1.7
hole 121   origin  x=-10.3 y=-8.92 z=1.7
hole 121   origin  x=12.875 y=4.46 z=1.7
hole 121   origin  x=12.875 y=-4.46 z=1.7
hole 121   origin  x=-12.875 y=4.46 z=1.7
hole 121   origin  x=-12.875 y=-4.46 z=1.7
hole 121   origin  x=-15.45 y=0 z=1.7
hole 121   origin  x=0 y=8.92 z=59.7
hole 121   origin  x=0 y=-8.92 z=59.7
hole 121   origin  x=2.575 y=4.46 z=59.7
hole 121   origin  x=2.575 y=-4.46 z=59.7
hole 121   origin  x=2.575 y=13.38 z=59.7
hole 121   origin  x=2.575 y=-13.38 z=59.7
hole 121   origin  x=-2.575 y=4.46 z=59.7
hole 121   origin  x=-2.575 y=-4.46 z=59.7
hole 121   origin  x=-2.575 y=13.38 z=59.7
hole 121   origin  x=-2.575 y=-13.38 z=59.7
hole 121   origin  x=5.15 y=0 z=59.7
hole 121   origin  x=5.15 y=8.92 z=59.7
hole 121   origin  x=5.15 y=-8.92 z=59.7
hole 121   origin  x=-5.15 y=0 z=59.7
hole 121   origin  x=-5.15 y=8.92 z=59.7
hole 121   origin  x=-5.15 y=-8.92 z=59.7
hole 121   origin  x=7.725 y=4.46 z=59.7
hole 121   origin  x=7.725 y=-4.46 z=59.7
hole 121   origin  x=7.725 y=13.38 z=59.7
```

```
hole 121   origin  x=7.725 y=-13.38 z=59.7
hole 121   origin  x=-7.725 y=4.46 z=59.7
hole 121   origin  x=-7.725 y=-4.46 z=59.7
hole 121   origin  x=10.3 y=0 z=59.7
hole 121   origin  x=10.3 y=8.92 z=59.7
hole 121   origin  x=10.3 y=-8.92 z=59.7
hole 121   origin  x=-10.3 y=0 z=59.7
hole 121   origin  x=-10.3 y=8.92 z=59.7
hole 121   origin  x=-10.3 y=-8.92 z=59.7
hole 121   origin  x=12.875 y=4.46 z=59.7
hole 121   origin  x=12.875 y=-4.46 z=59.7
hole 121   origin  x=-12.875 y=4.46 z=59.7
hole 121   origin  x=-12.875 y=-4.46 z=59.7
hole 121   origin  x=-15.45 y=0 z=59.7
hole 123   origin  x=0 y=8.92 z=117.7
hole 123   origin  x=0 y=-8.92 z=117.7
hole 123   origin  x=2.575 y=4.46 z=117.7
hole 123   origin  x=2.575 y=-4.46 z=117.7
hole 123   origin  x=2.575 y=13.38 z=117.7
hole 123   origin  x=2.575 y=-13.38 z=117.7
hole 123   origin  x=-2.575 y=4.46 z=117.7
hole 123   origin  x=-2.575 y=-4.46 z=117.7
hole 123   origin  x=-2.575 y=13.38 z=117.7
hole 123   origin  x=-2.575 y=-13.38 z=117.7
hole 123   origin  x=5.15 y=0 z=117.7
hole 123   origin  x=5.15 y=8.92 z=117.7
hole 123   origin  x=5.15 y=-8.92 z=117.7
hole 123   origin  x=-5.15 y=0 z=117.7
hole 123   origin  x=-5.15 y=8.92 z=117.7
hole 123   origin  x=-5.15 y=-8.92 z=117.7
hole 123   origin  x=7.725 y=4.46 z=117.7
hole 123   origin  x=7.725 y=-4.46 z=117.7
hole 123   origin  x=7.725 y=13.38 z=117.7
hole 123   origin  x=7.725 y=-13.38 z=117.7
hole 123   origin  x=-7.725 y=4.46 z=117.7
hole 123   origin  x=-7.725 y=-4.46 z=117.7
hole 123   origin  x=10.3 y=0 z=117.7
hole 123   origin  x=10.3 y=8.92 z=117.7
hole 123   origin  x=10.3 y=-8.92 z=117.7
hole 123   origin  x=-10.3 y=0 z=117.7
hole 123   origin  x=-10.3 y=8.92 z=117.7
hole 123   origin  x=-10.3 y=-8.92 z=117.7
hole 123   origin  x=12.875 y=4.46 z=117.7
hole 123   origin  x=12.875 y=-4.46 z=117.7
hole 123   origin  x=-12.875 y=4.46 z=117.7
hole 123   origin  x=-12.875 y=-4.46 z=117.7
hole 123   origin  x=-15.45 y=0 z=117.7
hole 125   origin  x=0 y=8.92 z=175.7
hole 125   origin  x=0 y=-8.92 z=175.7
hole 125   origin  x=2.575 y=4.46 z=175.7
hole 125   origin  x=2.575 y=-4.46 z=175.7
hole 125   origin  x=2.575 y=13.38 z=175.7
hole 125   origin  x=2.575 y=-13.38 z=175.7
hole 125   origin  x=-2.575 y=4.46 z=175.7
hole 125   origin  x=-2.575 y=-4.46 z=175.7
hole 125   origin  x=-2.575 y=13.38 z=175.7
hole 125   origin  x=-2.575 y=-13.38 z=175.7
```

```
hole 125   origin  x=5.15 y=0 z=175.7
hole 125   origin  x=5.15 y=8.92 z=175.7
hole 125   origin  x=5.15 y=-8.92 z=175.7
hole 125   origin  x=-5.15 y=0 z=175.7
hole 125   origin  x=-5.15 y=8.92 z=175.7
hole 125   origin  x=-5.15 y=-8.92 z=175.7
hole 125   origin  x=7.725 y=4.46 z=175.7
hole 125   origin  x=7.725 y=-4.46 z=175.7
hole 125   origin  x=7.725 y=13.38 z=175.7
hole 125   origin  x=7.725 y=-13.38 z=175.7
hole 125   origin  x=-7.725 y=4.46 z=175.7
hole 125   origin  x=-7.725 y=-4.46 z=175.7
hole 125   origin  x=10.3 y=0 z=175.7
hole 125   origin  x=10.3 y=8.92 z=175.7
hole 125   origin  x=10.3 y=-8.92 z=175.7
hole 125   origin  x=-10.3 y=0 z=175.7
hole 125   origin  x=-10.3 y=8.92 z=175.7
hole 125   origin  x=-10.3 y=-8.92 z=175.7
hole 125   origin  x=12.875 y=4.46 z=175.7
hole 125   origin  x=12.875 y=-4.46 z=175.7
hole 125   origin  x=-12.875 y=4.46 z=175.7
hole 125   origin  x=-12.875 y=-4.46 z=175.7
hole 125   origin  x=-15.45 y=0 z=175.7
hole 125   origin  x=0 y=8.92 z=233.7
hole 125   origin  x=0 y=-8.92 z=233.7
hole 128   origin  x=2.575 y=4.46 z=233.7
hole 128   origin  x=2.575 y=-4.46 z=233.7
hole 128   origin  x=2.575 y=13.38 z=233.7
hole 128   origin  x=2.575 y=-13.38 z=233.7
hole 128   origin  x=-2.575 y=4.46 z=233.7
hole 128   origin  x=-2.575 y=-4.46 z=233.7
hole 128   origin  x=-2.575 y=13.38 z=233.7
hole 128   origin  x=-2.575 y=-13.38 z=233.7
hole 128   origin  x=5.15 y=0 z=233.7
hole 128   origin  x=5.15 y=8.92 z=233.7
hole 128   origin  x=5.15 y=-8.92 z=233.7
hole 128   origin  x=-5.15 y=0 z=233.7
hole 128   origin  x=-5.15 y=8.92 z=233.7
hole 128   origin  x=-5.15 y=-8.92 z=233.7
hole 128   origin  x=7.725 y=4.46 z=233.7
hole 128   origin  x=7.725 y=-4.46 z=233.7
hole 128   origin  x=7.725 y=13.38 z=233.7
hole 128   origin  x=7.725 y=-13.38 z=233.7
hole 128   origin  x=-7.725 y=4.46 z=233.7
hole 128   origin  x=-7.725 y=-4.46 z=233.7
hole 128   origin  x=10.3 y=0 z=233.7
hole 128   origin  x=10.3 y=8.92 z=233.7
hole 128   origin  x=10.3 y=-8.92 z=233.7
hole 128   origin  x=-10.3 y=0 z=233.7
hole 128   origin  x=-10.3 y=8.92 z=233.7
hole 128   origin  x=-10.3 y=-8.92 z=233.7
hole 128   origin  x=12.875 y=4.46 z=233.7
hole 128   origin  x=12.875 y=-4.46 z=233.7
hole 128   origin  x=-12.875 y=4.46 z=233.7
hole 128   origin  x=-12.875 y=-4.46 z=233.7
hole 128   origin  x=-15.45 y=0 z=233.7
hole 36   origin  x=0 y=8.92 z=290
```

```
hole 36   origin  x=0 y=-8.92 z=290
hole 36   origin  x=2.575 y=4.46 z=290
hole 36   origin  x=2.575 y=-4.46 z=290
hole 36   origin  x=2.575 y=13.38 z=290
hole 36   origin  x=2.575 y=-13.38 z=290
hole 36   origin  x=-2.575 y=4.46 z=290
hole 36   origin  x=-2.575 y=-4.46 z=290
hole 36   origin  x=-2.575 y=13.38 z=290
hole 36   origin  x=-2.575 y=-13.38 z=290
hole 36   origin  x=5.15 y=0 z=290
hole 36   origin  x=5.15 y=8.92 z=290
hole 36   origin  x=5.15 y=-8.92 z=290
hole 36   origin  x=-5.15 y=0 z=290
hole 36   origin  x=-5.15 y=8.92 z=290
hole 36   origin  x=-5.15 y=-8.92 z=290
hole 36   origin  x=7.725 y=4.46 z=290
hole 36   origin  x=7.725 y=-4.46 z=290
hole 36   origin  x=7.725 y=13.38 z=290
hole 36   origin  x=7.725 y=-13.38 z=290
hole 36   origin  x=-7.725 y=4.46 z=290
hole 36   origin  x=-7.725 y=-4.46 z=290
hole 36   origin  x=10.3 y=0 z=290
hole 36   origin  x=10.3 y=8.92 z=290
hole 36   origin  x=10.3 y=-8.92 z=290
hole 36   origin  x=-10.3 y=0 z=290
hole 36   origin  x=-10.3 y=8.92 z=290
hole 36   origin  x=-10.3 y=-8.92 z=290
hole 36   origin  x=12.875 y=4.46 z=290
hole 36   origin  x=12.875 y=-4.46 z=290
hole 36   origin  x=-12.875 y=4.46 z=290
hole 36   origin  x=-12.875 y=-4.46 z=290
hole 36   origin  x=-15.45 y=0 z=290
hole 4   origin  x=0 y=0 z=-116
hole 5   origin  x=0 y=0 z=-116
hole 6   origin  x=0 y=0 z=-116
hole 4   origin  x=0 y=0 z=-58
hole 5   origin  x=0 y=0 z=-58
hole 6   origin  x=0 y=0 z=-58
hole 4
hole 5
hole 6
hole 4   origin  x=0 y=0 z=58
hole 5   origin  x=0 y=0 z=58
hole 6   origin  x=0 y=0 z=58
hole 4   origin  x=0 y=0 z=116
hole 5   origin  x=0 y=0 z=116
hole 6   origin  x=0 y=0 z=116
hole 4   origin  x=0 y=0 z=174
hole 5   origin  x=0 y=0 z=174
hole 6   origin  x=0 y=0 z=174
hole 4   origin  x=0 y=0 z=232
hole 5   origin  x=0 y=0 z=232
hole 6   origin  x=0 y=0 z=232
hole 4   origin  x=0 y=0 z=290
hole 5   origin  x=0 y=0 z=290
hole 6   origin  x=0 y=0 z=290
hole 4   origin  x=0 y=0 z=348
```

```
 hole 5   origin  x=0 y=0 z=348
 hole 6   origin  x=0 y=0 z=348
 hole 3   origin  x=-7.875 y=-13.6399 z=4.2
 hole 3   origin  x=-7.875 y=-13.6399 z=34.2
 hole 3   origin  x=15.75 y=0 z=4.2
 hole 3   origin  x=15.75 y=0 z=34.2
 hole 12   origin  x=-7.875 y=13.6399 z=4.2
 hole 3   origin  x=-7.875 y=-13.6399 z=62.2
 hole 3   origin  x=-7.875 y=-13.6399 z=92.2
 hole 3   origin  x=15.75 y=0 z=62.2
 hole 3   origin  x=15.75 y=0 z=92.2
 hole 12   origin  x=-7.875 y=13.6399 z=62.2
 hole 39   origin  x=-7.875 y=-13.6399 z=120.2
 hole 39   origin  x=-7.875 y=-13.6399 z=150.2
 hole 39   origin  x=15.75 y=0 z=120.2
 hole 39   origin  x=15.75 y=0 z=150.2
 hole 12   origin  x=-7.875 y=13.6399 z=120.2
 hole 39   origin  x=-7.875 y=-13.6399 z=178.2
 hole 39   origin  x=-7.875 y=-13.6399 z=208.2
 hole 39   origin  x=15.75 y=0 z=178.2
 hole 39   origin  x=15.75 y=0 z=208.2
 hole 12   origin  x=-7.875 y=13.6399 z=178.2
 hole 3   origin  x=-7.875 y=-13.6399 z=236.2
 hole 3   origin  x=-7.875 y=-13.6399 z=266.2
 hole 3   origin  x=15.75 y=0 z=236.2
 hole 3   origin  x=15.75 y=0 z=266.2
 hole 12   origin  x=-7.875 y=13.6399 z=236.2
 media 1 1 30
 media 9 1 10
 media 9 1 20
 boundary 1

---------Remaining fuel columns removed for example input file---------

unit 22
com='irradiation tube column'
 rhexprism 8  18  406  -116
 hole 10   origin  x=5.4 y=9.35307 z=0
 hole 10   origin  x=5.4 y=-9.35307 z=0
 hole 10   origin  x=-10.8 y=0 z=0
 hole 4   origin  x=0 y=0 z=-126
 hole 5   origin  x=0 y=0 z=-126
 hole 6   origin  x=0 y=0 z=-126
 hole 4   origin  x=0 y=0 z=-68
 hole 5   origin  x=0 y=0 z=-68
 hole 6   origin  x=0 y=0 z=-68
 hole 4   origin  x=0 y=0 z=-10
 hole 5   origin  x=0 y=0 z=-10
 hole 6   origin  x=0 y=0 z=-10
 hole 4   origin  x=0 y=0 z=48
 hole 5   origin  x=0 y=0 z=48
 hole 6   origin  x=0 y=0 z=48
 hole 4   origin  x=0 y=0 z=106
 hole 5   origin  x=0 y=0 z=106
 hole 6   origin  x=0 y=0 z=106
 hole 4   origin  x=0 y=0 z=164
 hole 5   origin  x=0 y=0 z=164
```

```
 hole 6   origin  x=0 y=0 z=164
 hole 4   origin  x=0 y=0 z=222
 hole 5   origin  x=0 y=0 z=222
 hole 6   origin  x=0 y=0 z=222
 hole 4   origin  x=0 y=0 z=280
 hole 5   origin  x=0 y=0 z=280
 hole 6   origin  x=0 y=0 z=280
 hole 4   origin  x=0 y=0 z=348
 hole 5   origin  x=0 y=0 z=348
 hole 6   origin  x=0 y=0 z=348
 media 9 1 8
 boundary 8
unit 15
com='replaceable reflector graphite block column'
 rhexprism 1  18  406  -116
 hole 4   origin  x=0 y=0 z=-126
 hole 5   origin  x=0 y=0 z=-126
 hole 6   origin  x=0 y=0 z=-126
 hole 4   origin  x=0 y=0 z=-68
 hole 5   origin  x=0 y=0 z=-68
 hole 6   origin  x=0 y=0 z=-68
 hole 4   origin  x=0 y=0 z=-10
 hole 5   origin  x=0 y=0 z=-10
 hole 6   origin  x=0 y=0 z=-10
 hole 4   origin  x=0 y=0 z=48
 hole 5   origin  x=0 y=0 z=48
 hole 6   origin  x=0 y=0 z=48
 hole 4   origin  x=0 y=0 z=106
 hole 5   origin  x=0 y=0 z=106
 hole 6   origin  x=0 y=0 z=106
 hole 4   origin  x=0 y=0 z=164
 hole 5   origin  x=0 y=0 z=164
 hole 6   origin  x=0 y=0 z=164
 hole 4   origin  x=0 y=0 z=222
 hole 5   origin  x=0 y=0 z=222
 hole 6   origin  x=0 y=0 z=222
 hole 4   origin  x=0 y=0 z=280
 hole 5   origin  x=0 y=0 z=280
 hole 6   origin  x=0 y=0 z=280
 hole 4   origin  x=0 y=0 z=348
 hole 5   origin  x=0 y=0 z=348
 hole 6   origin  x=0 y=0 z=348
 media 9 1 1
 boundary 1
unit 90
com='control rods'
 cylinder 9  3.4  406  333.5
 cylinder 10  3.75  406  333.5
 cylinder 11  5.25  406  333.5
 cylinder 12  5.6  406  333.5
 cylinder 13  6.15  406  0
 cylinder 14  6.15  0  -68
 cylinder 15  6.15  406  -68
 media 7 1 -9 10
 media 8 1 -9 -10 11
 media 7 1 -9 -10 -11 12
 media 5 1 9
```

```
 media 5 1 -9 -10 -11 -12 13
 media 5 1 14
 boundary 15
unit 80
com='shutdown hole'
 cylinder 1  6.15  406  0
 media 5 1 1
 boundary 1
unit 40
com='control rod column #1: shutdown hole at 120 degree'
 rhexprism 8  18  406  -116
 hole 80   origin  x=-5.4 y=9.35307 z=0
 hole 90   origin  x=-5.4 y=-9.35307 z=0
 hole 90   origin  x=10.8 y=0 z=0
 hole 4   origin  x=0 y=0 z=-126
 hole 5   origin  x=0 y=0 z=-126
 hole 6   origin  x=0 y=0 z=-126
 hole 4   origin  x=0 y=0 z=-68
 hole 5   origin  x=0 y=0 z=-68
 hole 6   origin  x=0 y=0 z=-68
 hole 4   origin  x=0 y=0 z=-10
 hole 5   origin  x=0 y=0 z=-10
 hole 6   origin  x=0 y=0 z=-10
 hole 4   origin  x=0 y=0 z=48
 hole 5   origin  x=0 y=0 z=48
 hole 6   origin  x=0 y=0 z=48
 hole 4   origin  x=0 y=0 z=106
 hole 5   origin  x=0 y=0 z=106
 hole 6   origin  x=0 y=0 z=106
 hole 4   origin  x=0 y=0 z=164
 hole 5   origin  x=0 y=0 z=164
 hole 6   origin  x=0 y=0 z=164
 hole 4   origin  x=0 y=0 z=222
 hole 5   origin  x=0 y=0 z=222
 hole 6   origin  x=0 y=0 z=222
 hole 4   origin  x=0 y=0 z=280
 hole 5   origin  x=0 y=0 z=280
 hole 6   origin  x=0 y=0 z=280
 hole 4   origin  x=0 y=0 z=348
 hole 5   origin  x=0 y=0 z=348
 hole 6   origin  x=0 y=0 z=348
 media 1 1 8
 boundary 8

------Remaining control rod columns removed for example input file-----

unit 34
com='permanent reflector block'
 rhexprism 1  18  406  -116
 media 10 1 1
 boundary 1
global unit 16
com='arrangement of array of fuel, control rod, reflector columns to
create core'
 cylinder 1  162  406  -116
 cylinder 3  214.98  406  -116
 array 2 1  place 6 6 1 0 0 0
```

```
 media 10 1 -1 3
 boundary 3
end geometry
read array
ara=2 nux=11 nuy=11 nuz=1 typ=rhexagonal gbl=2
fill 16*34 22 8*34 44 15 73 15 42 4*34 20 15 31 30 18 32 31 15 21 2*34
15 72 20 61 26 62 21 74 15 2*34 43 29 60 25 8 27 63 33 45 2*34 15 30 19
24 23 14 17 32 15 2*34 22 71 28 65 8 64 28 75 22 3*34 15 40 29 70 33 41
15 6*34 15 8 15 15*34
end fill
end array
end data
end
```

APPENDIX B

EXAMPLE DANCOFF-MC INPUT FILE

DANCOFF-MC Input File with Results

(Close packed lattice of spherical pellets)

Input values

ILATTI	Lattice type [squ=1,hex=2,ssq=3,rho=4,ort=5]	:	4
ENVIR	Radius of the environment [pitches]	:	10.00000
IGREY	Grey effect ? [yes=1, no=0]	:	0
IGP	Is there any gap ? [yes=1, no=0]	:	0
ICL	Is there any clad ? [yes=1, no=0]	:	1
RFLU	Outside radius of the fuel region [cm]	:	0.02900
RGPU	Outside radius of the (outer) gap [cm]	:	0.00000
RCLU	Outside radius of the (outer) clad [cm]	:	0.04600
PITCH	Pitch [cm]	:	0.11600
STFLU	Sigma total of the fuel [1/cm]	:	0.00000
STCLU	Sigma total of the (outer) clad [1/cm]	:	0.37000
STMD	Sigma total of the (outer) moderator [1/cm]	:	0.40200
IANNUL	Lump type [non-annular=0, annular=1]	:	0
RFLIU	Inside radius of the fuel region [cm]	:	0.00000
RGPIU	Inside (smaller) radius of the inner gap [cm]	:	0.00000
RCLIU	Inside (smaller) radius of the inner clad [cm]	:	0.00000
STCLIU	Sigma total of the inner clad [1/cm]	:	0.00000
STMDIU	Sigma total of the inner moderator [1/cm]	:	0.00000
NCYCLE	Number of Monte Carlo cycles to be executed	:	5000000
SACCUU	Sufficient accuracy for the Dancoff factor	:	0.00001
IRAND	Randomize the start of the RNG ? [yes=1, no=0]	:	0

Results

NLUM	Number of lumps taken into account	:	5705
DANFU	Dancoff factor calculated	:	0.84930
SDEVU	Standard deviation of the Dancoff factor	:	0.00009
NCEXU	Number of cycles executed	:	5000000

APPENDIX C

CODE-TO-CODE BENCHMARK DATA

Prismatic Core Model Benchmark Problem Description

1. Effective Multiplication Factor with Control Rods Fully Inserted
    - Determine K-eff
    - Fully loaded fresh fuel core
    - Core temperature of 300 K
    - Control rods fully inserted in the core
    - Experimental results (experimental-to-code)
    - Calculated results from member countries (code-to-code)
2. Effective Multiplication Factor with Control Rods Fully Withdrawn
    - Determine K-eff
    - Fully loaded fresh fuel core
    - Core temperature of 300 K
    - Control rods removed from the core
    - Experimental results (experimental-to-code)
    - Calculated results from member countries (code-to-code)
3. Control Rod Position at Criticality (300 K)
    - Determine control rod position at which core is critical
    - Fully loaded fresh fuel core
    - Core temperature of 300 K
    - Control rod insertion levels adjusted on the same level, except for three pair of control rods in the outer most region in the side reflectors
    - The critical control rod position is measured from the bottom of the active core
    - Experimental results (experimental-to-code)

- Calculated results from member countries (code-to-code)

4. Control Rod Position at Criticality (418 K and 480 K)

- Determine control rod position at which core is critical
- Fully loaded fresh fuel core
- Core temperatures of 418 K and 480 K.
- Control rod insertion levels adjusted on the same level, except for three pair of control rods in the outer most region in the side reflectors
- The critical control rod position is measured from the bottom of the active core
- Experimental results for 418 K (experimental-to-code)
- Calculated results from member countries at 480 K (code-to-code)

5. Isothermal Temperature Coefficient (Effective Multiplication Factors for Different Temperatures)

- Determine K-eff for core temperatures of 300, 340, 380, 420, 460 and 480 K
- Fully loaded fresh fuel core
- Control rods held at critical position for 300 K core (determined in benchmark problem 3. above)
- Experimental results (experimental-to-code)
- Calculated results from member countries (code-to-code)

KENO6-VI Parameter Data:

- GEN=210 (number of generations to be run)
- NPG=1000 (number of neutrons per generation)
- NSK=10 (number of generations to be omitted when collecting results)
- FLX=yes (collect and print fluxes)

- FDN=yes (collect and print fission densities)
- PKI=yes (print input fission spectrum)
- FAR=yes (generate region-dependent fissions and absorptions for each energy group)
- GAS=yes (print region-dependent fissions and absorptions by energy group)
- Remaining parameters at default

Optional More Data Parameter Data:

- IIM=50 (max number of inner iterations to be used in the XSDRNPM calculation)
- ICM=100 (max number of inner iterations to be used for XSDRNPM)
- COF=3 (diffusion coefficient for transverse leakage corrections in XSDRNPM, use a flux and volume weighting across all zones)
- EPS=0.0001 (overall convergence criteria for XSDRNPM, smaller value tightens convergence)
- PTC=0.000001 (pointwise convergence criteria for XSDRNPM, smaller value tightens convergence)
- SCALE determines the Dancoff factor, but can be manually input in this section DAN(xx)=Dancoff factor

The Dancoff factor was determined using three separate methods: 1) DANCOFF-MC, 2) SUPERDAN (SCALE code system), and 3) From IAEA-TECDOC-1382. Benchmark problems were calculated for each above case, with the DANCOFF-MC case being utilized for the final model.

Control Rods Inserted	
VHTR Prismatic Core Model	**k-eff**
-Dancoff from IAEA report	0.7061 ± 0.0021
-Dancoff MC	0.7254 ± 0.0018
-SUPERDAN	0.7376 ± 0.0029
Member States IAEA report	
-Japan (MVP)	0.70699
-Netherlands (KENO V.a)	0.6983 ± 0.0005
(PANTHER)	0.751
-France (TRIPOLI4)	0.68396 ± 0.0003
-Russia (MCNP 4a)	0.7172 ± 0.0015
-USA (MCNP 4a)	0.6899 ± 0.005
Experimental	0.685 ± 0.010

Control Rods Withdrawn	
VHTR Prismatic Core Model	**k-eff**
-Dancoff from IAEA report	1.1136 ± 0.0017
-Dancoff MC	1.1255 ± 0.0018
-SUPERDAN	1.1477 ± 0.0023
Member States IAEA report	
-Japan (MVP)	1.14278 ± 0.00039
-Netherlands (KENO V.a)	1.1584 ± 0.0005
(PANTHER)	1.1595
-France (TRIPOLI4)	1.13833 ± 0.00090
-Turkey (MCNP 4b)	1.15641 ± 0.00095
-Russia (MCNP 4a)	1.125 ± 0.0015
-USA (MCNP 4a)	1.1400 ± 0.004
Experimental	1.1363 ± 3.6%

Critical Insertion Depths of Control Rods	
Core Temperature 300 K **VHTR Prismatic Core Model**	**Control rod critical position from the bottom of the active core (cm)**
-Dancoff from IAEA report	198.0
-Dancoff MC	181.6
-SUPERDAN	160.0
Member States IAEA report	
-Japan (MVP)	180.0
-Netherlands (KENO V.a)	170.5
(PANTHER)	161.5
-France (TRIPOLI4)	177.9
-Russia (MCNP 4a)	170.0
-Turkey (MCNP-4B)	164.0
-USA (MCNP 4a)	159.0
Experimental	177.5 ± 0.5

Critical Insertion Depths of Control Rods	
Core Temperature 418 K **VHTR Prismatic Core Model**	**Control rod critical position from the bottom of the active core (cm)**
-Dancoff from IAEA report	217.0
-Dancoff MC	195.7
-SUPERDAN	182.5
Experimental	190.3 ± 0.5

Critical Insertion Depths of the Control Rod	
Core Temperature 480 K **VHTR Prismatic Core Model**	**Control rod critical position from the bottom of the active core (cm)**
-Dancoff from IAEA report	221.0
-Dancoff MC	205.0
-SUPERDAN	190.0
Member States IAEA report	
-Japan (MVP)	198.9
-Netherlands (KENO V.a)	187.9
(PANTHER)	193.4
-Turkey (MCNP-4B)	190.0

Isothermal Temperature Coefficients

Results	Temperature coefficients (Δk/k per Kelvin X 10e-4)					
	ρ320	**ρ360**	**ρ400**	**ρ440**	**ρ470**	**ρAve**
VHTR Prismatic Core Model	-1.05	-0.71	-3.10	-1.77	-1.42	-1.61
Member States IAEA report						
-Japan (MVP)	-1.23	-1.66	-1.63	-1.56	-0.91	-1.40
-Netherlands (KENO V.a)						-1.42
(PANTHER)						-1.52
-France (TRIPOLI4)	-1.67	-1.61	-1.62	-1.64	-1.56	-1.62
-Russia (MCNP 4a)	-1.95	-1.73	-1.65	-1.77	-1.45	-1.71
Experimental	ρ345 = -1.34 and ρ405 = -1.42					

VITA

David E. Ames II graduated from the University of Utah in May 2004 with a Bachelor of Science degree in mechanical engineering and a minor in physics. He entered the nuclear engineering graduate program at Texas A&M University in August 2004, and received his Master of Science degree in August 2006. Future contact may be made by e-mail at deames_99@yahoo.com or by mail forwarded through the department of Nuclear Engineering, c/o Dr. Pavel V. Tsvetkov, Texas A&M University, College Station, TX 77843-3133